Aus der Klinik für Neurologie
der Heinrich-Heine-Universität Düsseldorf
Direktor: Univ.-Prof. Dr. Hans-Peter Hartung

Combining a mechanical micro-connector device and human umbilical cord blood stem cells to enhance functional improvement after complete spinal cord injury

Dissertation
zur Erlangung des Grades eines Doktors der Medizin
der Medizinischen Fakultät der Heinrich-Heine-Universität Düsseldorf

vorgelegt von
Theresa Sophie Kehl

2017

Als Inauguraldissertation gedruckt mit der Genehmigung der Medizinischen Fakultät der Heinrich-Heine-Universität Düsseldorf

gez.:

Dekan: Univ.-Prof. Dr. med. N. Klöcker

Erstgutachter: Univ.-Prof. Dr. H. W. Müller

Zweitgutachter: PD Dr. med. J. F. Cornelius

"Ever tried. Ever failed. No matter. Try Again. Fail Again. Fail Better."

S. Becket, Worstward ho (1983)

Zusammenfassung

Hintergrund: Eine Schädigung des Rückenmarks (RM) führt distal der Verletzung zu einer teilweisen oder vollständigen Lähmung, häufig begleitet mit einem Verlust an Empfindungen. Die Pathophysiologie nach RM-Verletzungen ist multifaktoriell und verläuft in mehreren Phasen. In aktuellen Behandlungskonzepten soll diese Tatsache durch die Kombination verschiedener Behandlungsansätze berücksichtigt werden. In vorausgegangen Studien unserer Arbeitsgruppe wurde ein mechanisches Mikrokonnektorsystem (mMS) etabliert, das im Ratten-Modell nach kompletter Transektion des thorakalen RM die Annäherung der spinalen Gewebestümpfe bewirkt und zudem über ein internes Kanalsystem die Versorgung mit Therapeutika lokal im Läsionszentrum über einen längeren Zeitraum gewährleistet. Zusätzlich konnte in unserer Arbeitsgruppe gezeigt werden, dass die Transplantation von aus humanem Nabelschnurblut gewonnenen Stammzellen, die auch als "unrestricted somatic stem cells" (USSC) bezeichnet werden, sowohl die axonale Regeneration, als auch die allgemeine, motorische Funktion verbessern.

Ziel: Das Ziel dieser Arbeit war im Ratten-Modell nach kompletter Transektion des thorakalen RM die Effekte einer kombinierten Behandlung mit mMS und USSC im Vergleich zu Einzelbehandlungen sowohl hinsichtlich der funktionellen motorischen Ergebnisse als auch mit immunhistochemischen Methoden im Verlauf zu untersuchen.

Methoden & Ergebnisse: Zur Prüfung der Hypothese, dass eine Kombinationstherapie den Einzelbehandlungen überlegen ist, wurden 60 mit Cyclosporin A immunsupprimierte Ratten einer kompletten mikrochirurgischen Transektion des thorakalen RM unterzogen. In der gleichen Operation fanden die anschließenden therapeutische Behandlungen statt. Es wurden 4 Gruppen à 15 Tiere gebildet: A) Kombinationstherapie (mMS + USSC), B) Monotherapie 1 (mMS + Kontrollmedium DMEM), C) Monotherapie 2 (USSC) und D) Kontrolle (DMEM). Zur Evaluierung der funktionellen Erholung wurden die Tiere in einem Intervall von 2 Wochen mit dem modifizierten Offenfeld-Lokomotionstest nach Basso, Beattie und Bresnahan über einen Zeitraum von 16 Wochen untersucht. Danach erfolgten verschiedene immunhistochemische (IHC) Färbungen zur Beurteilung von Gewebeerhalt, Gefäßeinsprossung und axonalem Regenerationverhalten. Mittels IHC ließ sich hier erstmals zeigen, dass USSC zielgerichtet in das Lumen des mMS migrieren. Die kombiniert behandelten Tiere der Gruppe A) zeigten die geringste Bildung von Zysten, ein vermehrtes Einsprossen von Blutgefäßen in das Lumen des mMS und die beste axonale Regeneration, teilweise mit erneuerter Myelinisierung. Darüber hinaus zeigte die kombiniert behandelte Tiere der Gruppe A) die besten funktionalen Fähigkeiten mit einer signifikanten Verbesserungen der allgemeinen Lokomotion.

Zusammenfassung & Ausblick: Im Rattenmodell einer RM-Verletzung konnte in dieser Arbeit die Überlegenheit einer kombinierten Behandlung mit mMS und USSC gezeigt werden. Im Hinblick auf einen möglichen klinischen Einsatz dieser Behandlungsprinzipien wären weitere Modifikationen vorstellbar, wie beispielsweise die Applikation zusätzlicher Therapeutika über das interne Kanalsystem oder ein biologisch abbaubares mMS. Interessant wären auch die Ergebnisse von mMS Implantationen nach Resektion des Narbengewebes im Modell einer chronischen RM-Verletzung.

Summary

Background: A spinal cord injury (SCI) leads to partial or complete paralysis and loss of sensory input below the level of injury. The pathophysiology of SCI is multifactorial and multiphasic and, therefore, it is likely that effective treatments will require combinations of different strategies. Previously, we used a mechanical Microconnector System (mMS) composed of polymethylmethacrylate, which was developed to reconnect transected spinal cord stumps: It holds the availability of drug application by a system of internal micro-channels. In another study we provided evidence that transplantation of unrestricted somatic stem cells (USSC) from human umbilical cord blood significantly improves axonal regeneration and functional improvement.

Purpose: The aim of the study was to modify the therapeutic approaches and to determine whether the combination therapy is superior to the individual therapies.

Methods & Results: To test the hypothesis that the combination therapy is superior to the individual therapies, immunosuppressed rats (n=60) received a complete spinal cord transection (TX) at level Th8. Immediately after SCI, the therapies were performed in the following therapeutic groups à 15 animals:
A) combination therapy (mMS + USSC), B) mono therapy 1 (mMS + control medium (DMEM)), C) mono therapy 2 (USSC) and D) control (DMEM). Over a period of 16 weeks, hindlimb function was evaluated biweekly in an open field test using a modified Basso, Beattie, Bresnahan Locomotor Rating Scale (mBBB). To further investigate tissue preservation, revascularization, and axonal regeneration, various immunohistochemical stainings (IHC) were performed.
Immunohistochemical staining revealed for the first time that USSC migrate into the lumen of the mMS. Decreased cavity formation, numerous blood vessels into the mMS lumen and enhanced axonal regeneration were observed in animals receiving the combination therapy. Combined treated animals (A) performed significantly and consistently better in the open field test.

Conclusion & Perspectives: The combination of the individually effective approaches (mMS, USSC) in a severe spinal cord injury model resulted in locomotor improvement that is superior to the individual treatments. Regarding potential clinical trials, further modifications such as the application of therapeutic drugs through the system of internal micro-channels, as well as a biodegradable mMS are conceivable. It will be exciting to implant the mMS in a chronic model of SCI after resection of the fibrotic tissue.

Contents

List of Figures

List of Tables

1 Introduction

1.1 Spinal cord injury

1.1.1 Epidemiology

Injuries to the spinal cord are radically life-changing events resulting in life-long severe impairments for the patients. Improved medical care could markedly reduce historical mortality rates of 80 %. Not only the survival rate but also the quality of life of patients suffering from spinal cord injury (SCI) could be improved, due to quality devices such as wheelchairs and rehabilitation programs. In comparison to high-income countries, the situation in low-income countries is totally different, illustrated in still high mortality rates and poor medical outcome [1]. In the report of the World Health Organization (WHO) influencing variables for the individual overall impact are delineated. According to that report, the age, the extent of injury, the availability and timing of resources and services, as well as the physical, social, economic, and attitudinal environment play a decisive role [1]. In addition to the psychological stress of each individual patient, SCI is a high-cost health condition although the incidence is comparatively low. Precise statistical data for prevalence, incidence, mortality, causes, and costs of SCI are sparse. Approximately 250000 to 500000 people / year suffer from SCI [1]. This correlates with an estimated global incidence of 40 to 80 new cases per million population per year [1]. There are no reliable sources about the global and regional prevalence of SCI. Due to retrospective, longitudinal study designs and global estimates from six different countries, the overall prevalence rate of spinal cord injury valued at about 2525 per million population, or 85 000 people, in 2010 [2, 1].

Cases of traumatic SCI predominate non-traumatic SCI cases with age-dependent variations: traumatic SCI is concentrated in younger populations while non-traumatic SCI is concentrated in older age groups. Traffic accidents, falls, violence, and sports accidents are the main causes of traumatic SCI; the transition from good health to permanent disability is often occuring within seconds [1]. Relating to the age distribution, two common peaks are reported: traumatic SCI are highest in younger populations (age 15–29), followed by a second peak in the elderly (age $\geq$ 60) [2, 1].

SCI produce devastating disabilities for the individual, the family, and society as a whole. It poses an enormous health impact due to occasion of high expenditures. Beside the annual costs for medical treatment and assistance, SCI produce incidental costs owing to lost productivity in this young affected population [2]. Direct socioeconomic effects include: higher lifetime unemployment rates, significant income losses, and long-term health care requirements and costs. Depression, reduced life expectancy, reduced likelihood to marry or remain married, and higher suicide rates are examples for psychological effects [3].

1.1.2 Spinal cord injury classification

Depending on the neurological outcome, SCI is classified in general terms of being neurologically "complete" or "incomplete". Complete SCI is defined as no motor or sensory function below the level of the spinal cord lesion after the end of the spinal shock phase. In contrast, incomplete SCI is defined as injury with remaining spinal cord tract function after the end of the spinal shock phase. In this regard, spinal shock phase is defined as the temporary condition following injury of the spinal cord that is characterized by physiological dysfunction with no motor and sensory function or autonomic reflexes, which usually ends after 24 to 72 hours [4].
The purpose of the SCI classification was to develop greater precision in the definitions and to determine sensory and motor levels separately [5]. Defined by the American Spinal Injury Association (ASIA), the neurological level of injury is the most caudal segment of the spinal cord with normal function on both sides of the body [6]. The ASIA Impairment Scale (AIS) ranges from A to E, where A is a complete SCI and E denotes normal sensory and motor function (Tab. 1.1).

Table 1.1: **American Spinal Injury Association (ASIA) Impairment Scale**

Grade	Degree of Severity	Definition
A	Complete	No sensory or motor function is preserved in the sacral segments S4-S5.
B	Sensory incomplete	Sensory but not motor function is preserved below the neurological level and includes the sacral segments S4-S5, AND no motor function is preserved more than three levels below the motor level on either side of the body.
C	Motor incomplete	Motor function is preserved below the neurological level, and more than half of key muscle functions below the single neurological level of injury have a muscle grade less than 3 (Grades 0–2).
D	Motor incomplete	Motor function is preserved below the neurological level, and at least half (half or more) of key muscle functions below the neurological level have a muscle grade >3.
E	Normal	Sensory and motor function is normal. Someone without a SCI does not receive an AIS grade.

In general, the higher the neurological level, the more devastating the injury. Based on the neurological level one can distinguish between tetraplegia and paraplegia in terms of complete cases. In terms of incomplete cases, one can distinguish between tetraparesis and paraparesis [6].
The spine can be divided into different regions: cervical (C1 to C7/Th1), thoracic (Th1 to Th11), thoracolumbar (Th11/Th12 to L1/L2), and lumbosacral (L2-S5), whereby

the cervical spine is the most common location for SCI, conditioned by its architecture. Approximately 55% of acute SCI occurs in the cervical region, the remaining 45% are homogeneously distributed; each level accounts for approximately 15% [7]. The clinical manifestations are correlated to the affected area. As mentioned above, high cervical injuries might lead to respiratory failure and lifelong physical dependence on ventilatory assistance.

1.2 Pathophysiology of spinal cord injury

1.2.1 Primary and secondary events after spinal cord injury

SCI interrupts the electrophysiological signal transduction and results in various neurological disabilities caused by the damage to the spinal pathways. The pathophysiology of SCI is multifactorial and multi-phasic, it can be subdivided into an acute, subacute, and chronic phase [8]. Aside from the direct damage to the spinal cord tissue, the functional loss is also conditioned by a cascade of biological events, described as "secondary injury" [9]. The idea of "secondary injury" was first postulated in 1911. Allen demonstrated the neurological improvements dependent on the removal of inflammatory fluid in injured dogs [9, 10]. This observations caused numerous scientists to deal with this subject. Targeting cascades are mediated by molecular pathways and signaling molecules. These cascades represent a complex response, which start only few minutes after trauma and can last for weeks [11, 9]. These mechanisms often lead to a massive aggravation of tissue damage and functional loss (see Fig. 1.1).

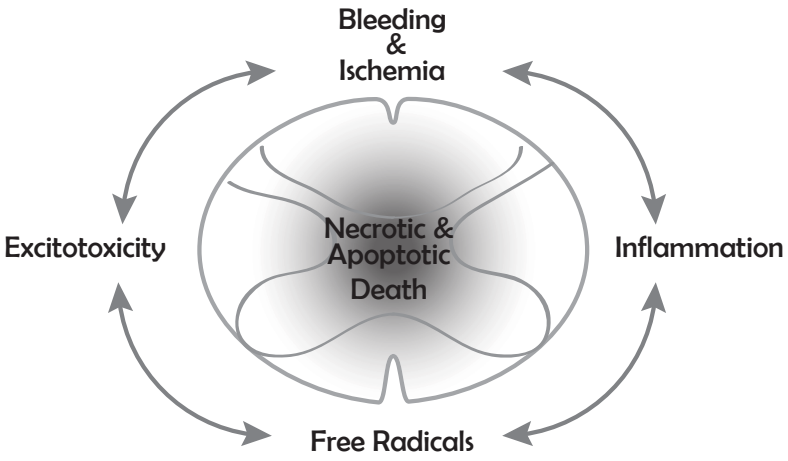

Figure 1.1: **Pathophysiologic processes after spinal cord injury**
Following spinal cord injury, different primary and secondary events interact and thus mutually reinforce each other. These processes are initiated by the initial trauma and finally lead to necrotic and apoptotic cell death. [Adapted from Kwon *et al.* [12].]

Secondary events inculde vascular changes (e.g. ischemia, edema, and disruption of blood-spinal cord barrier), disruption of ionic balance, free-radical production, apoptosis, and inflammation [9].

1.2.2 Regeneration failure after injury to the spinal cord

For a long time it was assumed that the mammalian central nervous system (CNS) was incapable of regeneration [13], in contrast to the peripheral nervous system (PNS) [14]. Santiago Ramón y Cajal, a pioneer in the field of SCI, summarized his studies on this matter in his seminal book "*Regeneration and Degeneration of the Nervous System*" [15]. The dogma of regenerative incapability could be refuted in 1981 by the work of David and Aguayo. They provided evidence that axons from nerve cells in the injured spinal cord and brainstem could elongate for long distances when the central nervous system (CNS) glial environment was replaced by that of peripheral nerves [16].

Many factors seem to be accountable for the poor regenerative capacity of CNS neurons. Axons of the adult mammalian CNS fail to regenerate after injury due to (1) the lack of stimulating environment, including missing growth promoting molecules and massive cell death, (2) the presence of regeneration barriers, mechanically conditioned by glia scar in addition to inhibitory molecules, and due to (3) the deficient growth potential of adult CNS neurons [17, 18, 19].

1.2.3 Scar formation - a physical and chemical barrier to regeneration

The complex molecular and cellular response (including primary and secondary injuries) following SCI leads to the formation of a lesion scar. By breakdown of the blood-brain/blood-spinal cord barrier hematogenous cells invade the lesion area and activate the inflammatory system by production of cytokines. Neural degeneration, cystic cavity formation, activation of glial cells are the consequences of these mechanisms. Two types of scarring tissue eventually form the lesion scar: The fibrous component in the lesion center and the surrounding glial part in the peri-lesion areas, those two components are separated by the *glia limitans* [20, 21]. A schematic illustration of the SCI lesion scar is presented in Fig. 1.2.

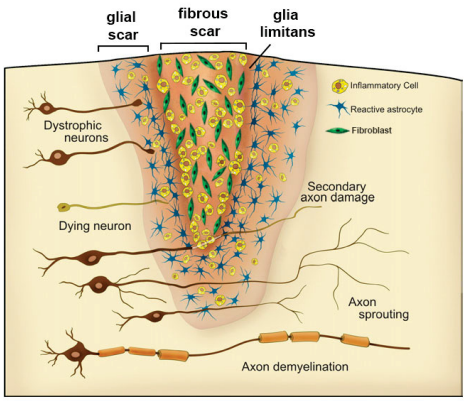

Figure 1.2: **Scar formation, secondary damage and wound healing after spinal cord injury**
The complex molecular and cellular response following spinal cord injury induces the formation of a lesion scar: A fibrous scar consisting of a dense extracellular matrix network and invading cells (e.g. fibroblasts and inflammatory cells), and a glial scar, which is mainly formed by reactive astrocytes. After contact with astrocytes invading meningeal cells form the glial limitans which presents a barrier to regenerating axons. [Modified from Fitch and Silver 2008 [19].]

Cellular components of the glial scar / Role of activated astrocytes

The glial scar not only represents a physical but also a chemical barrier to regeneration [22, 9, 19]. It is generally known that glial scars can inhibit both axon growth and myelination [23]. Therefore, it is clearly important to know what causes them to form. Additionally, and with regard to medical treatment, the knowledge of involved cells and inhibitory molecules is prerequisite for any manipulation [9]. In contrast to these adverse effects, reactive astrocytes, which are known as main components of the glial scar, convey survival advantages. However, reactive astrocytes are essential for wound healing by preventing an overwhelming inflammatory response, repair of the blood-brain/blood-spinal cord barrier, and limiting cellular degeneration [23, 24, 20].

Independent of the injury reason the cellular and molecular response is broadly the same. The immune system is significantly activated by non-CNS molecules entering the spinal cord parenchyma through the interrupted blood-spinal cord barrier [21]. In lesions where the dura mater is still intact, the scar is mainly composed of astrocytes and the inflammatory response is relatively bland. The glial scar is not merely a fixed construction, but rather an evolving structure, with different cells arriving and participating at different times. Astrocytes, microglia, and oligodendrocyte precursors are the main cell types involved in cellular events after SCI [25, 24].

The inflammatory response is mainly attributable to a switch to the reactive state of pre-existing cells followed by increased production of inhibitory molecules and hypertrophy [26, 9]. An increased expression of glial fibrillary acidic protein (GFAP) can be observed by immunohistochemistry.

In its final form, the glial scar consists mainly of a meshwork of astrocytes, connected and tightly interwoven with cells of different origin (e.g. oligodendrocytes, macrophages, microglia, and endothelial cells) via tight and gap junctions [27]. In time, the glial scar is becoming more rubbery, tenacious, and growth-blocking.

Fibrotic scar

The fibrous scar is located in the lesion core (Fig. 1.2) and consists of a dense extracellular matrix (ECM) network including collagen type IV (ColIV), fibronectin, and laminin [28, 29, 30]. The scaffolding is mainly composed of ColIV, other molecules, such as laminin and entactin, are further associated and interwoven with the fibrous scar [31]. Astrocytes and invading fibroblasts cooperate to lay down a continuous basal lamina on the out-facing astrocytic surface and to re-establish the glia-pial barrier referred to as the glia limitans [32, 20]. The lesion site seems to be sealed off by the fibrotic scar and leukocytes infiltration is enclosed [20]. The fibrous scar is further associated with other components such as growth inhibitory molecules [28].

Growth inhibitory molecules

Different inhibitory molecules of the extracellular matrix are increased following SCI [25]. Reactive astrocytes up-regulate, chondroitin sulfate proteoglycans (CSPGs) [33],

semaphorin 3 [34], ephrin B2 [35] and tenascin [27]. Furthermore, Oligodendrocytes promote the production of myelin-associated inhibitors (e.g. NogoA [36] or myelin-associated molecule (MAG) [37] and oligodendrocyte-myelin glycoprotein (OMgp) [38]) [39]. The entirety of these molecules creates a long-lasting non-permissive environment for regeneration in the CNS [19, 40].

1.3 Treatments - endless opportunities to achieve one goal

There are numerous different ways of treating SCI. Contemporaneously with the growing understanding of the molecular processes and the pathophysiology, more and more therapeutic approaches were tested. Since it has been shown that regrowth of only a few axons can lead to the improvement of some respectable motor or sensory functions, many research groups have focused on identifying the factors and mechanisms which are responsible for the failure of regrowth with the aim to improve axonal regeneration [41]. In simplified terms and for comparison of clinical trials, therapeutic approaches can be divided into four broad categories [42]:

- Neuroprotection and pharmacotherapy
- Surgery
- Stimulation of axonal regeneration
- Rehabilitation

In this section, the diverse therapeutic approaches will be presented with the focus on stem cell based therapies and mechanical adaptation strategies that have been investigated for SCI, (Fig. 1.3):

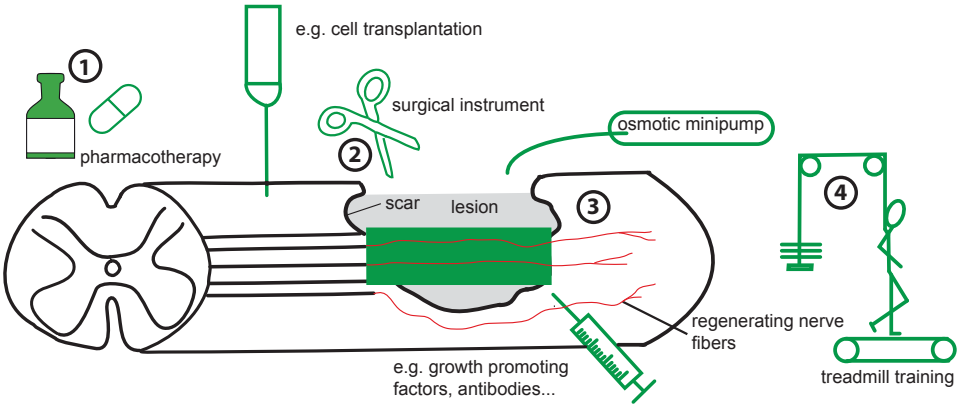

Figure 1.3: **Different strategies to repair the injured spinal cord**
Therapeutic approaches to treat the injured spinal cord include: (1) neuroprotection and pharmacotherapy, (2) surgical decompression and stabilization, (3) stimulation of axonal regeneration through e.g. implanting bridge devices, cell transplantation, and treating the lesion with growth promoting factors or nerve attractants by osmotic minipump or injection, and (4) rehabilitation through e.g. treadmill training. [Based on Schwab 2002 [43].]

Neuroprotection and pharmacotherapy

Neuroprotection includes agents such as steroids or other anti-inflammatory agents (e.g. interleukin-10 (IL-10)[44] and cyclooxygenases (COX-1 and COX-2) [45, 46, 47]) to counteract the secondary injury mechanisms in SCI [42]. While numerous approaches were attempted in animal models, just a few reached clinical state. To date, neuroprotection alone has not produced a significant recovery after SCI [42].

Surgery

Decompression and stabilization are the main goals of surgical interventions [48]. The optimal timing is still controversially discussed. Pre-clinical studies reveal biological benefits of early surgical decompression in animal models. If clinically safe and feasible, surgery should be performed within 24 h. Early surgical intervention has the potential to improve clinical, neurological, and functional outcome [48].

Regenerative Strategies

Numerous scientific working groups all over the world try to develop new strategies to stimulate axonal regeneration. Numerous factors and mechanisms have already been identified: E.g. Neurotrophic factors, blocking the inhibitory effects of myelin [49, 36], suppression of fibrous scarring through application of an iron chelator 2,2'-bipyridine-5,5'-dicarboxylic acid (BPY-DCA) [50, 28, 51], designs to bridge the gap with transplantation of matrices, scaffolds and other bioengineering strategies [52], and cell replacement therapies (Schwann cells [53], macrophages [54], olfactory ensheathing glia (OEG) [55], stem cells and many other). These examples represent just a small extract of the wide range of possibilities.

Rehabilitation

Additional rehabilitation strategies such as treadmill training seem to have supportive effects for the prevention of myatrophy and spasticity. Additionally, the axonal regeneration and spinal cord plasticity as well as the functional outcome could be increased by regular training [56, 57].

1.4 Efforts to bridge the gap - Functional requirements and realization of different approaches

1.4.1 Critical design parameters

Suturing or glueing of spinal cord tissue is unsatisfactory and due to the texture of the tissue sometimes unconvertible, in many cases even harmful. Suturing of the *dura mater* leads to a restricted adaptation. In fact, it has been shown, that suturing of the *dura mater* reduces the spinal cord lesion gap, cystic cavitation, and connective tissue scar

formation in the model of hemisection [58] and in the model of a complete transection [59]. Suturing of the *dura mater* only allows an indirect adaptation. In contrast, glueing enables a direct adaptation, but the glue acts as a regeneration barrier, comparable to the scar. Regenerated axons cannot cross long tissue gaps to re-enter tissue beyond the lesion. Those tissue gaps are the result of the original trauma combined with secondary injury processes. In addition, resection of the fibrotic tissue, as part of a surgical intervention, also leaves a gap in animals with chronic SCI [60]. When a large lesion has arisen from secondary injury, regenerated axons remain at the border of the lesion unable to cross the tissue defect on their own due to the absence of a cellular and extracellular environment [61]. Several strategies to bridge spinal cord tissue gaps have been developed in the past few years. Cell transplantation has probably been the most widely investigated strategy to restore the tissue defect. But recent years have witnessed a significant increase in the application of bridging devices. Tissue engineering is an emerging field of SCI research. Bioengineering offers opportunities not only to replace lost tissue but also to provide mechanical support, to counteract secondary injury, to suppress scar formation, to guidance axonal regrowth, to act as a drug delivery system and much more [52]. Bridging devices differ in the following parameters: cellular or acellular bridges, natural or synthetic materials or composite materials, non-degradable or degradable materials, and the different designs [62, 63, 64].
Thus, application of scaffolds provides optimal conditions for a combinatorial treatment [65]. Critical design parameters for nerve guidance channel function are shown in Fig. 1.4.

Designs and Macro-architectures

Gels, sponges, tubes, and matrices are typical designs of bridging devices used in the experimental field of SCI. Each of these has advantages and disadvantages. Viscous gels are advantageous for filling in a small area (e.g. in a cystic cavity) and might act as vehicles for cells or drugs. In comparison, sponges may fill up wider tissue defects. Disadvantages of gels and sponges include their mechanical weakness. In contrast, tubes and channels provide the pathways for axonal regrowth across long tissue gaps [52]. Axonal regeneration of the CNS is more complicated compared with that of the PNS, because of the non-permissive environment after (experimental) CNS injury. Nerve guidance channels have been used to bridge PNS injuries for many years. Based on the success of nerve guidance channels in the PNS, much focus has been directed to their application in the CNS. However, the complexity of the CNS requires adjustments regarding the designs of the CNS guidance channels [64]. The mechanical properties should be similar to those of the native spinal cord [62]. Further parameters, such as morphology, architecture, porousness, and surface components have an essential influence on the outcome [62]. A summarizing presentation of typical architectures of scaffolds used for SCI repair is given in a review by Wang *et al.* in 2011. Inventive and creative research groups came up with new designs by mimicking spinal cord cross sections. Such designs might enhance the functional organization due to improved specificity. Thus, separation of functional pathways with tract-specific growth-enhancing strategies might be possible [63, 66]. Compared to a single-lumen tube, multichannels provide a larger surface area [62]. The microstructure is important with regard to the mechanical properties and the surface-to-volume ratio

[62, 63]. To maximize the stability with simultaneous consideration of maximal system surface, the application of honeycombed devices seems to have beneficial effects. The optimal design of CNS guidance channels is thereby expected to become increasingly complex and quite different from the optimal PNS guidance channels [64].

Biocompatibility

Biocompatibility is a critical factor for the implantation of a bridging device. Contact-mediated guidance of scaffolds are able to promote axonal regeneration. To optimize those possibilities, surfaces of the scaffolds can be modified to prevent rejection or avoid adverse immune reaction and to mimic a natural extracellular matrix. However, with regard to clinical trials, scaffolds must be easily sterilizable to prevent infection [67].

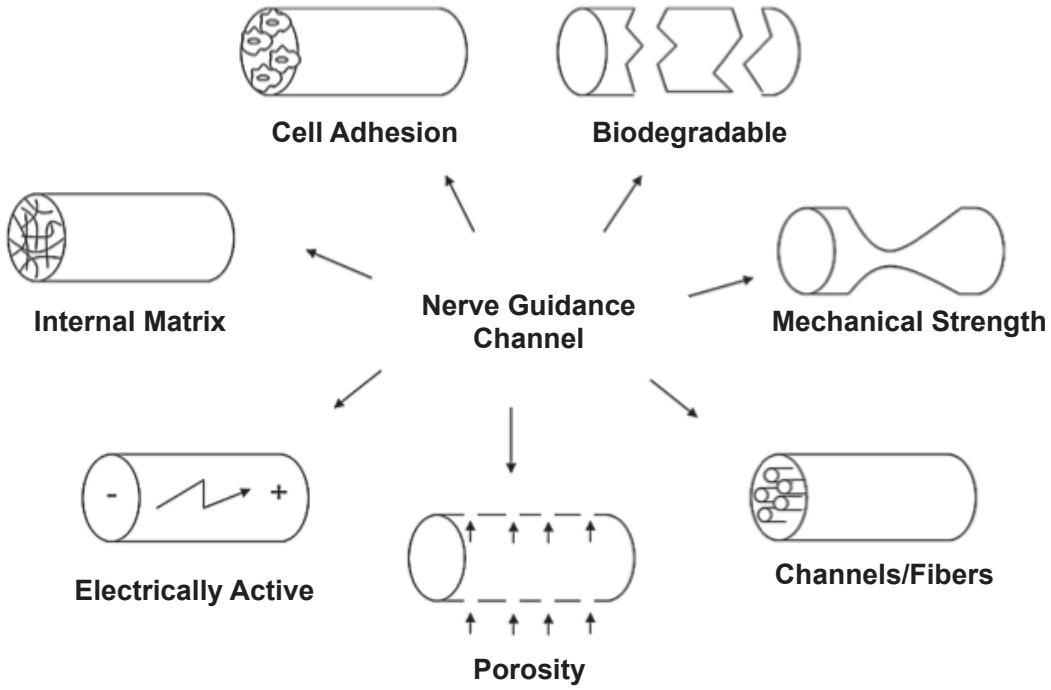

Figure 1.4: **Key elements of nerve guidance channels**
Different design parameters for nerve guidance channels. The realization of these parameters are crucial for the therapeutic effects. [Designed by Straley *et al.* 2010 [64].]

Biodegradability

Regarding biodegradability, different therapeutic approaches exist with special characteristics. Non-degradable channels, however, are often made of synthetic materials. Synthetic materials include advantages of uniform and controlled synthesis techniques. Due to permanent implantation, the risk of an inflammatory response is increased. In some cases, a secondary surgery to remove this material will be necessary, which might cause further complications [68]. The permanent stay otherwise provides continous mechanical rigidity. A controlled degradation rate and the toxicity of degradation products can be ignored in non-degradable devices. In contrast to non-degradable channels, degradable channels are

often accompanied by complex designs, since the degradation rate should be manipulable for a timely and controllable degradation. The materials should be digestable by existing enzymes simultaneous to nerve regeneration. Natural materials, from which the majority of the degradable designs consist of, might cause problems in uniformity and controlled fabrication. Further, limited purification might induce a rejection reaction. A non-negligible factor is the potential toxicity of degradation products. Compared to synthetic materials, natural materials are often more cell adhesive, which facilitate combinatorial treatment with cell transplantation. The scope of synthetic materials, however, can be maximized by modification of specific characteristics including e.g. surface modification or the possibility to act as a drug or gene delivery vehicle. [64, 69]

1.4.2 Materials of different nerve guidance channels

Examples of common degradable and non-degradable materials used for nerve guidance channels in the model of spinal cord injury are given in Table 1.2.

Table 1.2: **Common degradable and nondegradable materials used for nerve guidance channels**

Degradable materials	Non-degradable materials
Collagen	Polymethylmethacrylate (PMMA)
Chitosan	Poly(2-hydroxyethyl methacrylate) (PHEMA)
Fibronectin	poly(2-hydroxy- ethyl methacrylate-co-methyl methacrylate) (PHEMA-MMA)
Alginate	Poly[N-(2-hydroxypropyl)methacrylamide] (PHPMA)
Agarose	Poly(acrylonitrile-co-vinylchloride) (PAN/PVC)
Hyaluronic acid (HA)	Carbon filaments
Poly(glycolic acid) (PGA)	Silica
Poly(lactic acid) (PLA)	
Poly-β-hydroxybutyrate.	
Polycarbonate	
Polyethylene glycol (PEG)	

1.4.3 The mechanical Microconnector System (mMS)

Previously, Brazda *et al.* described a novel implantable microconnector system (mMS), which was developed for the purpose to re-connect the separated stumps of the severely injured rat spinal cord [66]. On the one hand the mMS leads to stabilization of the damaged spinal cord tissue. On the other hand, the mMS has several additional advantages: minimal distance to overcome by regenerating axons due to adaptation of the tissue stumps, the

possibility of infusing pharmacological substances directly into the lesion center, and the adjustable design of the connector system (size, material, etc.) [66]. Detailed information of structure and mechanics are given by Brazda *et al.* [66] and in Fig. 3.1.

1.5 Stem cell transplantation as a promising therapeutic strategy

Cell transplantation has been one of the most widely investigated strategies in the field of SCI. Especially, the transplantation of stem cells has arisen in recent years. Numerous experimental studies have indicated beneficial effects of different stem cell types on both, functional recovery and axonal regeneration [70, 71, 72].

In simple terms, a stem cell is defined by its ability of self-renewal and its potential to differentiate into specialized cell types [73]. Stem cells can be described and distinguished by their source. In general, stem cells can be considered as embryonic and postembryonic stem cells depending on their differentiation potential.

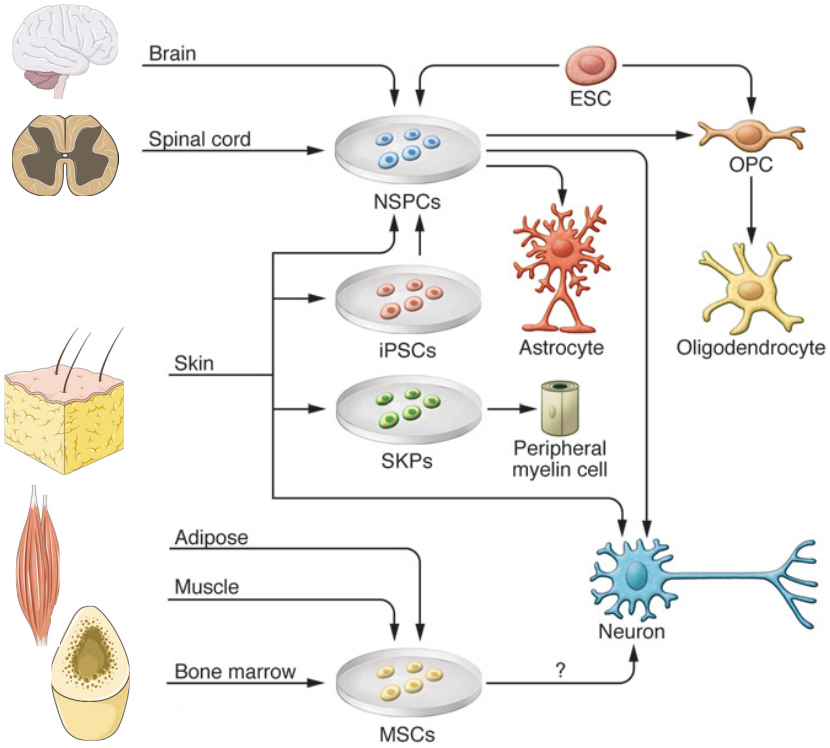

Figure 1.5: **Different sources of stem cells for transplantation into the injured spinal cord**
Stem cells from different sources can be transplanted into the injured spinal cord. This illustration gives an overview of the different origins with main focus on postembryonic stem cells. These cells can be propagated in cell culture and pre-differentiated before transplantation. Neural stem cells and progenitors (NSC/NSPC) can be isolated from the fetal and adult spinal cord and brain and differentiated into both neuronal (neuron) and glial cells (i.e. oligodendrocyte and astrocyte). Skin-derived precursors (SKP) have the potential to be used for autologous transplantation with the possibility to differentiate into peripheral neurons and Schwann cells. Reprogramming methods can be used to generate induced pluripotent stem cells (iPSC). Mesenchymal stem cells can be harvested from different tissues, such as muscle and bone marrow, and they have the potential for differentiation into neural lineages in vitro. ESC = embryonic stem cell(s), OPC = oligodendrocyte progenitor cell(s), MSC = Mesenchymal stem cell(s). [Modified from Mothe *et al.* [74] with medical illustrations from "http://smart.servier.com".]

1.5.1 Embryonic stem cells

Embryonic stem cells (ESC) are derived from the inner cell mass of a blastocyst and can differentiate into nearly all cell types due to their pluripotency. Under defined conditions, ESC can be cultured on a large-scale, which allows expanding to a clinically sufficient number. These features make the transplantation of ESC a promising approach in the field of SCI. Unfortunately, ESC have a predisposition to form teratomas or other tumors, necessitating pre-differentiation prior to grafting [74]. The first human ESC trial of transplantation with the object to reproduce promising preclinical data was approved by the US Food and Drug Administration (FDA) in 2009 [74].

Besides these prospects, the use of ESC presents a serious ethical dilemma, because isolating the embryo blast or inner cell mass results in destruction and death of the blastocyst. Furthermore, ESC occasionally show poor survival post transplantation [75].

1.5.2 Postembryonic stem cells

Postembryonic stem cells can be further classified as adult or rather somatic stem cells and induced pluripotent stem cells (iPSC). On the one hand they can be harvested from a fetus, on the other hand they are found in mature tissues of different organs such as bone marrow, muscle, skin, spinal cord, brain, and others [74]. Related to their tissue specificity, somatic stem cells comprise, among others, the following stem cell types. The different stem cell types will shortly be summarized in the section below, particularly with regard to therapeutic application in SCI: hematopoietic stem cells (HSC), neuronal and their progenitor stem cells (NSC/NSPC) and mesenchymal stem cells (MSC).

Unlike stem cells of embryonic or fetal origin, using adult stem cells avoids ethical and moral problems as well as teratogenic and oncogenic risks [70].

Hematopoietic stem cells (HSC)

HSC are the multipotent stem cells of the blood system with the ability of self-renewal. HSC express the hematopoietic progenitor cell antigen CD34. They can rise to both the myeloid and lymphoid blood lineages; HSC not only have the differential potential for hematopoietic lineages of cells but they can further differentiate to nonhematopoietic linegages of cells, such as neural lineage cells [76, 77, 78]. Additionally to the bone marrow, HSC can isolated either from the peripheral blood after mobilization or from human umbilical cord blood. The transplantation of HSC is widely known and well established for the treatment of hematopoietic diseases such as leukemia. They also seem to have therapeutic benefits after SCI [79].

Mesenchymal stem cells (MSC)

MSC were originally found in bone marrow and described as “marrow stromal cells” [80]. Additionally to bone marrow, they could be identified in many other tissues, such as adipose tissue, umbilical cord, and other tissues. Several studies reported beneficial effects

of MSC in the model of SCI [81, 82, 83]. These studies suggest the potential of MSC to promote axonal regeneration and to enhance tissue sparing due to neuroprotection, whereby the precise mechanisms are not fully understood. Based on the experimental success, clinical trials have been performed and are still ongoing to determine the safety, feasibility, and therapeutic outcome of BM-MSC [84, 85].

Neural stem cells and their progenitors (NSC/NSPC)

NSC and NSPC seem to be the most promising cells for stem cell therapy for SCI, as they can easily give rise to mature neurons, astrocytes, and oligendendrocytes [86, 87]. It is necessary for the implanted stem cells to be compatible with the endogenous spinal cord cells. Therefore, NSC were the obvious first choice [88]. Indeed, many studies reported improved functional outcome after the transplantation of NSC/NSPC into injured spinal cord [71]. A registry of government and privately supported clinical trials from all countries is available (http://www.clinicaltrials.gov) [74]. The tumorigenicity should be considered, since one patient developed several neuroblastoma derived from the graft [89]. Further studies will be necessary to determine and enhance safety of these therapies.

Induced pluripotent stem cells (iPSC)

IPSC have to be treated separately in the group of postembryonic stem cells. They are generated by reprogramming mature, fully differentiated cells into a pluripotent state [74]. IPSC are easily available, as they can be produced directly from the SCI patient, e.g. by reprogramming skin cells, differentiating, and transplantation back to the same patient. Therefore, autologous transplantation is possible [74].

1.5.3 Potential of different stem cells in (pre-)clinical studies

The potential to generate various cell types created great interest in pre-clinical and clinical investigations. Promising results of stem cell therapy have been obtained in experimental models of SCI. A variety of stem cell types have been examined as therapeutic strategies for SCI including further characterization, isolation, and *in vitro* differentiation [74]. Stem cell transplantation after SCI has several aims: (1) facilitation of regenerating axons to cross any barriers, cysts or cavities, (2) functional replacement of lost cells, and (3) creation of a supportive environment for axon regeneration involving neuroprotection [79]. Beneficial effects of stem cell therapy are basically multifactorial and often difficult to attribute to one single mechanism [71]. Importantly, timing of transplantation such as acute, subacute, or chronic, the host microenvironment, as well as the phenotype and purity of the transplanted cells crucially influence the efficacy of cell replacement [90].

1.5.4 Umbilical cord blood as productive stem cell source

Isolation of HSC from human umbilical cord blood (CB) is a widespread method and accepted alternative to bone marrow and peripheral blood mobilization in the therapy of hematological malignancies. Not only HSC can be isolated from umbilical cord blood, but also MSC and MSC-like cells.

USSC characteristics and comparison to MSC

In 2004, Kögler and colleagues detected an additional stem cell type in the cord blood with an even broader differentiation potential than CB-MSC, named unrestricted somatic stem cells (USSC) [91]. USSC and CB-MSC have several properties in common such as their osteogenic and chondrogenic *in vitro* and *in vivo* differentiation potential. In contrast to CB-MSC, USSC are characterized by their lack of adipogenic differentiation potential [92]. It has been demonstrated that USSC express DLK-1/PREF-1 (delta-like-1/preadipocyte factor-1) which seem to be responsible for the lack of adipogenic differentiation potential of USSC [93]. In addition, CB-MSC and USSC clearly vary in their immunological behavior [94, 95]. USSC differ from CB-MSC by a HOX-negative expression profile [96].

According to their distinct properties, USSC possess longer telomeres associated with a higher proliferative potential. Thus, USSC are regarded as being of a biologically younger state [93]. Interestingly, USSC showed no tumorigenic potential as revealed in a 16 months study in which xenograft tumorigenicity was tested in immunodeficient mice [97].

An absolute advantage of umbilical cord blood cells and especially of USSC is the simple extraction. USSC can be purified in a GMP (good manufacturing practice) -grade status and can be easily expanded in a clinical scale without any ethical concerns; an invasive intervention is not necessary [97, 98].

Under specific medium incubations *in vitro,* USSC can differentiate into neuronal-like cells [99, 100]. Up to now, an *in vitro* differentiation to functional neurons failed after XXL-induction, co-cultivation with primary neural cell cultures and organotypic slices, although the microRNA profile indicated a differentiation into immature neural cells [100, 101]. Further characteristics of USSC include high expression of various interleukins (e.g. IL-1ß, IL-6) and growth factors like stromal cell-derived factor-1 (SDF-1), hepatocyte growth factor (HGF), and vascular endothelial growth factor (VEGF) [102, 101]. A detailed phenotypic characterization of USSC and their cytokine production was described by Kögler *et al.* in 2005 [102] and the comparison to CB-MSC in 2006 [103].

Transplantation of USSC in the injured spinal cord

USSC are a promising human stem cell source for clinical application in SCI. In previous studies, Schira *et al.* provided evidence that transplantation of USSC significantly improved the axonal regeneration and functional recovery in an acute model of SCI in rats [98, 101]. They revealed that grafting of USSC into the vicinity of a dorsal hemisection injury at thoracic level Th 8 resulted in HGF-directed migration and accumulation within the lesion area. In addition, USSC transplantation reduced the lesion size. The beneficial effects were accomplished without neural differentiation or long-lasting persistence of the grafted USSC [101, 98]. Paracrine mechanisms as well as cell-cell interaction might be responsible for the regenerative effects.

In the present study, the transplantation of USSC has been combined, for the first time, with the implantation of the mMS.

1.6 The complete transection - the "gold standard" to demonstrate axonal regeneration

A great number of experimental animal models of SCI have been developed in recent years. They not only differ in the injury mechanism, but also in the species of the experimental animals, mainly including rats, mice, dogs, rabbits, and pigs [104]. Rats and mice are the most common SCI models, both because of cost and accessibility, easy to care for, and because of the existence of well-established functional analysis techniques [105, 9]. On the basis of these animal models, an enhanced knowledge of the pathophysiology and secondary mechanism of SCI could be acquired, which contributed to a better understanding of novel therapeutic strategies. Experimental SCI models should preferably fulfill specific conditions: They should reflect and simulate aspects of clinical SCI; they should be reliable, controlled, and reproducible [104, 106]. Depending on the aspects to be investigated, different experimental models are used. Complete or incomplete transection, as well as contusion and compression models are commonly used. Less common models include hypoxia and ischemia models [105, 107].

To evaluate the effectiveness of therapeutic interventions to promote axonal regeneration and functional recovery, transection models are more appropriate than contusion models [108], although most human SCI are quite different from the transection models. Most humans suffer an acute trauma which corresponds most closely to a 'dura-intact' compression and/or contusion injury model [107, 109]. Nevertheless, the model of complete SCI is often seen as the "gold standard" to demonstrate axonal regeneration [110], since complete transection enables unambiguous distinction between regenerated and spared axons, always provided that the transection was done properly [111, 110]. If the chosen therapeutic strategy requires implantation of a scaffolding biomaterial, complete transection of the spinal cord will be essential to accommodate the device [112]. Complete transection models represent a good way for initial evaluation of tissue engineering strategies, particularly of those targeting axon regeneration [112]. Complete spinal cord injury should not only be considered suitable for an acute SCI model, but also for chronic SCI models, since neurosurgeons could imagine resection of scar tissue leaving a large tissue gap comparable to a transection model [60].

For the present study, a complete transection model was used to enable the implantation of the mechanical Microconnector System (mMS) to investigate axonal regeneration.

2 Aim of This Thesis

Spinal cord injury (SCI) is still a devastating condition. The electrophysiological signal transduction is interrupted resulting in a range of deficits due to damage of the spinal pathways. The permanent loss of motor and sensory function frequently leads to lifelong physical dependence for the affected patient. Research has remarkably increased the knowledge of SCI in recent years. Numerous treatment strategies were developed on the basis of detailed findings of mechanisms and pathophysiology involved in injury- and recovery-related processes [113]. Despite major achievements in experimental, preclinical, and even in clinical conditions, there is currently no effective treatment available for SCI. As already outlined above, the pathophysiology of SCI is multifactorial and multiphasic. The overall aim of SCI research to enhance locomotor function will require a combination of different strategies. Therefore, I have combined the following two therapeutic approaches: grafting of stem cells and implantation of a microconnector device.
On the one hand numerous pre-clinical studies have indicated that transplantation of different stem cell types have beneficial effects on regeneration after SCI. Schira *et al.* provided evidence that the transplantation of unrestricted somatic stem cells (USSC) significantly improves axonal regeneration and functional recovery in a rat model of hemisection [98].
On the other hand, the mechanical Microconnector System (mMS) was developed for the purpose to re-adapt separated spinal cord stumps of completely transected rat spinal cords in a sub millimeter range [66]. In long-term studies, Estrada et *al.* showed beneficial effects on stabilization, cellular invasion, and axonal regeneration resulting in improved functional outcome.

The aim of this thesis was to combine these independently effective approaches to further enhance the individual effects. In particular, the investigative approach intended to answer

1. whether USSC reveal migratory potential and survival in the lesion or respectively in the lumen of the mMS after transplantation into completely transected spinal cords
2. whether USSC transplantation leads to enhanced axonal regeneration and subsequently improved functional recovery in complete SCI
3. whether the combination further enhances regenerative axon growth and prevents tissue loss, and
4. whether the combination results in motor improvement that is superior to the individual treatments.

3 Materials and Methods

3.1 Buffers, solutions, and antibodies

Buffers and solutions

Table 3.1: **Buffers and solutions overview**

Buffers and solutions	Composition / Manufacturer
PB (phosphate buffer) 0.2 M, pH 7.4	28.8 g Na_2HPO4 (Merck) 5.2 g NaHPO4 (Merck) ad 1000 ml aqua bidest
PBS (phosphate buffered saline) 0.1 M, pH 7.4	50 ml 0.2 M PB 9 mg NaCl ad 1000 ml aqua bidest
NGS (normal goat serum), 10 %	500 µl ad 5 ml PBS
DS (donkey serum), 5 %	500 µl DS (Sigma) ad 10 ml PBS
Sucrose for cryoprotection 30 %	30 g sucrose ad 100 ml PBS
Triton X-100	0.3 % 30 µl Triton X-100 (Sigma) ad 10 ml PBS
PFA (paraformaldehyde) 4 %, pH 7.4	40 g PFA powder (Merck) ad 1000 ml 0.1 M PB pH titration with 5 M NaOH
Gelatine, 10 %, for tissue embedding	10 g DifcoTM gelatine (BD) ad 100 ml 0.1 M PB 60 °C for dissolving, 37 °C for embedding
Paraffin for tissue embedding	100 g paraffin (Merck) 5 g wax (Cera Alba, Caelo) 56 °C
Fluoromount G for tissue mounting	Southern Biotech
Immu-Mount for tissue mounting	Thermo Scientific

Primary Antibodies

Table 3.2: **Primary antibodies**

Antibody	Class	Antigen	Dilution	Manufacturer
GFAP	ms IgG	glial fibrillary acidic protein	1:500	Chemicon
GFAP	rb IgG	glial fibrillary acidic protein	1:1000	Dako
TH	rb IgG	tyrosine hydroxylase	1:750	Abcam
5HT	rb IgG	5-hydroxytryptamine, Serotonin	1:40	Biologo
CGRP	gt IgG	Calcitonin gene-related peptide	1:1500	Serotec
PAM	ms IgG	phosphorylated neurofilament	1:1000	Covance
vWF	rb IgG	von Willebrand factor (factor VIII-related antigen)	1:1000	Dako
ED1	ms IgG	ED1 phagocytizing macrophages and microglia	1:1000	Serotec
hNuc	ms IgG	human nuclei	1:500	Millipore
NF	rb IgG	Neurofilament (recognizing NEF-L, NEF-M and NEF-H)	1:1300	Biotrend
P0	ck IgG	Myelin protein zero	1:100	Abcam
S100	rb IgG	S100 calcium binding protein	1:1000	Sigma Aldrich
CTB	gt IgG	Cholera Toxin beta Subunit	1:80000	List Biological Laboratories

Secondary antibodies

Table 3.3: **Secondary antibodies**

Antibody	Class	Dilution	Manufacturer
Alexa Fluor® 488 anti-mouse	dk IgG	1:500	Molecular Probes
Alexa Fluor® 594 anti-mouse	rb IgG	1:30	Molecular Probes
Alexa Fluor® 647 anti-mouse	dk IgG	1:500	Molecular Probes
Alexa Fluor® 488 anti-rabbit	dk IgG	1:500	Molecular Probes
Alexa Fluor® 594 anti-rabbit	dk IgG	1:500	Molecular Probes
Alexa Fluor® 488 anti-goat	dk IgG	1:500	Molecular Probes
Alexa Fluor® 488 anti-chicken	dk IgG	1:500	Molecular Probes
Oregon Green® 488		1:1000	Molecular Probes

Tracer substances and reagents

Table 3.4: **Tracer substances and reagents**

Substance	Dilution	Manufacturer
DAPI (4,6'-Diamino-2-phenylindole)	1:10.000	Roche Diagnostics
Sudan Black	0.3%	Fluka
Biotinylated Dextran Amine (BDA) MW 10 000	10%	Molecular Probes
Cholera Toxin B Subunit (CTB)	1%	List Biological Laboratories

3.2 Therapeutic components used in these studies

3.2.1 The mechanical Microconnector System - design, structure, and mechanics

The mMS consists of two elliptical discs with a thickness of 350 µm and outer diameters of 1.7 mm and 2.7 mm (corresponding to the oval cross section of the thoracic rat spinal cord)

constituting the delimiting sidewalls of a microchamber with a surface of 3.6 mm². The distance between the two discs is 300 µm adding up to a total thickness of the assembled mMS of 1000 µm [66]. As shown in Fig. 3.1 A, the mMS possesses a honeycomb structure consisting of about 55 honeycombs with an inner diameter of 265 µm each. This structure provides high mechanical stability with as little material as possible. The rough surface allows the adherence of the spinal cord stumps to the wall is possible and the retraction of the stumps after removal of the vacuum pump is prevented. The mMS can be placed between the two stumps of the severed spinal cord (Fig. 3.1 B) before a vacuum can be applied to re-connect the transected stumps in a submilimeter range. The required force was calculated and tested by *in vitro* and *in vivo* experiments. The internal channel system allows pharmacological drug application with a homogenous distribution within the mMS chamber (Fig. 3.1 C).

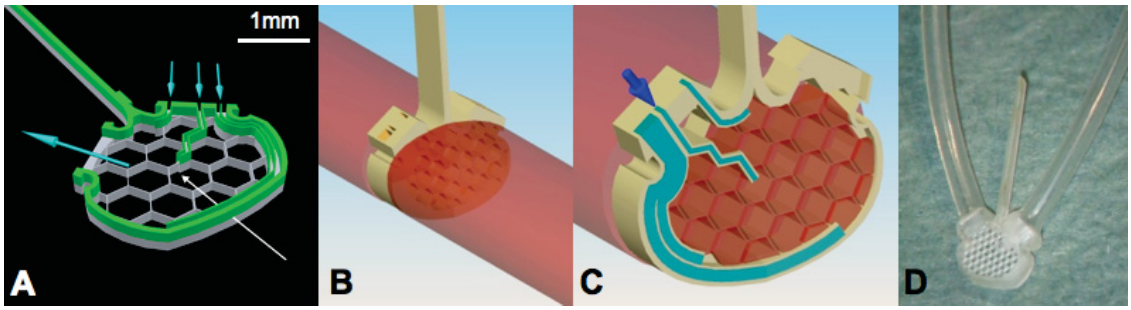

Figure 3.1: **The mechanical Microconnector System - general design and operation principle**
(A - C) Schematic drawing: (A) The general design with honeycomb structure, (B) Implantation of the mMS into the spinal cord lesion, (C) Distribution of pharmacological drugs within the mMS lumen via internal micro-channels. Infusion is depicted by blue arrow. (D) Photographic picture of the mMS and the tubes for the vacuum pump and for different infusions. [Modified from Brazda *et al.* 2013 [66].]

3.2.2 Unrestricted Somatic Stem Cells - Cell Culture

The following procedures were performed by working group members. They are no independent work. They are listed for the sake of completeness. A vote (# 4746) of the ethical commission of the Medical Faculty was granted for the use of human cord blood-derived unrestricted somatic stem cells (USSC) in spinal cord transplantation in rat.

Isolation, Expansion, and Characterization of USSC

The USSC population was provided by the group of Professor Gesine Kögler from the Institute for Transplantation Diagnostics and Cell Therapeutics, Heinrich Heine University Medical Center Düsseldorf. Initially, USSC were generated from 94 cord blood sample and isolated as previously described [91]. To obtain the mononuclear cell fraction, a standard Ficoll-gradient separation was used followed by ammonium chloride lysis of red blood cells. Subsequently, the cells were washed and plated in culture flasks to grow in the presence of dexamethasone. Adherent cell colonies were selected for expansion. Therefore, USSC were incubated in DMEM (Lonza) containing 30 % heat-inactivated fetal bovine serum (FBS, Lonza), 2 mM glutamine (Gibco) and penicillin/streptomycin (100 U / ml, Gibco).

Cells were incubated at 37 °C in 5 % CO_2 in a humidified atmosphere. USSC of passages 6 to 8 were used.

Freezing and storage of USSC

Once the USSC reached 80 % confluency, they were detached from culture flasks using trypsin / EDTA (1x, 0.05 %; Gibco) for 3 min at 37 °C. To stop the trypsin reaction DMEM / 10 % FBS were added and cells were centrifuged for 5 min at 1200 rpm. Subsequently USSC were resuspended in culture medium, which was gently mixed 1:1 with freezing medium containing DMEM / 40 % FBS and 20 % DMSO (Sigma). Immediately, cells were frozen at -20 °C for 30 min and afterwards at -80 °C over night. Ultimately, tubes were transferred into liquid nitrogen and stored until thawing and usage.

3.3 Experimental animals and surgical procedure

3.3.1 Animals

Adult female Wistar rats weighing 260 - 300 g were used. During the experiments, animals were housed in groups of 3 - 4 rats per cage under standard conditions with a 12 h light/ 12 h dark cycle. Germ-free water and pelletized dry-food were available *ad libitum*.

Institutional guidelines for animal safety and comfort were adhered to, and all surgical interventions and pre- and post-surgical animal care were provided in compliance with the German Animal Protection law (State Office, Environmental and Consumer Protection of North Rhine-Westphalia, LANUV NRW: AZ 87-51.04.2011.A023, AZ 8.87-50.10.34.08.315, and AZ 84-02.04.2014.A195). The license to perform animal experiments was granted by PD Dr. med. vet. Martin Sager in May 2011.

The Table 3.5 provides an overview of the experimental animal groups.

Table 3.5: **Experimental animal groups**

Treatment	Survival time	Animals / group
TX + USSC	7 days	n = 6
TX + USSC	3 days	n = 4
mMS + USSC	3 days	n = 5
TX + DMEM	16 wpo	n = 15
TX + USSC	16 wpo	n = 15
mMS + DMEM	16 wpo	n = 15
mMS + USSC	16 wpo	n = 15

TX = complete transection, mMS = mechanical Microconnector System, USSC = unrestricted somatic stem cell, DMEM = Dulbecco's modified Eagle medium, wpo = weeks post operation, n = number

3.3.2 Spinal cord preparation of the and complete spinal cord transection

During all surgical procedures, animals were placed on a heating pad at 37 °C to maintain body temperature.

Adult female Wistar rats were anesthetized with isoflurane (Forene, Abbott, Germany; 2-3 % in O_2 and N_2O at a ratio of 1:2) and with bolus injection of Caprofen (s.c. 5 mg/kg, Rimadyl ®). To control the narcosis, the absence of reflexes was observed. To prevent the animals' eyes from dehydrating they were covered with Bepanthen ® ophthalmic ointment (Roche, Basel, CH). All instruments were disinfected with 70 % ethanol before usage. After shaving and disinfection of the animals' backs with Incidur (Ecolab), a midline incision was made along the thoracic vertebrae (Th6 - Th10) and the skin was opened to expose the underlying paravertebral muscles. Adipose tissue between the blade bones was carefully removed from the muscles. Using a small muscles clamp (Fine Science Tools, Burlington, USA), the muscles above the thoracic vertebrae were retracted. Henceforth, all surgical steps were done under microscopic control (stereotactic microscope; Stemi DV4 Spot, Carl Zeiss). Following laminectomy at thoracic level Th8/9, the spines and vertebral arches were removed using a Friedman-Pearsons micro-rongeur (FST 16020-14). The spinous processes of Th7 and Th10 were clamped and stabilized using a stereotactic device (Small Animal Adaptor, David Kopf Instruments) to allow a controlled operation procedure. Care was taken not to damage any blood vessels, especially the lateral spinal arteries. After elevating the *dura mater* with fine forceps, it was opened with a transverse 5 mm cut using fine eye scissors. While retaining the lateral cut end of the opened *dura mater*, a spinal cord hook (Fine Science Tool) was carefully inserted into the *subarachnoidic* space between *dura mater* and *arachnoidea* without damaging the meninges. To avoid damage of the meninges, care had to be taken that the forceps or spinal cord hook were not pricking into the *pia* or *dura mater*. The hook was slowly rotated to place around the spinal cord and then the spinal cord was slightly lifted upwards for approximately 1-2 mm and separated from the *dura mater* to see a gap at the ventral side between spinal cord tissue and *dura mater*. The complete spinal cord transection was made with the aid of fine eye scissors, which resulted in the retraction of the transected cord leaving a small gap between the two segments. To ensure complete transection, two small spatulas were used to gently pull the segments apart. This complete transection leads to a highly reproducible lesion. For further information see [66] and [114].

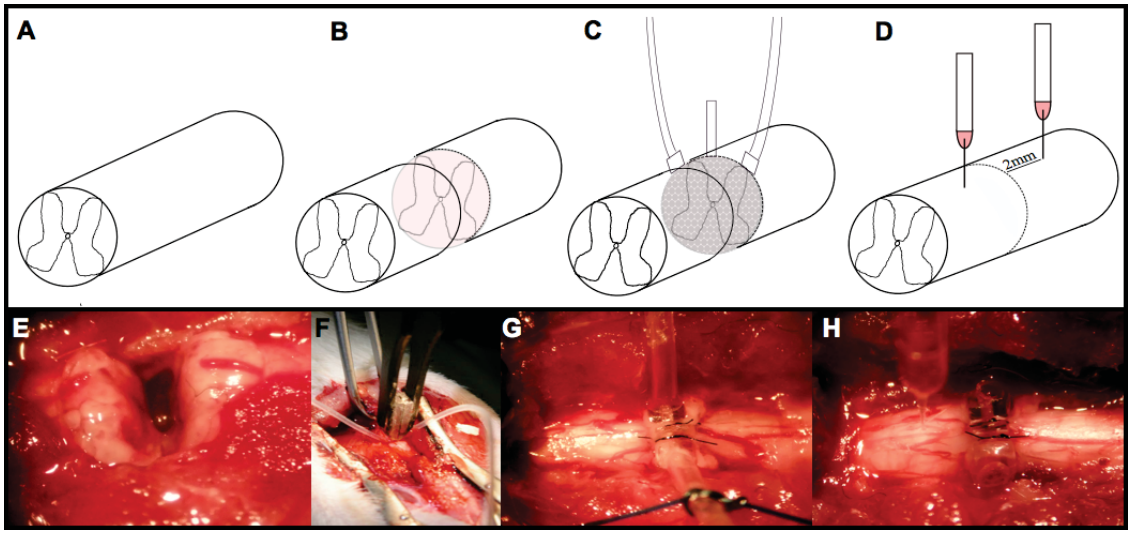

Figure 3.2: **Complete spinal cord transection, implantation of the mMS, and stem cell transplantation - Surgical procedure**
(A - D) Schematic drawings: (A) A spinal cord segment with grey matter and the central canal, (B) Spinal cord segments after complete transection, (C) The implantation of the mMS into the spinal cord lesion, (D) The injections of stem cells / DMEM (Medium) 2 mm rostral and caudal to the lesion. (E - H) Photographic images through a surgical microscope (except for F): (E) A gap following complete spinal cord transection at thoracic level Th 8 / 9, (F) The mMs implantation using stabilization forceps, (G) suturing of the *dura mater* above the mMS, and (H) USSC grafting performed with a glass capillary 2 mm rostral and 2 mm caudal to the mMS.

3.3.3 Implantation of the mechanical Microconnector System

For implantation, the mMS was held by the stabilization forceps of a custom made holding device (Fig. 3.2 F) and lowered into the spinal cord tissue gap with the two tubes positioned to the lateral sides of the vertebrae [66]. To ensure stabilization of the mMS, the tubes were temporarily sutured to the muscles using nonresorbable 4-0 threads (Ethicon ®, vicryl) at the side of the vertebrae (Fig. 3.2 G). After opening and removing of the holding device the mMS connector pin was removed by cutting with a pair of fine scissors. The *dura mater* was sutured with 9.0 threads (Ethicon ®) above the mMS (Fig. 3.2 G). One of the tubes was sealed by clamping, the other one was attached to the vacuum pump. The separated stumps were sucked into the mMS lumen by a gentle negative pressure which was applied for 10 min and monitored by sensors; the required pressures were documented in the operative report (335 - 365 mbar). Both tubes were cut close to the mMS and removed. The detailed surgical procedure is shown in Fig 3.2.

3.3.4 USSC grafting into the spinal cord

Immediately after implantation of the mMS, USSC grafting was performed with a glass capillary 2 mm rostral and 2 mm caudal to the lesion site/mMS at 1.3 mm, 1.0 mm, 0.7 mm, and 0.4 mm depth as previously described [98] (Fig. 3.2 D & H). The glass capillary (Deiberit 502; Dr. Böhme & Schöps Dental) was attached to a 10 µl syringe (701LT; Hamilton). Two µl containing a suspension of 100000 cells in DMEM were injected slowly within 4 min at each injection site. Beginning one day prior to surgery and daily thereafter

for three weeks postoperation, all experimental animal groups were immunosuppressed with cyclosporine A (15 mg/kg s.c., Sandimmun ®, Novartis)

3.3.5 Surgical procedure for migration analysis

To further characterize the migration potential of USSC in a complete spinal cord transection model and after mMS implantation, short term *in vivo* experiments were performed. Adult rats received a highly reproducible complete transection at thoracic level Th 8/9 as described above. Immediately after transection or mMS implantation, 2 x 10^5(2 x 2 µl) USSC were transplanted at a distance of 2 mm rostral and 2 mm caudal to the lesion site or the mMS device. To prevent reflow, the transplantation was performed with a glass capillary at 1.3 mm, 1.0 mm, 0.7 mm, and 0.4 mm depth and the USSC were slowly injected within 4 min at each injection site. All rats were immunosuppressed with cyclosporine A to reduce rejection reaction.

3.3.6 Post-operative care

Immediately after USSC/DMEM grafting, the muscles and skin were sutured layer by layer with resorbable threads (Ethicon ®, vicryl 4-0). The animals received a subcutaneous injection of 2 x 2.5 ml NaCl (0.9 %) at 36 °C for rehydration after surgery. The animals were observed until full consciousness was regained. Post-operative care included prophylactic daily oral antibiotics (Baytril ®, Bayer Health Care) administration for one week. Daily manual bladder emptying was performed when necessary (two times per day). The animals were routinely inspected for any signs of infection, dehydration, or injuries with appropriate veterinary assistance as needed.

3.3.7 Anterograde axonal tracing of corticospinal tract

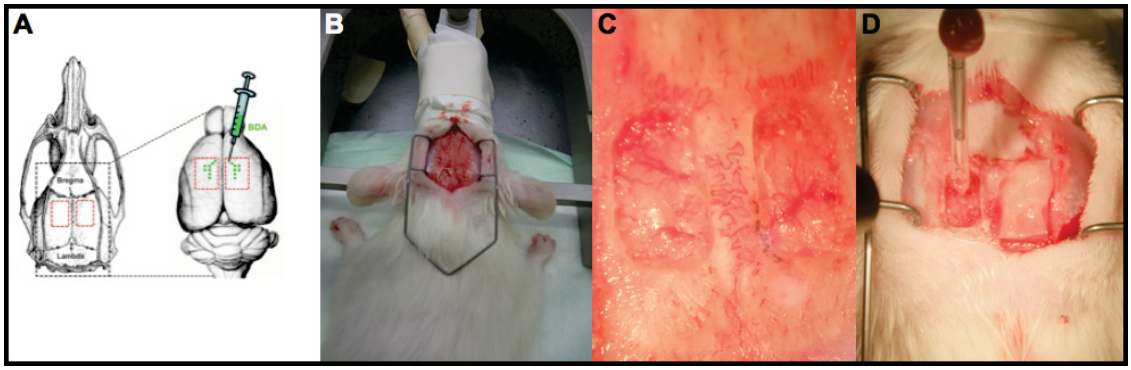

Figure 3.3: **Axonal tracing of the corticospinal tract**
(A) Schematic illustration of injections of biotinylated dextran amine (BDA) into the sensorimotor cortex of the rat; the rat skull with the stereotaxic reference points bregma and lambda. Red rectangles represent the area of craniotomy, the green points illustrate the injection sites. [[115], modified by Brigitte Koeni.] (B - D) Photographic pictures: (B) The animal's head was fixed in the small animal adaptor at both external acoustic meati. The skin was shaved and the cranium was exposed. (C) The craniotomy was done along the sagittal and coronal suture by using a drill. (D) A glass capillary was used to performe the BDA labeling. Eight injections were performed stereotactically into the sensorimotor cortex of each hemisphere.

According to a previously published protocol [30] the anterograde tracing was performed in anesthetized animals three weeks prior to sacrifice. The head of the animal was fixed in a small animal adaptor at both external acoustic meati and at the front teeth (See Fig. 3.3 B). After shaving and skin incision, the cranium was exposed and the periosteum was removed (see Fig. 3.3 B). Craniotomy was done along the sagittal and coronal suture using a drill (ø 1.4 mm, Fine Science Tools), (see Fig. 3.3 C). Subsequently, the tracing was performed by injection of multiple small volumes (0.2 µl each) of biotinylated dextran amine (BDA; 10 %; Molecular Probes) into the brain. For injection, a glass capillary (40 - 60 µm in diameter) was fixed with sealing wax onto a Hamilton microliter-syringe (10 µl). Eight injections at a depth of 1.2 mm were made stereotactically (Kopf sterotactic frame) into the sensorimotor cortex of each hemisphere for tracing of the CST (see Fig. 3.3 D). The coordinates (in regard to Bregma) for injection into layer V of the sensorimotoric cortex are shown in Tab 3.6 and Fig. 3.3. The coordinates were determined with the aid of Paxinos' and Watson's Stereotaxic Atlas of the Rat Brain (1982) and have been established by Susanne Hermanns in modification of a lab protocol of Dr. Rag Grill, University of Texas, Houston [30]. To avoid leakage of BDA at the injection points, the syringe was removed with a 2 minute delay. After this tracing, the skin was stitched using metal clips (Michel).

Table 3.6: **Coordinates for BDA injections into the layer V of the rat brain in regard to Bregma**

Bregma A/P	left L	left L	right L	right L
- 0.08	+ 0.20		- 0.20	
- 0.13	+ 0.22		- 0.22	
- 0.18	+ 0.24	+ 0.29	- 0.24	- 0.29
- 0.23	+ 0.24	+ 0.29	- 0.24	- 0.29
- 0.28	+ 0.24		- 0.24	
- 0.33	+ 0.24		- 0.24	

A/P: anterior/posterior, L: lateral

3.3.8 Anterograde labeling of axons in the thoracic spinal cord

For labeling of regenerating fibers extending into the lesion site, anterograde intraspinal axon tracing was performed rostral to the lesion at Th 7 one week prior to sacrifice. Animals were re-anesthetized with isoflurane and the thoracic area was re-opened analogous to the first surgery. Using a glass capillary attached to a Hamilton microliter-syringe (10 µl), biotinylated dextran amine (BDA, 10 %, MW, 10.000, Molecular Probes) was injected into the spinal cord 3 mm rostrally to the lesion / mMS site as shown in Fig 3.4. Injections of BDA were applied (0.1 µl each): at the midline at the depths of 1.5 mm (ventral *funiculus*), 0.8 mm (dorsal CST), and 0.5 mm (cuneate and gracile *funiculi*) from the *pia mater*; at 1 mm laterally from the midline on each side at the depths of 1.2 mm, 0.8 mm, and 0.4 mm (lateral *funiculi*) from the *pia mater*.

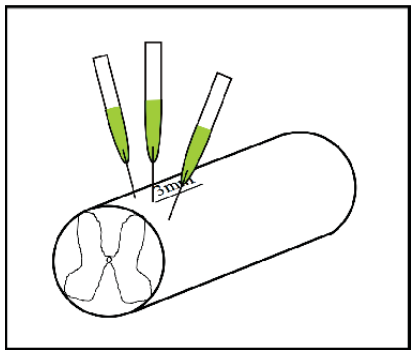

Figure 3.4: **Axonal tracing rostral to the lesion site**
Axons were labeled with biotinylated dextran amine (BDA) through tracer injections into the spinal cord 3 mm cranial to the lesion site.

3.3.9 Anterograde labeling of ascending sensory axons

Five days prior to sacrifice, the sensory sciatic afferents were anterogradely labeled with 1 % cholera toxin beta (CTB, List Biological Laboratories). Four Animals of each group were re-anesthetized and both thighs were shaved and disinfected. Using a scalpel (Nr. 20; Bayha, Tuttlingen, D) a skin incision was made along the femur. The muscles *biceps femoris* and *gluteus superficialis* were separated and then forced apart by a muscle retractor to expose the sciatic nerve at mid-thigh level (Fig. 3.5 A). In preparation for the following step, a ligature (Vicryl 4-0, Ethicon) was loosely placed proximally to the origin of the tibial and peroneal nerves after the nerve was raised and stabilized by a fine spatula (Fig. 3.5 C). Distal to the ligature, a small incision was made into the epineurium. The tip of a glass capillary attached to a Hamilton microliter-syringe and angled to the nerve, was inserted up to 2 mm deep through the incision (Fig. 3.5 D). 2 µl of 1 % CTB were gently injected over 3 min. To reduce leakage of CTB, the glass needle was left in place for 4 min. Afterwards, the syringe was removed and the suture was immediately tightened around the nerve. Finally, the sciatic nerve was crushed with a fine forceps proximally to the injection site for 10 sec to allow sufficient uptake of CTB. Upper hindlimb muscles and skin were sutured in layers. Anterograde labeling was performed bilaterally following this protocol.

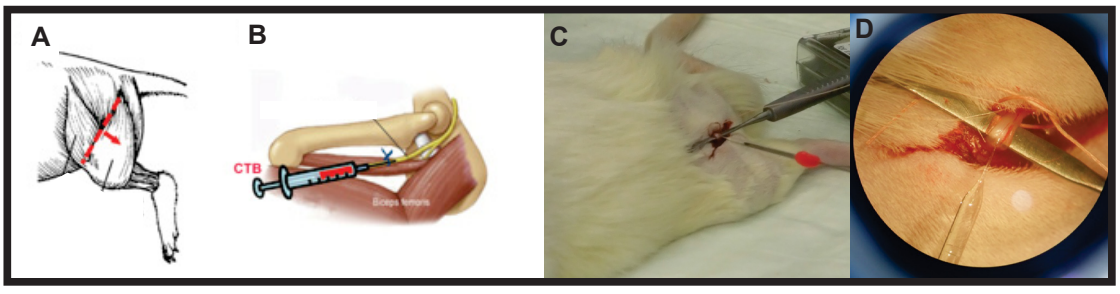

Figure 3.5: **CTB labelling of sciatic afferents**
(A + B) Schematic illustrations of CTB tracing: (A) Separation of the leg muscles to expose the sciatic nerve (modified from http://www2.sluh.org/bioweb/fieldbio/labsheets/ratmuscles2.png), (B) Schematic illustration of CTB injection into the sciatic nerve (modified by Brigitte Koenig from http://origin.ars.els-cdn.com/content/image/1-s2.0-S0165027013000071-gr1.jpg). (C + D) Photographic images of the procedure. (D) Photographic picture of CTB injection in higher magnification. The glas capillary of the Hamilton syringe was angled to the neve and inserted up to 2 mm deep.

3.3.10 Animal sacrifice

Tissue preparation for immunohistochemistry and axon tracing was performed as previously described [51, 28]. In brief, the animals were anesthetized with Narcoren ® (Merial) and transcardially perfused with ice-cold PBS for 2 min and subsequently with 4 % PFA (Merck) for 15 minutes using a perfusion pump (505S, Watson-Marlowe) with a pump rate of 25 ml/min. Spinal cord segments of approximately 6 cm length were dissected and post-fixed in 4 % PFA for 24 h at 4 ℃. Spinal cord pieces containing the lesion area were extracted surgically from the remaining tissue using a fine rongeur, forceps, and a scalpel blade.

3.4 Tissue preparation

Gelatine sections

The isolated spinal cords were pre-incubated in PBS overnight at 4 ℃. The spinal cord pieces were transferred to heated (60 ℃) 10 % gelatine (Difco, BD, Franklin Lakes) and then cooled down to 37 ℃; 0.1 % sodium azide (merck) were added to prevent fungal infestation. The spinal cord pieces were incubated in the gelatine overnight at 37 ℃. Plastic embedding molds (Peel-A-Way® Embedding Molds, Polysciences INC) were filled with a thin layer of gelatin and after gelling the spinal cord segments were parasagittally placed on top of the gelatine layer. Step by step, the molds were gently filled with cooled-down (< 37 ℃) gelatine until the tissue was completely covered. After incubation at room temperature for at least 30 min, the molds were stored for complete gelation for approximately 2 - 3 days at 4 ℃. Following this, gelatine blocks were incubated overnight in 4 % PFA at 4 °C. One day prior to slicing, the molds were cut into shape, transferred to 30 % sucrose and kept at 4 °C overnight. The spinal cord tissues were frozen in Tissue-Tek® compound (Sakura Finetek Europe B.V, Alphen aan den Rijn, NL) on a tissue holder and parasagittally cut into 50 µm thick sections on a freezing microtome (Thermo Scientific Microm HM650V). The sections were collected in 24-well plates pre-filled with PBS solution.

Paraffin sections

For some pilot studies the lesion-containing part of the spinal cord was embedded in paraffin to perform histological examinations. Therefore, the spinal cord pieces were transferred into PBS and incubated overnight at 4 °C. The paraffin embedding procedure was then started by dehydration with ethanol (EtOH):

Dehydration

EtOH 70 %: 30 min

EtOH 90 %: 60 min

EtOH 100 %: 3 x 60 min

methyl benzoate: overnight

On the next day, the spinal cords were transferred to benzene. After 15 min the molds were filled up with paraffin to a 10 % benzene/paraffin mix. After an incubation time of 30 min at 59 °C the benzene/paraffin mix was replaced by pure paraffin for 1 h and incubated at 59 °C. Two additional paraffin changes (incubation time 1 h at 59 °C, each) were made before the spinal cords were finally incubated in pure paraffin over night at 59 °C. On the next day, the spinal cord segments were parasagittally aligned and embedded in molds. After hardening of the paraffin blocks, they were cut parasagittally into 10 µm thick sections on a paraffin-microtome (RM 2035, Jung). The sections were transferred into a ~ 40 °C warm water bath to mount them on HistoBond® slides (Marienfeld) and subsequently dried on a heating plate. Finally, the sections were incubate at 56 °C for 10 hours.

Freezing-microtome Sections

Tissue preparation was performed as mentioned above. Segments containing the lesion area were transferred from PBS into 10 % sucrose at 4 °C for 24 h two to three days prior to sectioning. Specimens were incubated in 30 % sucrose at 4 °C for three to four days until the tissue had completely sunken into the solution. The respective spinal cord pieces were cut on a freezing-microtome (HM 430, Microm) at 50 µm thickness for improved visualization of potentially regenerated axon fibers and for improved stability of the mMS area. Segments, parasagittally oriented, were freeze-mounted onto the microtome cutting area using Tissue-Tek® compound (Sakura). Serial sections of 50 µm thickness were cut (cutting temperature: -28 to -24°C) and collected in 24-well plates (Costar) pre-filled with PBS. Care was taken that the specimens were mounted in diagonal orientation with the dorsal part of the spinal cord pieces facing away from the steel blade.

3.5 Histological staining protocols

Immunohistochemistry (IHC) enables identification of tissue components by the interaction of target antigens with specific antibodies tagged with a visible label [116]. Through IHC it is possible to visualize e.g. the distribution and localization of regenerated axons and specific cell types (for example: Schwann cells, astrocytes, and endothelial cells of blood vessels).

Trichrome staining

Trichrome staining presents an easy and fast way to delineate connective tissue in histological samples and was used to overview the tissue quality. Based on a polychrome protocol described by Bancroft *et al.* [117] the staining was performed using three different solutions (Tab. 3.7). The dyes in solution A stain muscles, fibrin, cytoplasm, and erythrocytes red, whereas fibers like collagen are colored green by solution C. Solution B is essential for the differentiation of the staining.

Table 3.7: **Compounds of Masson's trichrome solutions**

Solution A	Solution B	Solution C
0.5 g Acid Fuchsin 0.5 g Xylidine Ponceau 198 ml aqua bidest. 2 ml acetic acid	1 g Phosphomolybdic acid 200 ml aqua bidest.	2 g Light Green SF yellowish 200 ml aqua bidest. 4 ml acetic acid

First, sections were washed in aqua bidest. Second, the sections were immersed in solution A for 10 min, followed by rinsing with aqua bidest. Third, the sections were immersed in solution B for 5 min and subsequently rinsed in aqua bidest. Then the sections were incubated for 10 min in solution C followed by a last rinsing step in aqua bidest. After this, the sections were mounted on microscope slides and dehydrated with ethanol: 50 %, 70 %, 90 %, 2 x 100 %, 1 min each. Afterwards, the sections were transferred to RotiHistol® (2 x 3 min) and embedded in DPX (Fluka).

3.5.1 Demasking of antigens

The following demasking strategies were used (if necessary):

- Protease XXIV: 0.05 % in TRIS buffer, incubation of sections: 7 min at 37 °C ; PBS: 2 x 5 min

- Citrate buffer: 10 mM citrate buffer concentration, incubation of sections: 8 min microwave (600 W); cooling-down period for 30 min; PBS: 2 x 5 min

- Triton X-100: 0.1 % in PBS, incubation of sections at room temperature (RT): 10 min; PBS: 2 x 5 min

- NaBH4: 1 % in PBS at RT; incubation of sections: 10 min at RT; PBS: 2 x 5 min

3.5.2 Immunofluorescent staining of paraffin sections

Deparaffinization and rehydration: Xylene: 2 x 10 min; EtOH 100 %: 3 x 5 min; EtOH 90 %: 1x 5 min; EtOH 70 %: 1x 5 min; EtOH 50 %: 1 x 5 min; PBS: 2 x 5 min

Methods for demasking of antigens (if necessary): as described in 3.5.1

Blocking: 5% normal serum: 1 h at RT

Primary antibodies: incubation overnight (ON) at 4 °C PBS: 2 x 5 min

Secondary antibodies + DAPI (light-excluded): 1 h at RT PBS: 1 x 5min; EtOH 70 %: 1 x 5 min; Sudan Black: 1 x 7 min; EtOH 70 %: rinse 5 x; aq. bidest.: 2 x 5 min

Mounting: Fluoromount-G TM (Southern Biotech)

3.5.3 Immunohistochemical staining of gelatine sections

To visualize regenerated axons, vascularization, and myelinated axons, as well as the localization of the transplanted USSC, parasagittal spinal cord sections embedded in gelatine

were stained free-floating on a shaker using 12-well-microtiterplates. This technology enables staining through the entire thickness of 50 µm sections. The axon staining procedure was started by washing the sections in PBS (3 x 10 min). After washing, sections were blocked with 5 % normal serum and permeabilized with 0.03 % Triton X-100 (Merck) for 1 h at RT to prevent nonspecific antibody binding. Subsequently, sections were incubated with the primary antibodies. Incubation with primary antibodies directed to neurofilament protein (NF), phosphorylated neurofilament (PAM), 5-hydroxytryptamine (5-HT), tyrosine hydroxylase (TH), calcitonin gene-related peptide (CGRP), endothelial cells (von Willebrand factor, vWF), P0 (Myelin protein zero), and human nuclei (hNuc) was carried out ON at 4 °C. For fluorescent BDA-visualization, all animals were anterogradely traced either in the sensorimotor cortex or rostral to the lesion at thoracic level 7. Sections were incubated ON with Oregon Green® 488 at 4 °C. Every section was additionally stained for glial fibrillary acidic protein (GFAP; ms/rb 1:500/1:1000, Chemicon/Dako) ON at 4 °C to identify the (GFAP-negative) lesion area. All antibodies were diluted in PBS containing 0.3 % Triton X-100 and 5 % normal serum. Applied antibodies and the used respective concentrations are listed in Table 3.2. Antibodies against the animal type of origin of the first antibody were used as secondary antibodies. Normal serum of the animal type of origin of the secondary antibody was used as blocking agent. Cell nuclei were labeled with 4,6'- diamidino-2-phenylindoline (DAPI). Additionally, the P0 staining procedure was started with ethanol dehydration: EtOH 50 %, 70 %, 90 %, 95 %, 100 %, 95 %, 90 %, 70 %, 50 % each for 2 min. After incubation of primary and secondary antibodies, the Sudan Black procedure was executed.

Before secondary antibodies (listed in Table 3.3) were applied (except Oregon Green stained sections), specimens were rinsed with PBS (3 x 10 min). Sections were incubated for 3 - 4 h at RT, followed by a last rinsing step in PBS (3 x 5 min). After the staining procedures, sections were mounted on adhesive microscope slides (HistoBond®, Marienfeld) and coverslipped either with Immu-Mount (Thermo Scientific) or Fluoromount G (Southern Biotech) and stored at 4 °C.

3.6 Analysis and Documentation

Documentation of immunohistological stainings

Images were taken either with a fluorescence microscope (Axioplan2, Zeiss or BZ-8000 Keyence fluorescent digital microscope) or a confocal laser scanning microscope (LSM 510, Zeiss). The digitalized pictures were saved in TIF format. Projections from z-stacks were assembled using LSM image browser (Zeiss).

Exclusion of animals

Due to particular criteria, individual animals had to be excluded from the behavioral and histological studies. Possible exclusion criteria:

1. Premature death due to infection
2. Serious infection, indicated by loss of weight more than 20% of the primordial weight
3. Incomplete transection (retrospective, through histological examination)
4. Complications during surgery

Blinding procedure

Following complete transection, each animal was assigned either to a mMS groups or to a control group of animals. Furthermore, the USSC treatment was also applied in a blinded manner, i.e., the surgeon did not know whether the DMEM contained USSC or not. After surgery the animals received a random tail number by a third person who kept the key secret. After finishing the behavioral and histological analyses the key was broken by the third person. Therefore, the procedure was considered to be a double-blinded study.

3.7 Histological evaluation

3.7.1 Quantification of TH- and 5-HT-positive axon profiles

For the quantification of TH-positive and 5-HT-positive axon profiles in the lesion area and up to 2 mm caudal to the lesion, five to six 50 µm parasagittal spinal cord sections from analogous regions were stained for each neurotransmitter and for each animal. Respective sections were analyzed using the 20x-objective of a Nikon Diaphot 300 fluorescent microscope. Only TH-positive and 5-HT-positive structures which could clearly be identified as regenerated axons were taken into account for evaluation. Therefore, specific characteristics described by Steward *et al.* [111] were used for the quantification. Due to partly high background noise, axon profiles were counted manually. GFAP-antibody was used to label reactive astrocytes and to clearly delineate the borders of the fibrous scar. The scar area was defined by lack of immune reactivity to GFAP antibody. The 40x-objective was used for confirmation whenever the identification was ambiguous.

3.7.2 Analysis of blood vessel density

The following blood vessel analysis was performed by Lei Zhang during an internship.

The vWF staining was used for the analysis of blood vessel density. 50 µm thick sections double stained for vWF and GFAP were used for the evaluation.

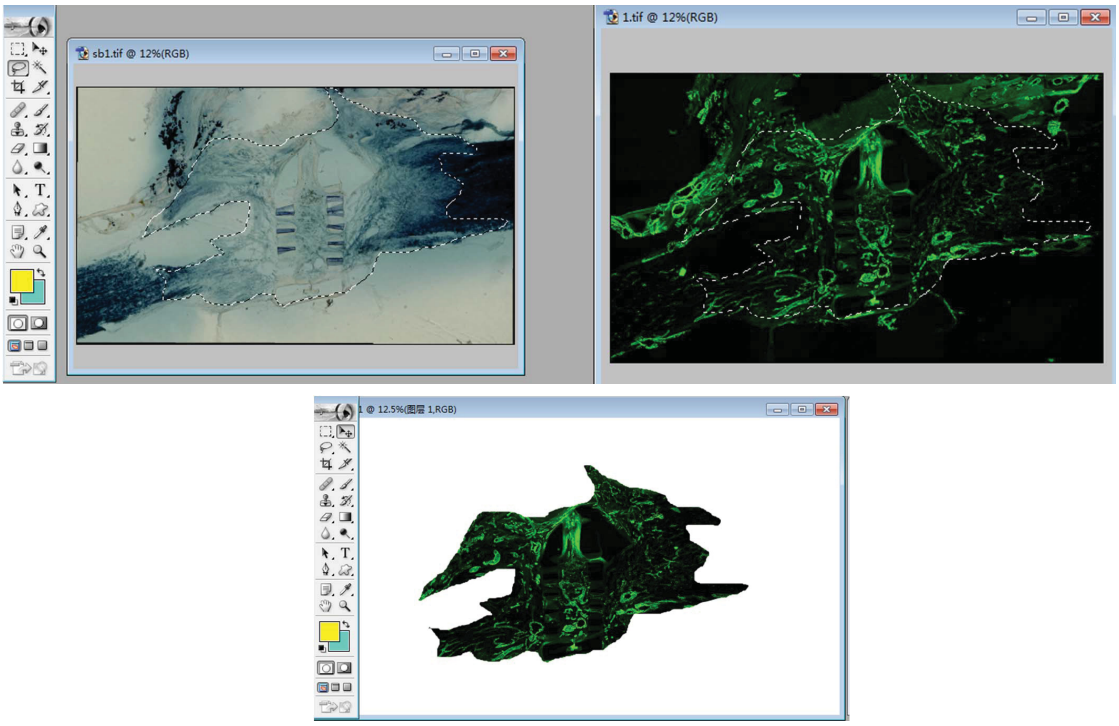

Figure 3.6: **Scar area outline for blood vessel analysis**
50 µm thick parasagittal spinal cord sections were stained for vWF and GFAP. GFAP was used to identify the scar area. The area was outlined using ImageJ software. vWF pixels were highlighted with a constant threshold value. The scar outline was subsequently transferred to the corresponding vWF image. (Generated by Lei Zhang.)

To identify the scar area, GFAP and Sudan Black were used. The scar area was defined

by lack of immune-reactivity to the GFAP antibody. Subsequently, the area was outlined using ImageJ Software (see Fig. 3.6). A defined grid was placed on top of the scar area image. The blood vessel density was then calculated as the number of points falling on the blood vessels divided by the total number of points falling on the scar area (see Fig. 3.7). Care was taken to distinguish between blood vessels and background. Since clear demarcation of neighboring blood vessels was not possible, the blood vessel density represents a relative rather than an absolute value.

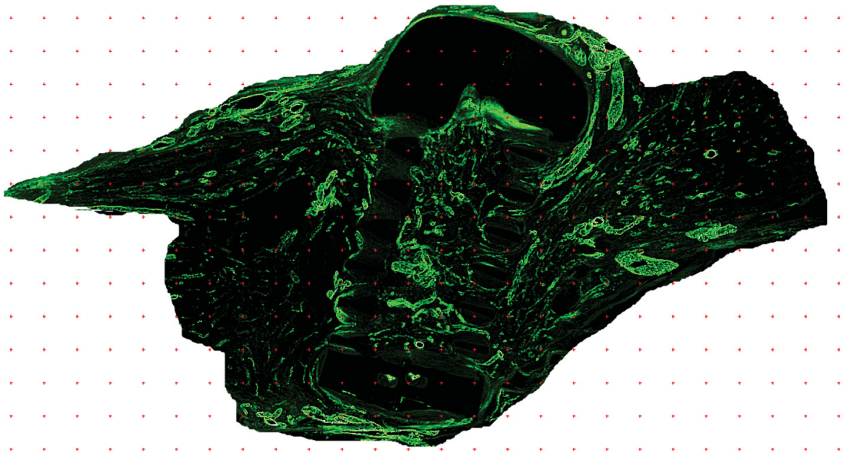

$$\text{Blood Vessel Density} = \frac{\text{Number of points falling on the blood vessels}}{\text{Number of points falling on the scar area}}$$

Figure 3.7: **Calculation of blood vessel density**
The scar area was transferred to the corresponding vWF image, a grid was overlaid to calculate the blood vessel density. Blood vessel density was defined as the quotient of the number of points falling on the blood vessels divided by the total number of points falling on the scar area. (Generated by Lei Zhang.)

3.7.3 Analysis of cysts and spared tissue

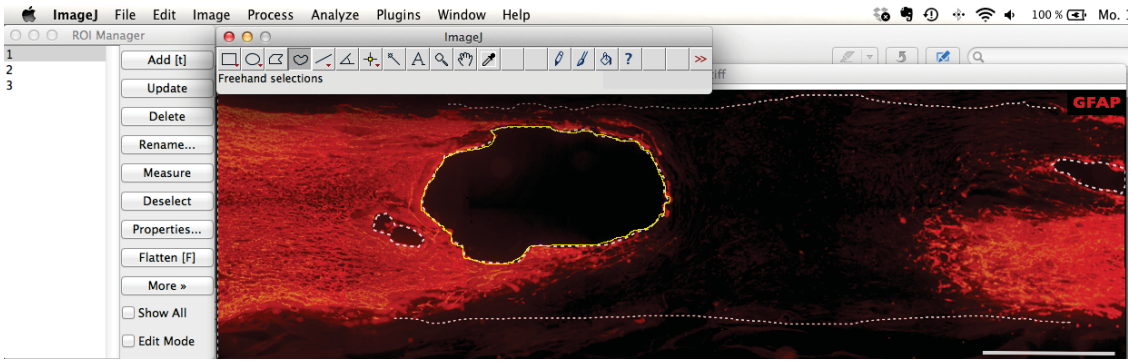

Figure 3.8: **Cyst formation analysis**
A 50 µm thick parasagittal spinal cord section stained for GFAP at 19 weeks post operation. Example for the analysis using Image J (and the ROI Manager), cysts were outlined using the freehand selection. Red = GFAP positive, dashed line represent dorsal and ventral limit of the spinal cord. Scale bar 500 µm.

Cyst areas (mm^2) were defined as fluid filled cavities. For measurement, parasagittal spinal cord sections were stained for GFAP at 19 weeks post operation. Three sections

of each animal (one central section and two equidistant sections lateral from the center section of the spinal cord) were included in the quantitative analysis. The center section of the spinal cord was detected by the presence of the central canal. Images of every single section were taken with a fluorescence microscope (BZ-8000 Keyence fluorescent digital microscope). Single images were merged to one total picture. Cyst areas were measured by drawing contours around them using Image J, an illustrative model is given in Fig. 3.8. To set the scale, the scale bar of the corresponding picture was used. Using the "Freehand selection", it was possible to collect detailed informations. Every cyst was outlined and numbered. The raw data were transferred to the ROI Manager and subsequently analyzed. The mean size was calculated and the number of cysts per section was counted. A semi-quantitative group analysis was performed due to defined limits, shown in Tab. 3.8.

Table 3.8: **Cavitation analysis**

dimensions	averages
0	0 - 0.2 mm^2
+	0.2 - 0.5 mm^2
++	0.5 - 1.5 mm^2
+++	1.5 - 3.5 mm^2
+++	$\geq$ 3.5 mm^2

A cavity index was calculated as quotient of numbers of animals times cavity points divided by numbers of animals.

The following analysis was performed by Lei Zhang during his internship.

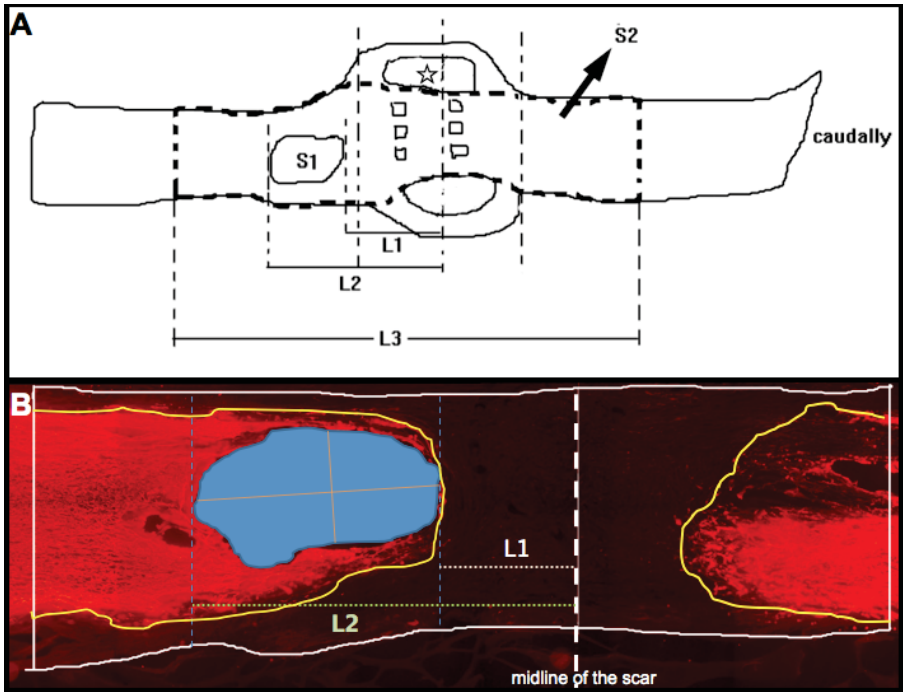

Figure 3.9: **Cyst locations and spared tissue**
(A) Schematic stencil to investigate the location and area of cysts and spared tissue. L1: proximal length from the cyst to the center of the scar area, L2: distal length from the cyst to the center of the scar area, L3: fixed length for all sections (14 mm), S1: area of the cyst, S2: area of the whole tissue, S2-S1 = area of the spared tissue, ☆: areas without tissue caused by the mMS (excluded); B: example of one specific section to demonstrate investigation. (Pictures created by Lei Zhang.)

To further investigate the location of the cysts and the percentage of the spared tissue, Lei Zhang used a schematic stencil which is shown in Fig. 3.9.
Six animals per group and two sections of each animal were included in this further examination. The cyst areas were measured as described above. The spinal cord area was limited rostrally and caudally to a total length of 14 mm (L3). The spared tissue area (mm^2) was calculated by subtracting the cyst areas (S1) from the whole tissue area (S2): S2 - S1 = area of the spared tissue. The proximal and distal lengths of each cyst were marked to make a point about the location. The documentation sheet is shown in Fig. 3.10. To determine the cyst area percentage, the cyst area was divided by the outlined spinal cord area from the same section. Finally, the cyst locations and percentages were correlated with the mBBB scores at wpo 14.

LOCATION	SCAR LENGTH	CYSTS AREA &LENGTH		S2	SPARE TISSUE AREA
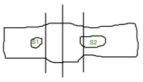		S1	L1		
			L2		
		S2	L1		
			L2		

Figure 3.10: **Decimation sheet for cyst location and spared tissue area**
Decimation sheet to inscribe informations about location, lengths, cyst areas, and spared tissue areas. S1: area of the cyst, S2: area of the whole tissue, L1: proximal length from the cyst to the center of the scar area, L2: distal length from the cyst to the center of the scar area. (Sheet created by Lei Zhang.)

3.8 Functional evaluation

3.8.1 Assessment of spasticity

During the behavioral testing, increased spastic locomotion patterns were observed from time to time. We designed a scale to assess similarities and differences between the groups based on the BBB rating scale [118]. To develop the scale, we documented movement patterns displayed by rats during the behavioral testing. The scoring sheet was generated whereby frequency, amplitude, and affected body regions (tail, hind limbs, toes) could be documented (Fig. 3.11). Spasticity of the hind limbs received a higher relevance compared to spasticity of tail and toes. The scoring is listed in Tab. 3.9.

Table 3.9: **Spasticity score**

Score	Frequency	Amplitude	Affected Body Segment
0	No		
1	Occasional	Weak	Tail / toes
2	Occasional	Weak	Hind limbs
3	Occasional	Weak	Hind limbs + tail / toes
4	Occasional	Large	Hind limbs + tail / toes
5	Frequent	Weak	Tail / toes
6	Frequent	Weak	Hind limbs
7	Frequent	Weak	Hind limbs + tail / toes
8	Frequent	Large	Hind limbs + tail / toes
9	Consistent	Weak	Hind limbs (+ tail/toes)
10	Consistent	Large	Hind limbs (+ tail/toes)

No: 0%, O = occasional: observed in $< 50\%$ of the time, F= frequent: 51-94%, C = consistent: $> 95\%$

3.8.2 Open field locomotor score

The behavioral testing and the consequent analyses were carried out blinded with regard to the treatment of the animals. Hindlimb function was evaluated biweekly in an open field test using a modified Basso Beattie Bresnahan locomotor rating scale (mBBB) developed by Antri *et al.* [119] over 16 weeks. The modified version of the BBB (mBBB) is better suited for rats with complete spinal cord transection due to the spread of lower BBB values (0-10). The standard BBB open field test was originally developed for partial lesions [118]. Conditioned by the lesion model and due to the fact that animals of the present study were neither trained nor tested on a treadmill, further modifications of the test procedure and of the mBBB scale were necessary [119]. To emphasize delicate distinctions, an additional criteria for evaluation of the general activity ratio was added in the scoring sheet. This was indicated due to the fact that we observed very different locomotion patterns: Some of the animals showed the combination of occasional movement in general with frequent right-left alteration, large amplitude, and frequent body weight support, whereas other animals showed frequent movement in general without any right-left amplitude and just a weak amplitude and no body weight support.

Tier_____ Datum_____ wpo_____ Scorer _____ Videos: ja / nein

Movement								Trunk position		Movement general			R-L Alterations	Amplitude		weight supp. L	weight supp. R	Plantar paw placement L	Plantar paw placement R	tail position	Spasm		
Hip		Knee		Ankle						L	R	rate									general	Amplitude	affected body parts
L	R	L	R	L	R	L	R							L	R								
no	no	no	no	no	no	mid		no	no	O	no			no	no	no	no	slack			hind limbs		
								weak limb jerks	weak limb jerks	F	O	weak	weak	O	O	O	O	up	O	weak	tail		
S	S	S	S	S	S			yes	yes	C	F	large	large	F	F	F	F	general movement	F	large	toes		
E	E	E	E	E	E						C			C	C	C	C						

Figure 3.11: **Documentation sheet for functional evaluation**
Complete documentation sheet for the functional evaluation for both the functional improvement and to asses spasticity.
wpo = weeks post operation, R = right, L = left; No: 0%, O = occasional: observed in < 50% of the step cycles, F= frequent: 51-94%, C = consistent: > 95%, S = slightly, E = extensively, supp = support.

In conclusion, in the present study, the modified version of the BBB (mBBB), which is already well-established in our research group, was used. Further modification in terms of additional distinct locomotor improvements were necessary. The modified scoring sheet is shown in Fig. 3.11 and the complete rating scale is listed in Tab. 3.10.

The testing procedure was executed as described elsewhere [118]. Animals were placed in a Plexiglas® open field with a side length of 1 m, the floor was covered with a rubber mat. For evaluation, the movement of each animal was videotaped over a time period of 4 min per trial and subsequently analyzed. During the video grab, rats were continually encouraged to move. To prevent stagnation, rats were enticed to move every time they remained stationary for longer than 15 - 20 sec. Care was taken not to touch the tail and/or hindquarters during testing due to stimulating effects for motor performance. Although video analyses are not recommended for the regular BBB due to the inability to evaluate toe clearance [120], video recordings in the case of animals with complete transection, which never reached the level where they show toe clearance, are very useful for close monitoring because repetitions of the video sequences are always possible. For the final evaluation, the mBBB scores of both hindlimbs were averaged. Different diagram types were used for the graphical representation. Different illustration facilities enable to set various priorities.

Graphical Representation using the program language R

The following analysis was performed by Dr. Wolfgang Kaisers from the Biologisch-Medizinisches Forschungszentrum (BMFZ) of the Heinrich Heine University of Düsseldorf.

The program "R" was used for the graphical representation in the form of non-parametric regressions. R is a language and free software environment for statistical computing and graphics [121]. Based on the data of the scatterplots, continuous smooth functions for each group were calculated using "ggplot stat smooth" function (ggplot version 1.0.1, stat_smooth) [122]. For further descriptions of this function see: http://docs.ggplot2.org/0.9.3.1/stat_smooth.html. Numbers of observation < 1000 require smoothing methods. *Stat_smooth* uses *loess* for smoothing. LO(W)ESS (locally (weighted) scatterplot smoothing, or LOcal RegrESSion) is a non-parametric regression method, combining multiple regression models in a k-nearest-neighbor-based-meta-model by using "Least squares"; LOESS was originally proposed by Cleveland [123]. A flexible modeling is reached by this smoothing. The default level for confidence intervals, which was also used in this study, is 95 %. In this way, the curves should best represent the relationship between the variables.

Table 3.10: **Modified BBB (mBBB) score**

Score	General Movement	R-L Alteration	Amplitude	Body weight support	Plantar foot placement
Level 1					
0	No				
1	Weak limb jerks				
Level 2: rhythmic movements/dorsal foot placement					
2	Occasional	No	Weak		
3	Occasional	No	Large		
4	Occasional	Occasional	Weak		
5	Occasional	Occasional	Large		
6	Occasional	Frequent	Weak		
	Frequent	Occasional	Weak		
7	Occasional	Frequent	Large		
	Frequent	Occasional	Large		
8	Frequent	Frequent	Weak		
9	Frequent	Frequent	Large		
Level 3: alternating movements / dorsal foot placement/occasional body weight support					
10	Occasional	Yes	Weak	Occasional	
11	Frequent	Yes	Large	Occasional	
Level 4: body weight support / plantar foot placement					
11	Yes	Occasional	Large	No	Occasional
12	Yes	Occasional	Large	Occasional	Occasional
13	Yes	Occasional	Large	Occasional	Frequent
14	Yes	Occasional	Large	Frequent	No
	Yes	Frequent	Large	No	Occasional
15	Yes	Occasional	Large	Frequent	Frequent
	Yes	Frequent	Large	Occasional	No
16	Yes	Frequent	Large	Occasional	Occasional
17	Yes	Frequent	Large	Frequent	No
18	Yes	Frequent	Large	Frequent	Occasional
19	Yes	Frequent	Large	Frequent	Frequent
20	Yes	Consistent	Large	Occasional	No/Occasional
21	Yes	Consistent	Large	Occasional	Frequent
	Yes	Consistent	Large	Frequent	No/Occasional
22	Yes	Consistent	Large	Frequent	Frequent
	Yes	Consistent	Large	Consistent	Yes

R-L: right-left, No: 0%, Yes: $\geq$ Occasional, Occasional: observed in $< 50\%$ of the step cycles, Frequent: 51-94%, Consistent: $> 95\%$.

4 Results

4.1 Stem cells migrate into the injured spinal cord and the mMS lumen

In order to investigate the migration potential of USSC in the model of a complete transection as well as after mMS implantation, we performed short time experiments and used a specific anti-human nuclus antibody (hNuc) to clearly identify these human stem cells. Three weeks after their transplantation (wpt), USSC were detectable in the lesion centre (Fig. 4.1 A) of completly transected spinal cords. USSC migrated from the injection site (Fig. 4.1 A, red arrow) to the lesion centre (Fig. 4.1 A, white arrow). They not only migrated into the lesion center, but also into the lumen of the mMS (Fig. 4.1 B and C). In contrast, when USSC were injected into the uninjured spinal cord, the cells remained at the injection site.

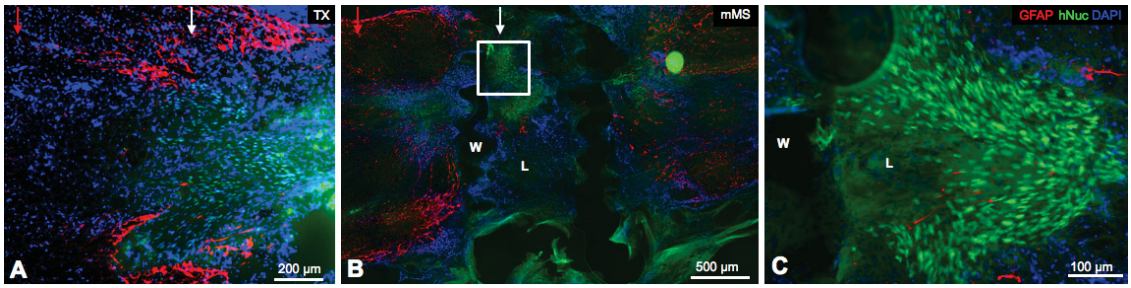

Figure 4.1: **Unrestricted somatic stem cells migrate into the lesioned spinal cord and into the mMS lumen**

(A) Three weeks after their transplantation, USSC (stained against human nuclei, hNuc, in green) have migrated from the injection site (red arrow) into the lesion center (white arrow), 50 µm parasagittal section of the TX lesion area, lesion area defined as GFAP (in red) -negative area. (B) USSC migrated into the mMS lumen three weeks after mMS implantation and USSC transplantation. (C) Magnification of framed area in B. W = mMS wall, L = mMS lumen, TX = complete transection, mMS = mechanical Microconnector System.

4.2 Combination of mMS and USSC prevents cavity formation after spinal cord injury

4.2.1 General tissue preservation

Trichrome staining was performed to get a complete overview of the tissue preservation of all animals. With regard to the mMS group it has been noticed that the majority of the mMS devices were placed in a nearly vertical position and did not tip over (Fig. 4.2 C and

D). In some cases, the tissue preparation was accompanied by some difficulties regarding to section processing. Small pieces were broken out of the tissue during cutting with the freezing-microtome, other small pieces of PMMA were washed out during staining of the tissue sections. In general, most of the mMS lumens were filled completely with tissue, regardless whether treated additionally with USSC or medium.

This experiment revealed the frequent occurrence of big cyst formations. Cyst formation to this extent was not seen before in our previous studies. Fig. 4.2 shows representative images of the trichrome staining for the different animal groups (with and without the mMS device). On the one hand examples of good tissue preservation are given and on the other hand those images of big cysts. Those observations promoted us to further analyze the precise cyst localization, cyst areas in total and in percentages, and the comparisons between the groups.

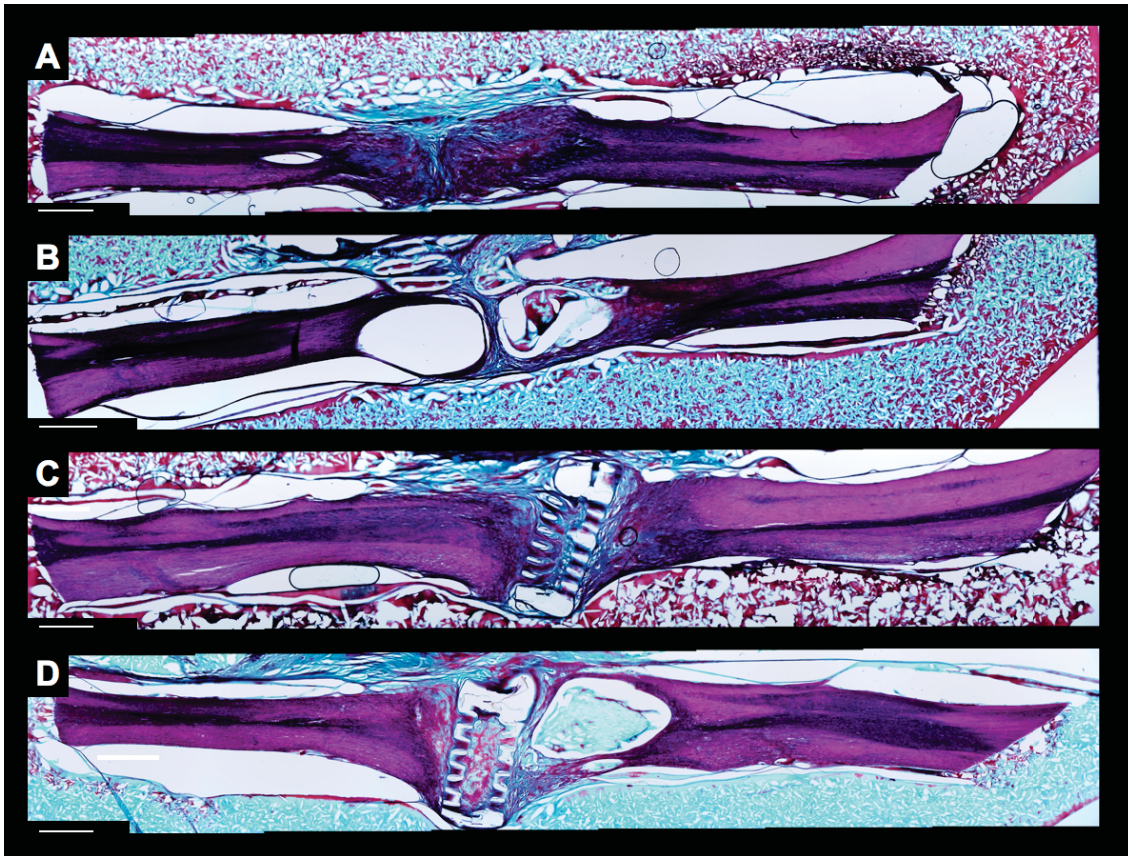

Figure 4.2: **Exemplary images of general tissue preservation**
(A-D) Exemplary images of 50 µm gelatin-embedded parasagittal spinal cord sections from differently treated animals at 19 weeks post operation (wpo), trichrome staining. (A) Examples of good tissue preservation in USSC and (C) mMS + USSC treated animals. (B) Examples of large cysts in Medium and (D) mMS + Medium treated animals. Scale bar = 1 mm.

4.2.2 Increased cyst formation rostral to the lesion

(These data were collected by Lei Zhang.)

The localization of cysts in the different animals was analyzed using the assessment sheets described in Fig. 3.9 and Fig. 3.10. An exemplary overview of different cyst localizations is given in Fig. 4.3. The 6 animals which achieved median mBBB scores (Fig. 4.3,

red numbers) were selected for each treatment group. Cyst localization of the different treatment groups are presented in columns. In addition to the corresponding mBBB, the average percentage value of the cyst area of each animal is given (Fig. 4.4, black numbers). Apart from the lesion site, cysts were more often found in the rostral direction (Fig. 4.3).

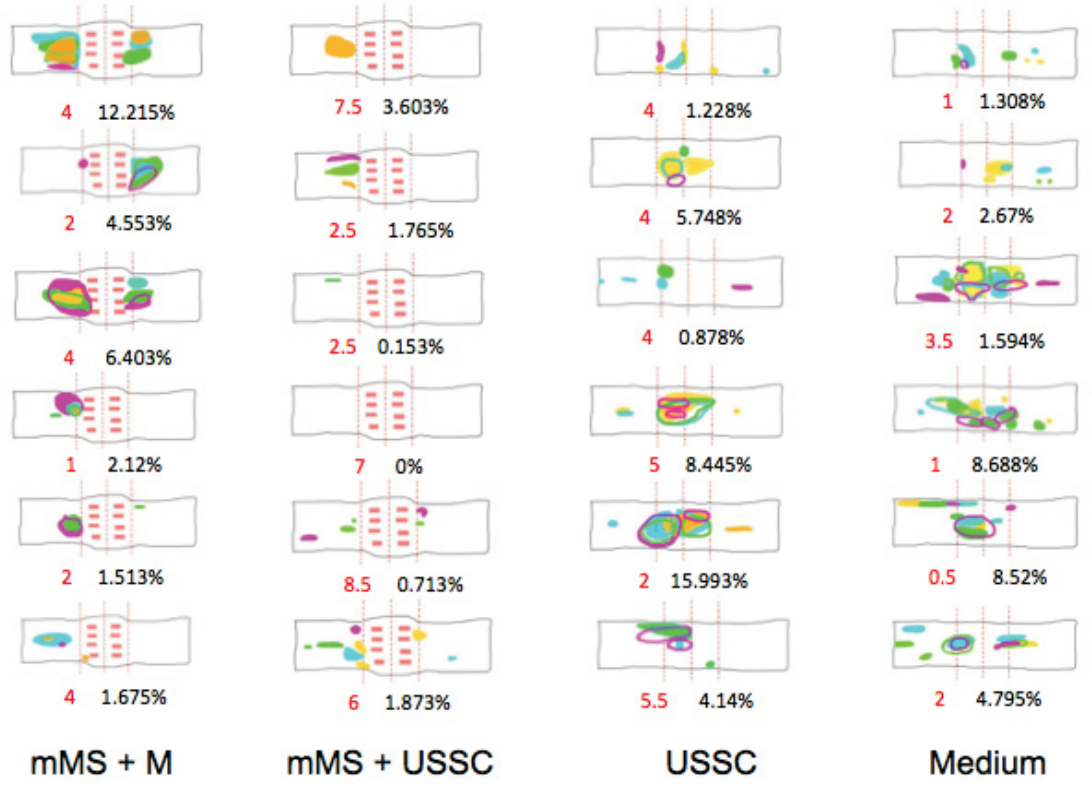

Figure 4.3: **Exemplary presentations of the different cyst localizations and percentages**
The different treatment groups are represented in columns, column 1: mMS + DMEM (Medium), column 2: mMS + USSC, column 3: USSC, column 4: DMEM (Medium). Analysis revealed increased cyst formation rostral to the lesion in general. In total, mMS + USSC treated animals showed less and smaller cyst formations. There are no obvious differences between the monotherapies. Numerous cysts appear only in Medium-treated animals. Red numbers: corresponding mBBB values at 14 weeks post operation (WPO), black numbers: corresponding cyst area in percent (%), defined in Fig. 3.9) mMS = mechanical Microconnector System, M = Medium.

As shown in Fig. 4.3, combined treated animals (mMS + USSC) showed less and smaller cysts in total, compared to the Medium group. A significant difference between the mMS + Medium and the USSC group could not be determined. Animals of the Medium group showed more and larger cysts with a greater spreading rostral and caudal to the lesion. A direct correlation between the mBBB scores and the cyst locations and size could not be observed.

4.2.3 Reduced cyst area in combination group

To elucidate the efficacy of mMS + USSC for tissue sparing and cyst formation after complete SCI, we measured the area of cavities and the total lesion area with GFAP staining at 19 weeks post operation (Fig. 4.4 A - C). Definitions of the precisely defined

areas are given in chapter 2.7.3. Based on these data, cyst area in percent (%) and spared tissue area (%) could be calculated. In general, a greater number of animals with only few and small cavities were detectable in the mMS + USSC group (Fig. 4.4 D, blue columns), compared to the other groups. In contrast, the control group showed a greater number of animals with cyst areas $\geq$ 1.5 mm² (Fig. 4.4 D, black columns).

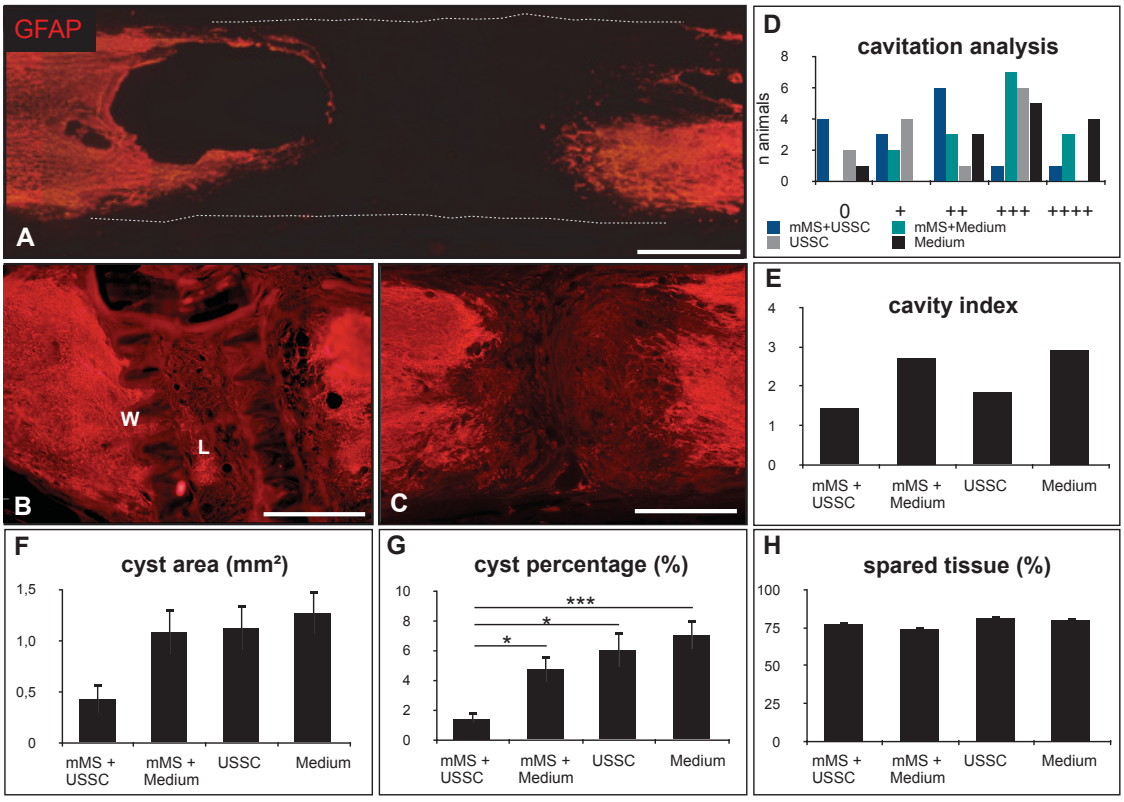

Figure 4.4: **Combination of mMS and USSC prevents cavity formation**
(A - C) Parasagittal spinal cord sections stained for GFAP (glial fibrillary acidic protein) at 19 weeks post operation (wpo). (A) Example of a large cyst after complete spinal cord transection. (B + C) Examples of good tissue preservation in mMS + USSC (B) and USSC animals (C). Scale bar = 500 µm. W = wall of mMS, L = lumen of mMS. (D) Quantification of cavity formation 0: $\leq$ 0.2 mm²; +: 0.2-0.5 mm²; ++: 0.5-1.5 mm²; +++: 1.5-3.5 mm²; ++++: >3.5 mm². A greater number of animals with only few and small cavities were detectable in the mMS + USSC group. The Medium group comprised more animals with larger cyst areas. (E) Cavity index: the number of animals x cavity points / number of animals. (F) Total cyst area in mm² of different treatment groups measured by using Image J. (G) Cyst area in percent (%): cyst area in mm² x 100 divided by total area in mm² (both defined in 3.9). Kruskal-Wallis with Holm-Bonferroni correction. *p $\leq$ 0.05, **p $\leq$ 0.01, ***p $\leq$ 0.001; n = 13 - 14 / group. (H) Spared tissue percentages (%): spared tissue (mm²) / total area (mm²), (both defined in 3.9). mMS + USSC could significantly reduce cysts formation compared to other treatments. Monotherapies (neither mMS nor USSC) also reduce cavity formation compared to the the medium group. A significant difference between the different groups relating to spared tissue could not be determined. Results are shown as mean ± SEM.

The cavity index was ascertained to allow a simplified and comprehensible representation of graphic D in Fig. 4.4. A major influence of USSC on suppression of cavity formation can be assumed by the cavity index (Fig. 4.4 E). The average areas of the cystic cavities were smaller in mMS + Medium and USSC animals compared to the control (Medium/DMEM) group. The combination of mMS + USSC further leads to reduction of the cyst area (Fig. 4.4 F) indicating a synergistic effect of mMS implantation and USSC transplantation to prevent cyst formation. Consequently, the cyst formation of mMS + USSC treated animals was significantly decreased (Fig. 4.4 G). A significant difference between the

animal groups relating to spared tissue could not be determined (Fig. 4.4 H).

Quantification of cavitation areas showed that, compared to control animals, USSC, mMS, and especially the combination lead to a decrease in cavity formation.

4.3 Combination leads to vascularization in close association with regenerated axons

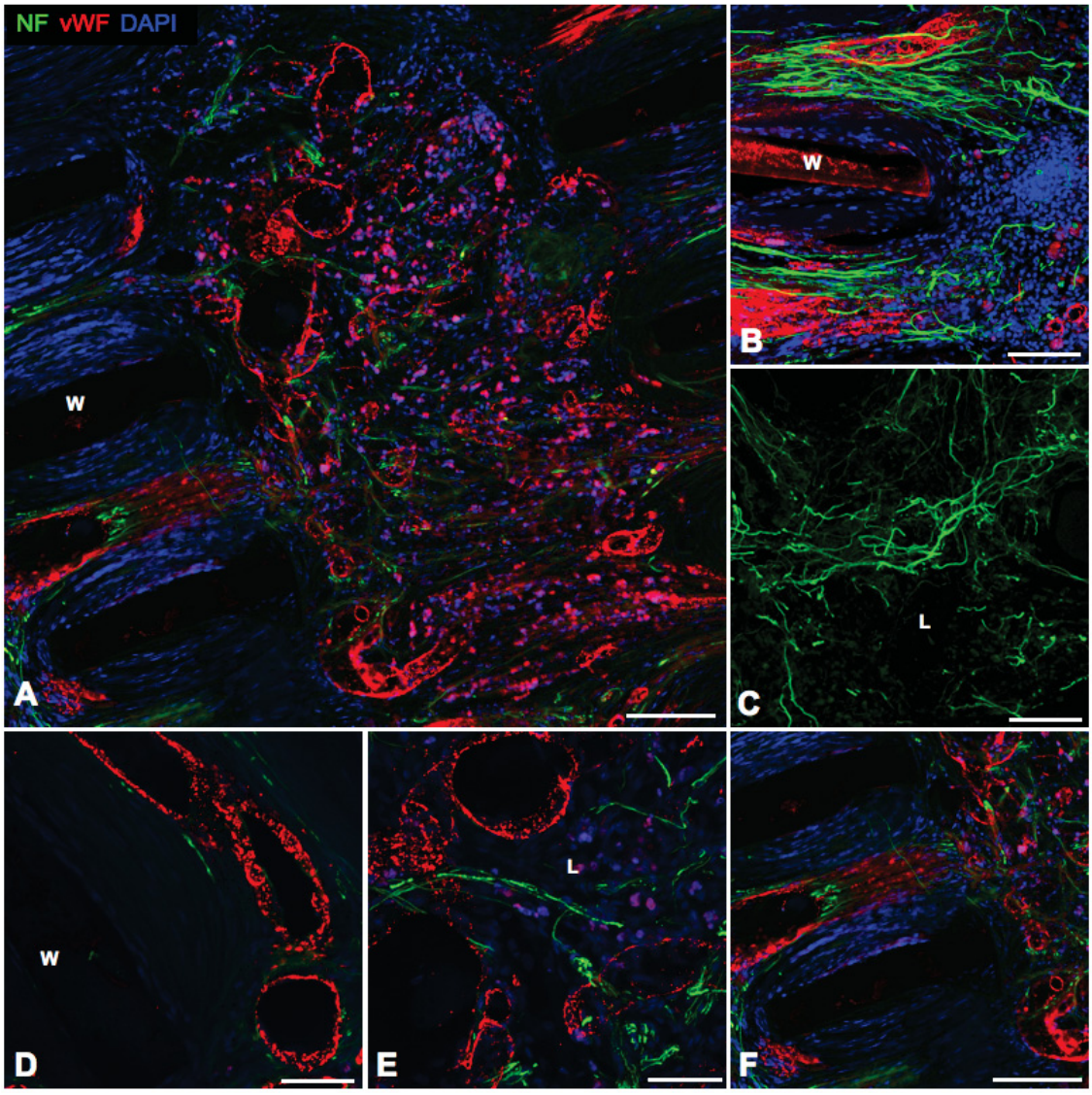

Figure 4.5: **Vascularization and axonal regeneration in the mMS lumen**
Regenerating axons are frequently found in close association with blood vessel-rich areas in the lesion center. (A - F), 50 µm parasagittal spinal cord section stained for neurofilament (NF) and endothelial cells (von Willebrand factor, vWF) to identify regenerated axons and vascularization at 19 weeks post operation, respectively. (B) Rostral mMS bridge and lumen. (C) NF-positive axons in the mMS lumen. (D) Caudal mMS bridge. (E) The mMS lumen. (D) Rostral mMS bridge and mMS lumen. Scale bar in A & F = 100 µm. Scale bar in B - E = 50 µm, W = wall of mMS, L = lumen of mMS. Green = NF-positive axons, Red = vWF-positive structures, Blue = DAPI.

Revascularization of damaged spinal cord tissue and thus the facilitated transport of supporting molecules and nutrients are important aspects for reparative events after SCI [124].

Immunohistochemical co-staining of von Willebrand Factor (vWF) and Neurofilament (NF) was performed to identify vascularization in the mMS lumen. Interestingly, numerous regenerating axons were frequently found in close association with vWF-positive structures (Fig. 4.5). The detection of vWF-positive endothelial cells revealed the ingrowth of newly formed blood vessels (BV) into the lumen of the mMS. It was possible to track the vessels' courses with the assistance of a confocal microscope (LSM 510, Zeiss). One can easily imagine the course of the BV, in particular in the Figures A, D - F of Fig. 4.5.

In both treatment groups receiving the mMS, BV could be observed. To evaluate the effects of the different treatments on revascularization, the calculation of BV density was performed as described above. The number of vWF-stained blood vessels was determined and related to the scar area (Fig. 4.6, A). The analysis revealed that the BV density of animals receiving the combination of mMS + USSC treatment was increased in comparison to the other groups (4.6), B. The BV density in the lumen of the mMS or in the lesion center was not statistically increased in treated groups when compared to the medium control.

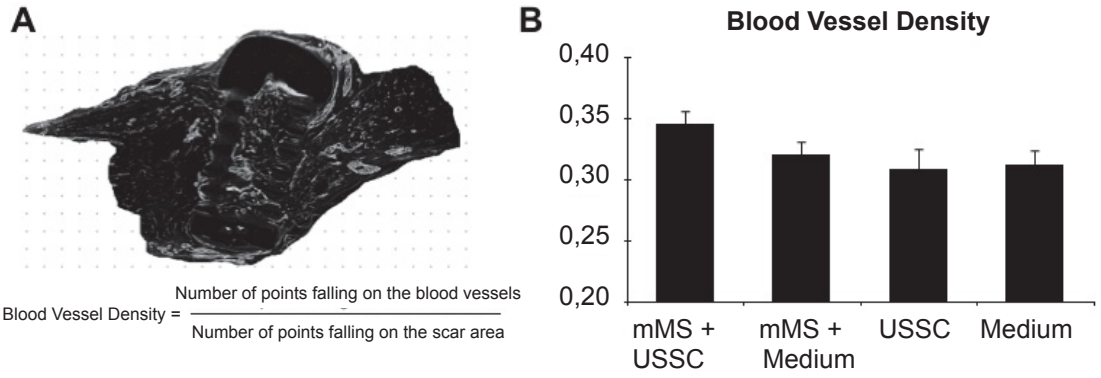

Figure 4.6: **Effect of different treatment modalities on blood vessel density**
(A) Calculation of blood vessel density. (B) Effects of different treatments on blood vessel density. Quantification of blood vessel density revealed enhanced vascularization in the combination group (mMS + USSC) compared to the other groups. A significant difference between the groups was not found. Results are shown as mean ± SEM.

Regenerated axons which were frequently found in BV rich areas (Fig. 4.5), were especially pronounced in the combination group. Long-distance courses of those blood vessels were particularly found in the mMS + USSC group.

4.4 Enhanced axonal regeneration after combination therapy

Axonal regeneration is one of the key aims in the field of SCI, since it has been shown that regeneration of only few axons can lead to partial recovery of locomotor and sensory function.

Due to high background signals in the lesion area, axons were counted manually. For the quantitative assay of TH^+ and 5-HT^+ axons five 50 µm parasagittal sections per staining were analyzed using the 20x objective of a Nikon Diaphot 300 fluorescent microscope. The 40x-objective was used for corroboration whenever the identification of single axon profiles was impossible at lower magnification. Axon profiles were counted under the microscope in the lesion area, defined as GFAP-negative zone. Only 5-HT^+ and TH^+ structures which could clearly be identified were counted.

Numerous axons involved in motor function (labeled with 5-HT ([5-hydroxytryptamine] serotonergic) and TH ([tyrosine hydroxylase] catecholaminergic) regenerated into the mMS lumen of USSC-treated animals, shown in Fig. 4.7. Quantitative analysis of TH^+ and 5-HT^+ axons revealed the positive influence of the combinatory treatment leading to enhanced axonal regeneration. Significant increase of TH^+ axons profiles was found in the mMS lumen or in the lesion area (GFAP-negative) and in the caudal spinal cord of mMS + USSC-treated animals compared to the control group. The number of regenerating axons was enhanced by more than threefold (**$p \leq 0.01$). A significant difference between the individual therapies compared to the control group could not be determined, although a trend of enhanced TH^+ axon ingrowth into the lesion area or mMS lumen could be observed. In addition, the number of regenerating axons in the combination group was two to three times higher than in the individual treatment groups, resulting in a significant difference between the mMS + USSC and the USSC only group (Fig.4.7, D). Those effects were not only seen in the lesion but also beyond (Fig. 4.7, E), also with a significant difference between the combination and the control group (**$p \leq 0.01$).

A similar pattern was seen in the quantitative analysis of 5-HT^+ axons. The total amount of 5-HT^+ axons was less compared to the TH^+ axons. However, the number of regenerating axons in the lesion/mMS lumen of the combination group was significantly enhanced compared to the control group (Fig. 4.7, F). Beyond the lesion, only few 5-HT^+ axons could be detected. Remarkably, the numbers of regenerating axons (5-HT^+ axons) were significantly enhanced in the USSC and mMS + Medium group compared to the control group (Medium) with further proof of the superiority of the mMS + USSC combination (Fig. 4.7, G).

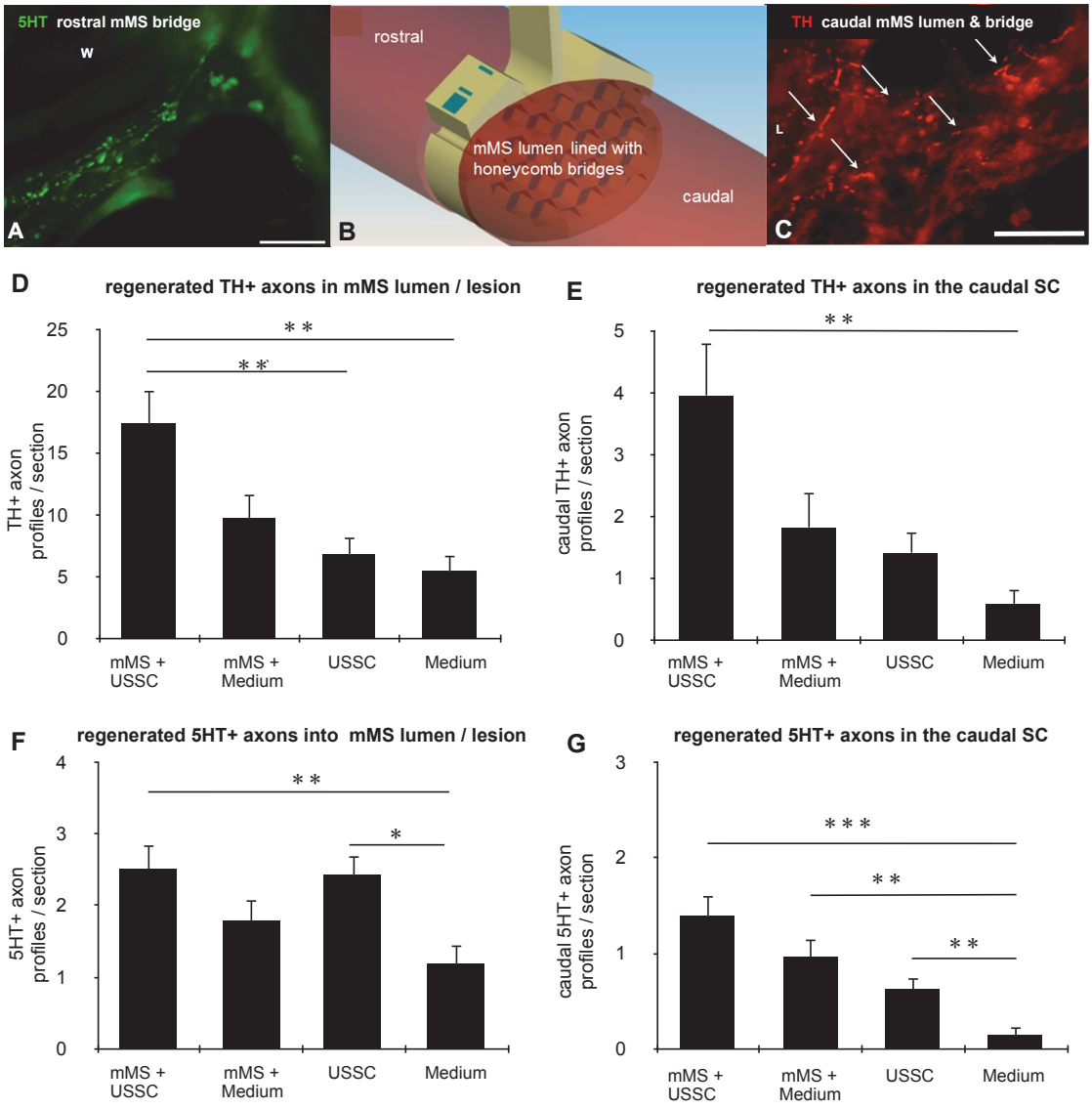

Figure 4.7: **Enhanced axonal regeneration of TH$^+$ & 5-HT$^+$ axons in combined treated animals**

Quantification of TH$^+$ and 5-HT$^+$ axon profiles. (A + C) Examples of axon regeneration into the mMS lumen and bridges in 50 µm parasagittal spinal cord sections stained for 5-HT (A, 5-hydroxytryptamine, green) and TH (C, tyrosine hydroxylase, red), 19 weeks post operation. (B) Schematic representation of the mMS (mMS lumen and bridges) with rostral and caudal spinal cord for a better orientation (Modification from Estrada et al., in preparation). Quantification of TH$^+$ profiles in the mMS lumen / lesion area (D) and in the caudal spinal cord (E). Quantification of 5-HT$^+$ profiles in the mMS lumen / lesion area (F) and in the caudal spinal cord (G). Quantification of regenerating axons revealed superiority of the mMS + USSC combination. Results are shown as mean ± SEM. Kruskal-Wallis with Holm-Bonferroni correction. *p ≤ 0.05, **p ≤ 0.01, ***p ≤ 0.001. W = Wall of mMS, L = Lumen of the mMS. Scale bars: A, C = 50 µm.

4.4.1 Remyelination after combination therapy

Myelination is important for the electrical insulation of axons and essential for a high signal transduction. In order to assess the regenerating axons, we performed a co-staining of PAM (panaxonal neurofilmaent marker) and P0, a distinct marker of peripheral myelin. As shown in Fig. 4.8, regenerating axons were frequently detected in close association with P0$^+$ structures.

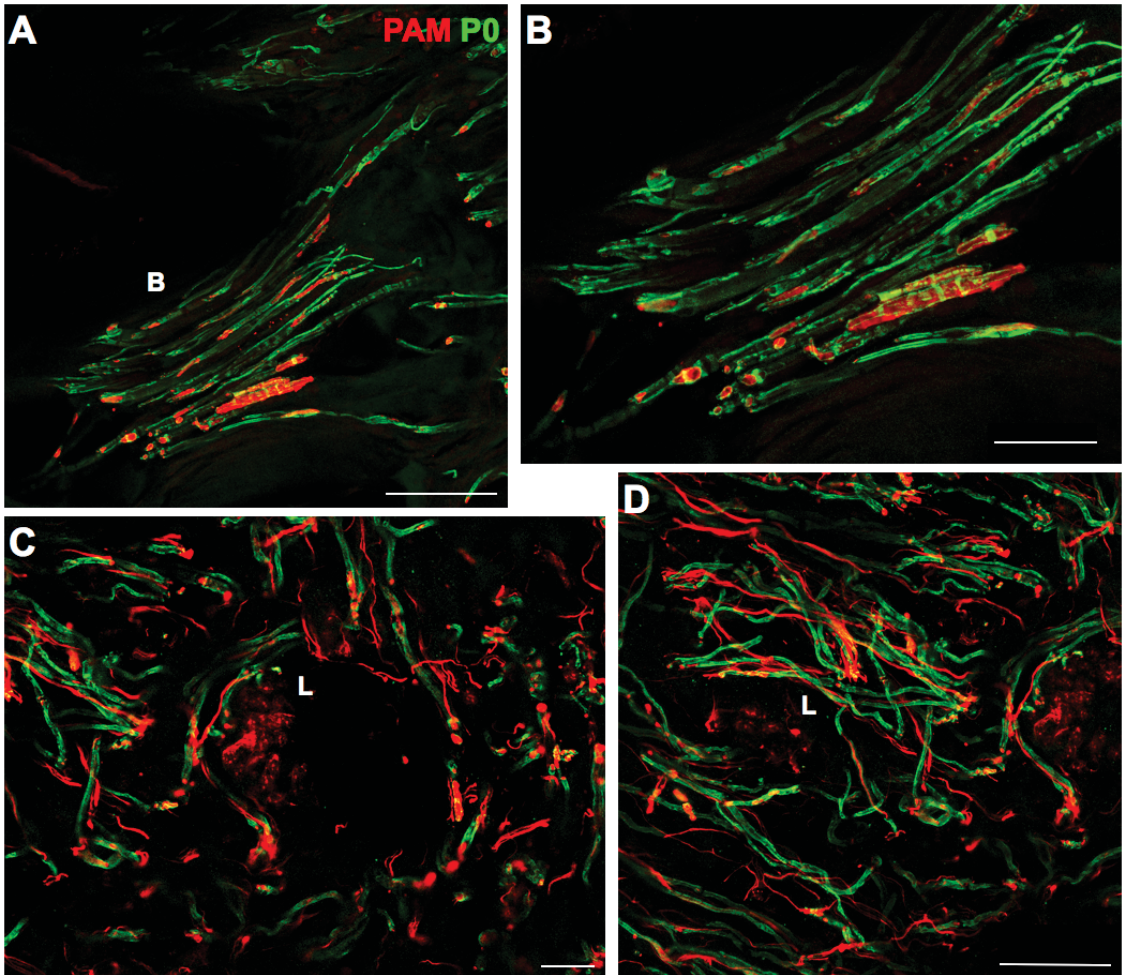

Figure 4.8: **Remyelination of regenerating axons**
(A - D) Immunohistochemical staining of 50 µm parasagittal sections of animals with combinatory treatments 19 weeks post operation (wpo), stained for PAM (phosphorylated neurofilament, red) and P0 (myelin protein zero, green). (A) Bridge area. (B) Higher Magnification of A. (C + D) Lumen of mMS. Numerous regenerating axons (PAM^+) in the mMS lumen and bridge areas are myelinated with peripheral myelin ($P0^+$). B = Bridge of mMS, L = Lumen of mMS. Scale bars: A = 100 µm, B + D = 50 µm, C = 20 µm.

Those $P0^+$ structures appeared in parallel strings. PAM^+ axons were ensheathed by $P0^+$ peripheral myelin. Staining against P0 showed that the detected myelin in the mMS was of peripheral origin. Co-staining of PAM and P0 was not only detected in the bridge areas (Fig. 4.8, A+ B), but also in the lumen of the mMS (C + D). Fig. 4.8 shows exemplary images of myelinated regenerating axons in the mMS of combined treated animals.

4.4.2 Regenerating axons of different origins invade the mMS lumen after mMS + USSC treatment

Since it has been shown that the majority of NF^+ axons not only comprised serotonergic (5-HT^+) and catecholaminergic (TH^+) axons, further characterization of regenerating axons was performed by using different antibodies and tracings as described above. Rostral BDA tracing and corticospinal tract (CST) tracing allowed the detection of further descending and newly regenerating axons. We could identify axons which had regenerated through the rostral mMS bridge (Fig. 4.9 A) into the mMS lumen (Fig. 4.9 C) and through the caudal

mMS bridge (Fig. 4.9 B) reaching even beyond the lesion. In addition, anterogradely labeled axons of the CST, which are known for their poor regenerating capacity, could be occasionally detected in the mMS lumen.

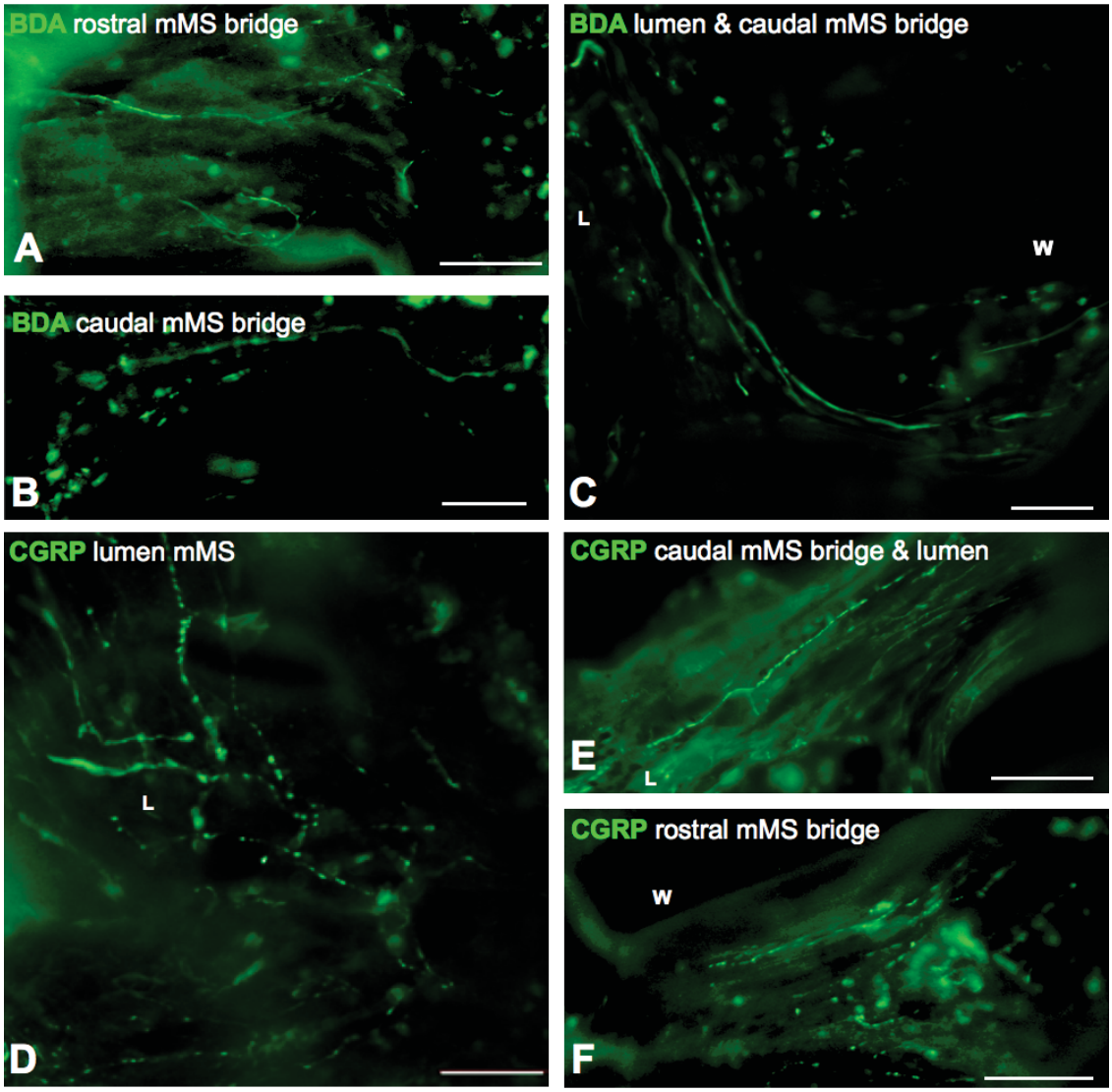

Figure 4.9: **Regenerating axons of different origins invade the mMS lumen**
Numerous axons involved in both motor function (rostrally traced BDA$^+$ axons (A-C)) and sensory function (CGRP$^+$ (D-F)) regenerated into the mMS lumen of combined treated animals. 50 µm parasagittal sections stained for BDA (biotinylated dextran amine, green) and CGRP (Calcitonin gene-related peptide, green). Different regions of the mMS are represented. BDA tracing was performed as described in 3.3 and 3.4. Scale bar = 50 µm, L = lumen of mMS, W = wall of mMS, 19 weeks post operation.

A similar situation appeared in the histological evaluation of ascending axons which are involved in sensory function (CGRP$^+$, Calcitonin gene-related peptide). CGRP$^+$ axons were identified not only in the caudal mMS bridges (Fig. 4.9 E) and lumen of the mMS (Fig. 4.9 E and D), but also in the rostral bridges (Fig. 4.9 F) and even a few rostral to the lesion.

4.5 Combination therapy leads to enhanced functional improvement after spinal cord injury

4.5.1 Combination (mMS + USSC) does not notably aggravate spasticity

Since we observed spastic movement patterns during behavioral testing we developed a scale (Table 3.9) to document the incidence. The results are shown in Fig. 4.10. Most of the animals showed spasticity scores between 1 and 2 resulting in occasional spasms of the tail and toes or of the hindlimbs with a weak amplitude. However, no differences were found between the groups using this assessment procedures that involves merely descriptive aspects.

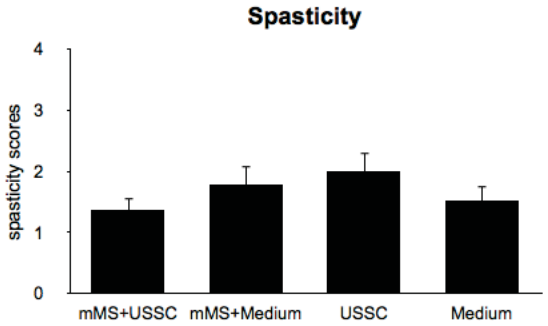

Figure 4.10: **Results of spasticity scoring**
The observed spasticity was measured by using the spasticity score in Tab. 3.9 dependent on frequency, amplitude, and the affected body segment of each animal. Animals of all groups showed spasticity. A significant difference could not be found. Results are shown as means ± SEM.

4.5.2 Improved locomotor function in combination group

As shown in Fig. 4.11 A, the mBBB scores decreased initially after injury and treatment to scores between 0 and 1, reflecting the complete transection of spinal cord pathways. Animals reaching higher mBBB scores in the first week post-injury were excluded from the functional testing due to incomplete transection. Within 5 weeks, a slight increase to average mBBB values of 2 could be observed in all groups. After 6 to 7 weeks a spread of the mBBB scores of the different treatment groups could be noted. Animals of the Medium group remained at level 1 with only weak limb jerks while the other groups improved their locomotor function to the level of rhythmic movements and dorsal foot placement. From wpo 9 to the end of the evaluation period, animals of the Medium group performed significantly lower than the animals of the mMS + USSC group with an average score of 1 - 2 (Fig. 4.11 A). In the same period, animals of the mMS + USSC group reached average scores between 6 - 9 resulting in a frequent movement pattern with coordinated right - left (R-L) alteration and large amplitudes (Fig. 4.11 A). The two monotherapy groups stayed between the two groups with an average performance of 4 - 6 points (Fig. 4.11 A).

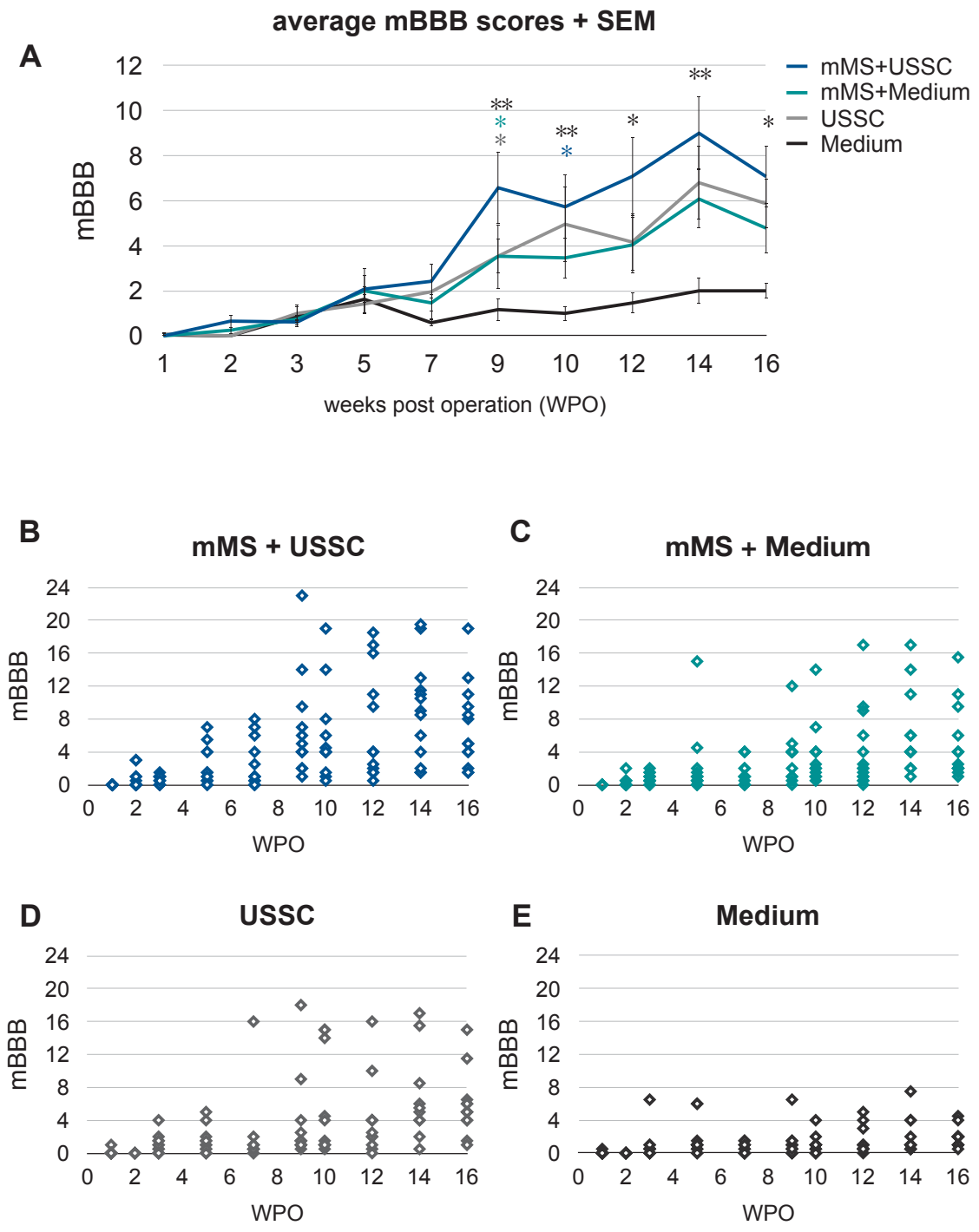

Figure 4.11: **The combination of the mechanical Microconnector System and USSC leads to enhanced functional performance**

(A) Time course of locomotor performance in a long-term study comparing the combined mMS + USSC animal group (n=13), monotherapy 1 (mMS + Medium; n = 14), monotherapy 2 (USSC; n = 13) and control group (Medium; n = 13). (A) Overall locomotor behavior assessed with an open field BBB locomotor scoring using a modified (mBBB) rating scale. Animals which received the combinatory treatment performed significantly better than TX control animals. Results are shown as means ± SEM. * $p < 0.05$, ** $p < 0.01$ (Mann-Whitney U test). Black * = mMS + USSV vs. Medium, cyan * = mMS + Medium vs. Medium, grey * = USSC vs. Medium, blue * = mMS + USSC vs. mMS + Medium.
(B - E) Scatterplot diagrams showing the individual mBBB scores of mMS + USSC (B), mMS + Medium (C), USSC (D) and of Medium (E) treated animals per test day. In contrast to the treated animal groups, none of the control (medium) animals reached a mBBB score of 8 or above.

From week 7 to the end of the observation period, always the same relations between the groups were ascertained. The Medium group always reached the lowest scores. The two monotherapy groups reached approximately the same values with consistently higher scores than the Medium group. Interestingly, the combination of those individually effective treatments led to a further improvement resulting in consistently and significantly higher scores compared to the Medium group (Fig. 4.11 A).

The implantation of the mMS and the transplantation of USSC and in particular the combination thereof lead to higher degree of variation

To show all scores of each individual animal, the data for each group are additionally presented in scatter plots (Figures 4.11 B to E) . Using this method of evaluation, the degree of variation for each group became apparent. The graph shown in Fig. 4.11 A alone would not show the heterogeneities in the groups with the pronounced inter-individual differences given within a group. Obviously, more treated animals (not only with USSC (Fig. 4.11 D) but also with the mMS (Fig. 4.11 C), and especially with the combination thereof (Fig. 4.11 B)) reached higher mBBB scores than animals of the Medium group (Fig. 4.11 E). The Medium group showed only minimal variability. Not a single individual of the Medium controls was able to reach the level of body weight support (Figures 4.11 E). In contrast, some individuals of the mMS + USSS group reached level 4 with mBBB scores around 20, resulting in alternating movements of large amplitude with occasional body weight support and with or without occasional plantar foot placement (Figures 4.11 B). Also, some animals of the monotherapy groups reached mBBB scores of 16 - 18. These values reflect a movement pattern of frequent R-L alternating, large amplitude, and occasional to frequent body weight support (Figures 4.11 C + D).

Animals of the combination group (mMS + USSC) showed higher mBBB thresholds

The histograms (Fig. 4.12 A - E) show the proportion (%) of each animal group that was able to reach the respective mBBB thresholds. All animals of the combination group reached at least a mBBB score of 4, whereas only 33 % of the Medium group reached this threshold. At least 75 % of the mMS + Medium as well as of the USSC group reached this level. More than 50 % of the combined treated animals and still 46 % of the USSC as well as 21 % of the mMS + Medium animals were able to achieve the critical threshold mBBB score 10, where animals show occasional body weight support to the alternating movements. Animals of the Medium group uniformly failed to this hurdle. Clearly, the percentage of animals reaching higher mBBB thresholds was higher in the combination group compared to all other groups (Fig. 4.12).

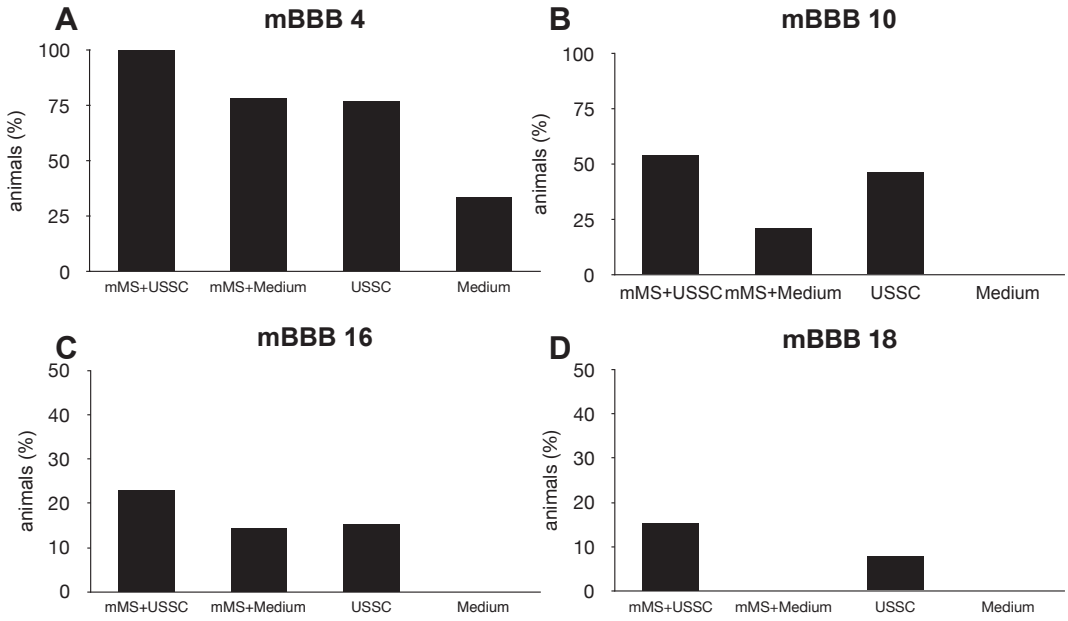

Figure 4.12: **Animals receiving combinatory treatment attain higher mBBB thresholds**

More animals of the combination group (MS + USSC) attained higher mBBB thresholds compared to the monotherapy groups (mMS + Medium or USSC) and the control group (Medium). Values are given as percentage of the number of animals per group.
The percentages of each group are given for the different thresholds: (A) mBBB 4, (B) mBBB 10, (C) mBBB 16, (D) mBBB 18. (B + C) Not a single animal of the Medium group reached the threshold 10 or 16. (D) Only animals treated with USSC (mMS + USSC or USSC only) reached the threshold of 18.

Combination of mMS + USSC results in improved motor function that is superior to the individual treatments

For a concluding presentation of the behavioral study, a non-parametric regression analysis was performed by Dr. Wolfgang Kaisers from the BMFZ (Biologisch-Medizinisches Forschungszentrum) of the Heinrich Heine University Düsseldorf. The curves, which should best represent the relationship between the variables, were calculated based on the scatterplots by using the free language R for statistical computing and graphics and the "ggplot stat_smooth" function. The default level for confidence intervals of 95 % was chosen. The curve progressions of Fig. 4.13 are comparable to those of Fig. 4.11 A and thereby they confirm the results of Fig. 4.11 B - E. The differences are statistically significant whenever the estimated value of one group (curve) lie outside of the range of the 95 % confidence interval (colored area) of another group. As a consequence, we could assume significant differences between all treatment groups compared to the control group (Medium) 6 to 8 weeks after operation. The comparison of the monotherapies (mMS + Medium vs. USSC) revealed no significant differences between them, visible through overlapping of the curves and colored areas. Animals of the combination (mMS + USSC) group further differed from those of both monotherapy groups (mMS + Medium vs. USSC), reaching significance around week 8.

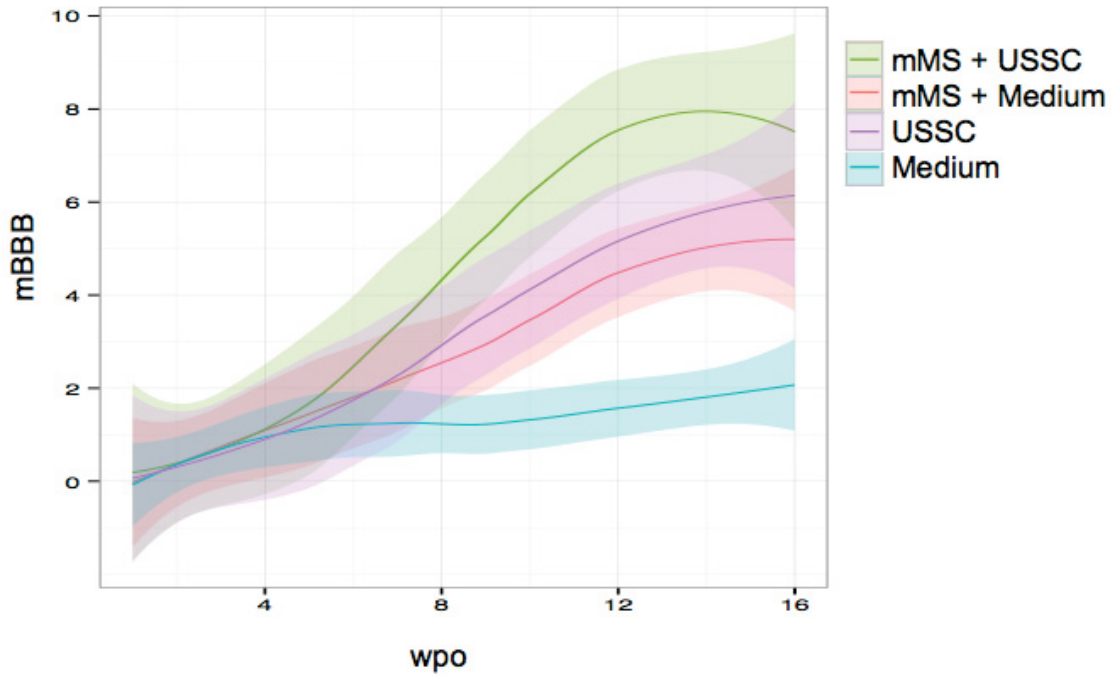

Figure 4.13: **The combination of the mMS and USSC results in improved motor function that is superior to the individual treatments**

Non-parametric regression analysis. Curves represent the relationship between mBBB scores achieved at the considered points in time. The default level for confidence intervals is 95 % and color-coded for each corresponding group. All treatment groups achieved significant functional improvement compared to the control group at approx. 8 weeks after operation. The combination results in improved motor function that is superior to the individual treatments with significant differences to both the mMS + Medium and the USSC group. The differences are statistically significant whenever the estimated value of one group (curve) lie outside of the range of the 95 % confidence interval (colored area) of another group.
The statistical model has been calculated using program R and the ggplot stat_smooth function. USSC = unrestricted somatic stem cells, wpo = weeks post operation, mMS = mechanical Microconnector System, mBBB = modified BBB. (The graphic was created by Dr. Wolfgang Kaisers at the BMFZ (Biological and Medical Research Center) of the University Düsseldorf.)

5 Discussion

Aim of this thesis was to modify and combine two individual therapeutic approaches to enhance functional improvement in a severe spinal cord injury (SCI) model in rats. Here, we could demonstrate, for the first time, that the implantation of the mechanical Microconnector System (mMS) in combination with the transplantation of unrestricted somatic stem cell (USSC) led to locomotor improvement that was superior to the individual treatments. There are a variety of possible aspects for the therapeutic success, which will be discussed.

5.1 USSC promote axonal regeneration by migration to the site of injury

We could demonstrate that USSC migrate into the lesion area of the completely transected spinal cord (Fig. 4.1) of immunosuppressed rats. Furthermore, after its transplantation, USSC were not only detectable in the lesion centre of the completely transected spinal cord, but also in the lumen of the mMS (Fig. 4.1 B and C). These observations confirm previous results where USSC were grafted in close proximity to a traumatic spinal cord injury [101]. The two studies merely differ in the type of spinal cord injury. Schira *et al.* transplanted USSC after dorsal hemisection, whereas in the present study USSC were grafted after complete transection and after implantation of the mMS, respectively. In contrast, USSC remained at the injection site when grafted into the uninjured spinal cord, which indicates that USSC are attracted by the spinal cord lesion site [101]. Since USSC were harvested from human umbilical cord blood, immunosuppression was necessary for survival of the stem cells in the environment of rat spinal cord. USSC survive for 3 weeks until withdrawal of immunosuppression.

The migratory potential of USSC is not unique for this type of stem cells. Other research groups have described the potential of migration of different types of stem cells (e.g. NSC [125] and MSC [126]) as well as in different lesion models (e.g. contusion [126, 127], clip injury [86], and hemisection) involving various animal species. Whenever the source and host of the stem cells differ in their origin of species, immunosuppression is essential for the survival of the cells. Another way to prevent rejection is the transplantation to animals of immunodeficient species [127].

In vivo and *in vitro* experiments can provide evidence for cell migration. In previous studies, various chemoattractants could be detected which initiate and accomplish the targeted migration. Among these are the stromal cell-derived factor 1 (SDF-1) [128, 129] and the hepatocyte growth factor (HGF). Schira *et al.* identified HGF as the responsible chemoattractant for USSC migration in SCI using an under-agarose chemotaxis *in vitro*

assay. Neutralizing HGF with a specific antibody (anti-HGF-AB) limited the migration of USSC [98]. The expression of the HGF receptor c-Met in USSC could be demonstrated previously, as well as the migratory potential after neuronal injury depending on HGF up-regulation [130].

Thus, our observations are in accordance with recent studies regarding the migratory potential of various stem cell types. Migration of transplanted stem cells is widely considered as absolutely essential to facilitate secretion, differentiation, axonal regeneration, and remyelination, as well as prevention of secondary damage and cyst formation *in situ*. Thereby stem cells can act as therapeutic delivery vehicles. The migratory potential of USSC is a natural advantage and opens up new possibilities relating to the release of therapeutic molecules into the lesion centre.

5.2 The mMS - an approach to combine different regenerative strategies in a single device

The results regarding the general tissue preservation reveal that the implantation of the mMS in combination with the transplantation of USSC led to stabilization of the spinal cord after a complete transection injury in rats. In most cases, the mMS device was inserted straight in the spinal cord and completely filled with spinal cord tissue. We could demonstrate the ingrowth of new vessels in close association with regenerating axons at long survival times. These observations confirm previous results of our research group [66]. On the one hand, these results are important for the reproducibility in the field of SCI [131] and, on the other hand, they are essential conditions for further assessments. Structural stability is one of the desirable properties of non-biodegradable bridging devices [52]. In accordance with preceding studies, tissue shrinkage at the lesion site was more common in the control groups without mMS implantation [66]. Retraction of the spinal cord stumps out of the mMS device was not observed in any case, even after release of the vacuum. This fact might be important for the therapeutic success of the mMS.

In the introduction, properties for ideal bridging devices are described; a schematic representation is given in Fig. 1.4. Some of the requirements have been met, some of them have not been met by the use of the mMS. In the following, some of these key elements (described by Straley *et al.* in 2010 [64]) and their practical realization in the mMS are discussed in detail:

- Mechanical Strength: It can be generally considered that mechanical properties should be similar to native spinal cord [62]. The question could arise whether the implantation of a relatively stable material into the environment of the elastic, gel-like consistency of the spinal cord causes further trauma. Indeed, those differences are obvious and the reason why some research groups prefer the use of gels [132]. Hydrogels have the internal properties to mimic the chemical, physical, and mechanical properties of the spinal cord tissue to promote cell adhesion and axonal regeneration [133]. In contrast, our observations revealed good integration of the mMS into the spinal cord and, moreover, the stabilization of the spinal cord without causing additional tissue damage by a foreign body reaction. Furthermore, the honeycomb structure provides high mechanical stability with minimal

material [66]. Additional advantages would be implicated by the use of a biodegradable version of the mMS, which is described in the following section.

- Biocompatibility / Biodegradability: Biocompatibility is a critical design parameter and crucial for axonal growth. Therefore, significant *in vitro* testing is important to additionally determine the regenerative capacity of a material [134]. Modifications of the surface are possible and partly essential to facilitate and enhance axonal regeneration. The mMS devices have passed numerous of such pre-tests. The potential for axonal regeneration could be demonstrated in several independent experimental studies. Briefly, biocompatibility and integration of the mMS were adequate, apparent by trichrome staining (see Figure 4.2) and ED1 staining. Additional pilot testing of a biodegradable version is on-going and initial successes could be achieved (data not shown). A biodegradable mMS would combine the optimal structural stability at early time points after the implantation with the possibility to regain flexibility after its degradation. The optimal time frame of degradation must be determined and tested to promote axonal regrowth by allowing the material to be replaced by regenerating cells and their extracellular matrix (ECM) [64].

- Channel system: Directed axonal regrowth can be facilitated by a longitudinal channel system of bridging devices [63]. Specific channel systems have been developed to mimic spinal cord tracts [63]. Thereby, tract-specific treatment would be conceivable [63]. Axonal regeneration further depends on the number and the diameter of these channels [135, 66]. The mMS is in concordance with such designs, due to its honeycomb structures. Additionally, the design is adapted for the rat spinal cord and can be adjusted depending on the extent of the lesion and on the treated species. The opportunity of adjustment is important for a potential clinical application.

- Cell adhesion / surface quality: The surface properties are critical for tissue cohesion. The effective roughened surface of the mMS' walls has to be large enough for an optimal adhesion of the spinal cord tissue after vacuum release. At the same time, the adhesion should not be too strong in order to prevent further injury due to the high forces needed to suck the tissue into the system [66]. Pre-tests revealed the need for optimization. Further modifications led to an optimized tissue stability within the mMS. The roughness was adjusted to support adhesion without disruption. Stump retraction was not observed.

- Porosity: As already outlined by previously [66], the mMS is designed without pores, although various bridging devices utilize pores for diffusion of nutrients and cells [62]. The mMS does not require additional pores because regenerating axons are provided with nutrients by the tissue within the lumen and subsequently by neovascularization (Fig.4.5) [66]. Additional important structures of the mMS are the four internal micro-channels which, allow a precise long-term drug infusion into the lesion center (see Fig. 3.1 C and D). Common delivery methods of drug application such as oral and intravenous administration are restricted after SCI since the diffusion of drugs across the blood-brain barrier is temporary and limited. [133]. The possibility of local drug application through the internal channel system of the mMS is a big advantage over other designs since direct and controlled drug application is facilitated by avoiding the blood–brain barrier.

- Electrical activity: The hypothesis that electrical stimuli have a positive influence on axon growth and remodeling led to the development of electrically active materials [64]. These modified guidance channels offer the ability for localized electrical stimuli to promote

axonal regeneration and growth directionality. This characteristic is often incompatible with some of the other properties such as biodegradability and cell adhesion [64]. Further studies with coated mMS for electrical stimulation are in progress.

- Internal matrices: Internal matrices have been implanted into injured spinal cord with the intention to increase the bioactivity of nerve guidance channels and to prevent their collapse [64]. Numerous materials to fill the implanted scaffolds have been investigated [64, 136]. Hydrogels, which are also being tested and established as independent regenerative scaffolds, have been frequently used for this purpose [132]. Using a vacuum pump to reconnect the separated spinal cord stumps after SCI, the mMS is completely filled with the original spinal cord tissue. Thereby, it is unlikely that the device would collapse and indeed we never observed this phenomenon. Complete filling is also important to prevent overturning of the mMS. An additional filling of the device was neither required nor implemented. It has to be considered whether filling with additional material might be useful. A potential application of growth factor solutions would be possible at different time points using the additional tubing system. Results of the histological evaluation regarding the general tissue preservation revealed the consistent filling within the mMS for the entire period of the long-term study.

Different key parameters (Fig. 1.4) have been reviewed and discussed here with regard to the practical realization of the mMS. Various of these requirements have been realized in the design of the mMS already. The realization and development of the mMS design was achieved in close cooperation with the Institute of Microsystems Technology (Technical University Hamburg-Harburg) and the BG Trauma Hospital Hamburg (Department of Trauma Surgery, Orthopedics and Sports Traumatology). Communications between biomaterial designers, neurobiologists, and surgeons are essential for the success of such a project.

In conclusion, the mMS is a promising device to adapt and stabilize the injured spinal cord. The field of application can range from severe traumatic injury with large tissue damage to substantial tissue loss after surgical resection of scar tissue (e.g. in chronic patients). Various of the key design properties are already implemented, other properties will be optimized. For example, a biodegradable mMS system is currently tested. The realization of every single key design parameter is not mandatory for a proper function. The reconnection of the separated stumps alone can be very effective. The mMS system is highly suitable for combination therapies e.g. due to potential (long-term) drug application via the tubing system to which a mini-pump can be connected.

5.3 Cyst formation - an insuperable barrier for axonal regeneration and functional improvement?

Tissue preservation, including the prevention of cyst formation, is generally considered as an important requirement for axonal regeneration and functional improvement after SCI [137, 138].

In contrast to previous studies, we observed more cyst formation while evaluating the general tissue preservation. Thus, we decided to further assess the influence of the different

treatment strategies on cyst formation. To investigate whether the mMS implantation, USSC transplantation, and the combination thereof could prevent cyst formation and enhance tissue preservation after SCI, the lesion size, spared tissue, and the total cyst area was measured. Additionally, the relative proportion of the cyst area to the rest of the tissue were quantified in all animal groups and compared as described elsewhere [139] with minor modifications. In the present study, we observed increased cyst formation compared to our previous studies [119, 98, 66]. Particularly, and in contrast to Brazda *et al.* [66], histological evaluation revealed enhanced cavity formations. Pressure force and duration of the vacuum application were considered as possible causes. All data of the minimally varying pressures were documented in the OP protocols. Significant differences between the applied pressures could not be determined and no correlation was found between pressure forces and cyst formation. Moreover, the observed cyst formation in the USSC and control (DMEM) groups could not be explained by changes regarding the mMS since the latter device was not implanted in both of these animal groups. Newly created short-time experiments revealed the different breeders as the most likely cause for the differences to our previous studies. Interestingly, rats of the control group showed more pronounced cyst areas compared to all other groups.

The importance of cyst prevention for functional improvement could be detected by comparing previous and present behavioral data of our research group. Increased cyst formation might explain the lower mBBB scores of the control groups.

The work presented in this thesis demonstrated the positive influence of USSC, the mMS, and, in particular, the combination thereof regarding to cyst formation. These observations are in accordance with other research groups, who highlighted the therapeutic success of different treatments. Pearse *et al.* described a significant reduction of cavitation following the transplantation of Schwann cells and olfactory ensheathing glia after contusion injury [140]. Pretreatment with methylprednisolone (MP) and Interleukin-10 (IL-10) further reduced cavitation [140]. In 2008, those results could be reproduced by Someya *et al.* using a similar experimental setup [139]. Both research groups used Schwann cells for subacute (1 week after SCI) transplantation after contusion injury. The two studies clearly differ in their source of Schwann cells, either obtained from sciatic nerves or derived from bone marrow stromal cells [139, 140]. Someya *et al.* discuss neuroprotective effects of Schwann cells by secreting different growth factors [139]. Similar mechanisms and functions of USSC related to neuroprotection have been described previously [102, 98]. SDF-1 (stromal cell-derived factor-1), HGF (hepatocyte growth factor), and VEGF (vascular endothelial growth factor) are examples of USSC-released factors with known neuroprotective effects [102]. The neuroprotective potentials of different stem cell types achieved through secretion of trophic factors and modification of inflammation are reviewed by Tetzlaff [71].

In addition to the molecular effects of different cell types, mechanical strategies appear to be supportive for the reduction of cyst formation. Dura closure as the simplest mean of surgical intervention seems to have beneficial effects [58]. Interestingly, Teng *et al.* implanted a polymer scaffold seeded with neural stem cells in the injured spinal cord after hemisection and tissue aspiration [141]. They observed cyst formation in some of the cells-only and lesion-control animals, but not in the animals treated with scaffold plus cells or scaffold-only animals. They hypothesized that the scaffold might impede

scarring and subsequent cyst formation . More importantly, they highlighted tissue preservation as the primary factor accounting for the improved locomotor function in the scaffold plus cells group [141]. In addition, Hakim *et al.* [142] emphasize that scaffold implantation results in reduced cyst formation. Significant reduction of cyst area was observed in polymer-implanted animals compared to transection-only animals, whereas no differences between polymer-implanted animals with or without Schwann cells were found [142]. Further combination of different treatments, such as a three-dimensional gelatin sponge scaffold and BM-MSC [143], led to the reduction of cavity formation in a severe SCI model. Additional groups demonstrated a decrease of cyst formation through implantation of scaffolds and transplantation of stem cells [134]. In some of these studies, a stronger effect of one of the combined treatments was shown. The respective effects of the individual treatments with USSC and mMS on cavitation appear to be very similar without a significant predominance of one of these treatments. A further reduction of cyst formation which is superior to those of the individual effects can, however, be achieved by the combination of both treatments.
Sharp *et al.* observed large cavities after scar removal [144]. This observation will gain importance in view of clinical application. In chronic patients, cyst formation after surgical scar removal might be detrimental for the functional outcome. Therefore, therapies to reduce and prevent cyst formation have to be developed. First, underlying reasons for cyst formation need to be further investigated. A possible explanation for cyst development might be secondary injury processes, similar to the tissue response after the acute injury as described in the introduction (for graphic representation see also Fig. 1.1). Already in 1999, Fitch *et al.* postulated that cascades of secondary tissue damage are responsible for progressive cavitation [138]. Detailed mechanisms of cyst formation are still not well understood and thus need to be investigated in the future.

The finding that the mMS is capable of reducing cyst formation is very important, particularly with regard to potential future clinical application. The mMS was also developed with the purpose to adapt and stabilize the injured spinal cord after surgical resection of scar tissue (e.g. for chronic patients). It is likely that effective therapy will require suppression of secondary injury and prevention of cyst formation.

5.4 Vascularization - a key element for axonal regeneration?

Blood vessels (BV) provide spinal cord tissue with nutrients and oxygen, as long as they are intact. Following SCI, numerous BV are directly or indirectly disrupted. Devascularization seems to be victim and contributor of secondary injury processes at the same time. Disruptions of BV result in ischemia, loss of autoregulation and microcirculation, hemorrhage, vasospasm, thrombosis, and electrolyte imbalances due to breakdown of the blood-brain barrier [145]. The endogenous angiogenesis often fails to establish proper vascularization [124].
For these reasons, vascularization seems to be one of the key regulators of axonal regeneration. Different therapeutic approaches have been shown to promote or enhance the growth of new vessels [124], e.g. different biomaterials [61]. VEGF is one of the key regulators of blood vessel formation [124, 146]. Attention should be paid to a proper

dosing when applying of VEGF as a therapeutic agent for SCI. A low dose can only achieve little effect, but a high dose can lead to vessels with morphological and functional changes or abnormalities [124]. Moreover, re-introduction of oxygen (reperfusion) can induce apoptosis (reperfusion injury) of neurons that initially survived causing extensive damage [124].
Besides those side effects, early revascularization is essential for the repair of tissue after SCI. The same applies to cells located in the center of scaffolds, which are also depending on adequate oxygen and nutrition supply. On this account, vascularization of the biomaterials is also very important [143]. As shown in Figure 4.5, regenerated blood vessels crossed the junction between mMS and the host tissue in the mMS + USSC group, suggesting that the tissue within the mMS became vascularized.
USSC and blood vessel formation seem to have complex interactions. As described above, formation of blood vessels is important for repair and survival of cells, including transplanted stem cells. On the other hand, stem cells, including USSC, have the potential to increase blood vessel formation. Insufficient angiogenesis leads to low stem cell survival rates. Thus, the survival and therapeutic efficacy of stem cells depends to a large extent on successful angiogenesis [124, 147]. We examined vascularization at 19 weeks post operation. In order to make a precise and explicit statement to early stages of revascularization further studies would be required.
Differentiation to endothelial cells or secretion of growth factors as well as paracrine effects are potential mechanisms of stem cells to enhance vascularization. USSC release various trophic factors, including VEGF [102]. VEGF was further described to exert neuroprotective effects [146]. We detected the highest blood vessel density in the mMS + USSC group (Fig. 4.6 B). However, no significant differences between USSC and Medium-treated groups could be observed with regard to tissue sparing (Fig. 4.4 H) and blood vessel density (Fig. 4.6 B).

Although there is general agreement about the importance of BV formation as a requirement for tissue preservation, axonal regeneration, and, consequently, functional improvement, there is still uncertainty about the quantity and quality of new blood vessels [124]. It should also be noted that statements to functionality of regenerated blood vessels cannot be provided just on the basis of immunohistochemical staining.

5.5 Axonal regeneration - an overestimated goal?

5.5.1 Which therapeutic approaches enable axonal regeneration after spinal cord injury?

As already pointed out in the introduction, improved axonal regeneration is a key goal in SCI treatment. It has been shown that regrowth of only a few axons can lead to the improvement of some important motor or sensory functions [41]. Tissue preservation, reduced cyst formation, and vascularization alone do not sufficiently explain the improved functional outcome in the mMS + USSC combination group. Neither the spared tissue (see fig. 4.4 H), nor vascularization (see fig. 4.6 B) showed significant differences between these groups. These results give rise to the assumption that axonal regeneration should

definitely be discussed as a possible reason for functional recovery. But which conditions have to be met for successful axonal regeneration?

There is a broad agreement that axonal regeneration is dependent on a balance of growth promoting and growth inhibiting molecules at the site of injury [148, 25, 149]. Many research groups have focused on identifying the factors and mechanisms which are responsible for the failure of regrowth with the aim to improve axonal regeneration. Based on this knowledge, a broad variety of repair strategies have been investigated. Growth factors and molecules that suppress inhibitors of neuronal regeneration are able to promote axonal regrowth by providing a more permissive environment [150]. The application of neurotrophic and other growth factors is one major strategy in experimental SCI. Neurotrophic factors, such as brain-derived neurotrophic factor (BDNF) [151] and Neutrophin 3 (NT-3) [152], promote axonal regeneration and functional recovery and enhance sprouting and neuronal survival [153]. Axonal regeneration has also been achieved by blocking the inhibitory effects of myelin due to immunological neutralization [49, 36], inhibition of Rho or cAMP (cyclic adenosine monophosphate) signaling pathways [154, 155], by suppression of fibrous scarring to prevent accumulation of inhibitors which boost the non-permissive environment, e.g. through application of an iron chelator 2,2'-bipyridine-5,5'-dicarboxylic acid (BPY-DCA) [50, 28, 51], by enzymatically counteracting inhibitory proteoglycans in the ECM via Chondroitinase ABC [156, 157], or by introduction of matrices, scaffolds, and other bioengineering strategies [52]. Cell and tissue transplantation, e.g. of peripheral nerve grafts [158, 159], Schwann cells [53], macrophages [54], olfactory ensheathing glia (OEG) [55, 160], and stem cells have the potential to support axonal regeneration. Beneficial effects are attributable to the replacement of lost cells, guiding regenerating axons and/or secretion of trophic factors. Especially the potential of stem cells reached great interest for SCI research, recently [73, 71]. Human and rodent ESCs have been transplanted into various animal models of SCI either as monotherapy or in combination with other established approaches [161, 162, 163]. Transplantation often led to both neuronal regeneration and functional recovery.
Tissue loss and cavity formation are consequences of SCI. Not only the non-permissive environment, but also a physical gap impede axonal regeneration. Therefore, it is likely that effective treatments will include strategies to replace lost tissue and to re-attach spinal cord stumps after complete SCI or scar resection. Several strategies to bridge this tissue gap have been developed and described, such as implantation of guiding channels, matrices, or scaffolds [64, 69, 52].

The present data provide evidence that the implantation of the mMS and the transplantation of USSC promote axonal regeneration after severe injury of the spinal cord. The combination leads to a further increase in axonal regeneration which is superior to the individual effects. For comparison with the current literature it is important to consider the severity of the SCI model, since it has been shown that axonal regeneration is often insufficient after complete transection of the spinal cord.
Yang et *al.* also showed enhanced BDA-positive fibers in the transplanted groups (transplantation of human umbilical mesenchymal stem cells) compared to the control group. Comparable with our results, the number of BDA-positive fibers, which spread through the lesion, was significantly lower than the number of BDA-positive fibers rostral to the lesion [164]. In addition, a large number of neurofilament-positive axons was detected in the

treated group [164]. A further characterization of the different origins of the neurofilament axons (e.g. 5-HT & TH) was not performed in this study.
In 2012, Lu et *al.* presented significant progress toward the goal of axonal regeneration following complete transection of rats' spinal cord. Two weeks post injury, they transplanted rat or human embryonic spinal cord neuronal stem cells suspended in a cocktail of growth factors (e.g. NT-3, BDNF, IGF-1, and HGF) and Calpain inhibitor embedded into a fibrin matrix. This cocktail improved the survival, growth, and integration of the transplanted stem cells and led to impressive long-distance axonal outgrowth. These early-stage neurons were sufficient to overcome the axon growth barriers in the adult CNS [68]. Among others, they grafted neural stem cells/progenitors from green fluorescent protein (GFP)-expressing rat embryos to track their fate, integration, process extension, and differentiation within the inhibitory milieu of the adult CNS [68]. Graft-derived spinal cord neurons extended large numbers of axons into the host spinal cord over very long distances [68]. Interestingly, the treated animals exhibited a significantly improved functional outcome with BBB values of 6 to 7 resulting in extensive movements of two to three joints [68]. Although we did not detected comparable lengths of regenerated axons, the animals of the combination group reached an improved functional outcome similar to the results of Lu et *al.*
In accordance to our results, Gao et *al.* observed excellent integration of an implanted scaffold four weeks after complete transection and implantation [165]. GFAP labeling also showed a partial upregulation of glial reactivity at interfaces with the lesion site. In addition to the anterograde BDA tracing of the reticulospinal tract, they immunohistochemically labeled serotonergic axons with an antibody directed to 5-HT [165]. The detected axonal growth was highly linear in orientation. A significantly greater number of axons penetrated scaffolds pre-filled with bone marrow stromal cells compared to the cell-free scaffolds. The penetrated axons spanned the full length of the lesion area; similar to our results demonstrated in fig. 4.5, 4.7, 4.8, and 4.9. However, Gao et al. did not observe motor axonal regeneration beyond the scaffold. In contrast, we could detect axons that regenerated beyond the lesion zone and the mMS. A comparison regarding the functional relevance did not include the locomotor evaluation.

In conclusion, it should be emphasized that axon growt and the description of location and origin of regenerated axons can easily be over-interpreted. The presence of regenerated axons alone does not provide sufficient evidence for an improved functional outcome. Therefore, the collected informations regarding axonal regeneration, tissue preservation, remyelination, vascularization, and functional outcome will provide a measure for the overall effectiveness of a treatment.

5.5.2 Remyelination - important for the proper function of the regenerating axons?

Demyelination (loss of myelin) and dysmyelination (abnormal myelination) are typical consequences of CNS injury and contribute to further functional disability [166]. Demyelination is caused by prolonged and dispersed oligodendrocyte cell death [167]. The process of spontaneous, endogenous remyelination is often insufficient and characterized by shorter internode segments, thinner myelin sheaths, and missing relationship between

axons and myelin [167, 166]. Regenerating axons require compact myelin sheaths for axonal conductance, nutrient supply, and, consequently, for proper function [168]. Thus, it is important to investigate the functional relevance of remyelination. The extent and quality of remyelination should be stringently correlated with functional parameters such as locomotion, sensory function, and autonomic functions [166]. Extensive remyelination has not been achieved under experimental conditions so far [166], although remyelination is hypothesized to be beneficial for functional recovery after SCI and it is target of numerous research groups [167]. This hypothesis is based on findings that remyelination is able to enhance functional improvement [167]. Different approaches exist to promote remyelination, of which the two most promising are: (1) Induction of endogenous oligodendrocytes (either progenitor cells or mature oligodendrocytes); and (2) transplantation of cells which have the intrinsic potential to produce myelin [166]. The application of chemokines, cytokines, and growth factors can support and/or enhance induction of oligodendrocytes in various experimental models. The approach to transplant cells with intrinsic remyelination potential was sufficiently tested with Schwann cells [53], olfactory ensheating glia [160], and stem cells (e.g. BMSC [169]) [166].

In order to investigate remyelination in our experimental setting, immunohistochemical staining against P0, a distinct marker of peripheral myelin, was performed. We found numerous regenerating axons (PAM-positive) in close associations with P0, suggesting remyelination of axons within the mMS from peripheral cells. Possible explanations for the origin of these myelin-producing cells need to be studied. Previous results of mMS treated animals indicate Schwann cells as a contributor for the compact myelin sheaths, confirmed using electron microscopy. The fact that endogenous Schwann cells migrate, proliferate, and invade into the injured spinal cord has repeatedly been demonstrated [170]. Several strategies and treatments have been considered to regulate and support their migratory potential. First, the question why these peripheral cells invade the injured CNS have to be answered. Under normal circumstances, Schwann cells are strictly located in the peripheral nervous system (PNS). These cells are rigorously separated from astrocytes by the *glia limitans* [170]. Injury-induced breakdown of the *dura* and *glia limitans* facilitate peripheral Schwann cells to migrate from the dorsal root entry zone to the lesion site [170]. Alternative sources of Schwann cells and their precursors such as bone marrow have to be detected using reliable labeling techniques [170]. Relevant knowledge about mechanisms and function of Schwann cells regarding myelination could be gained from their transplantation into the injured spinal cord [71]. Schwann cells are one of the most commonly transplanted and thus most extensively studied cell types for treatment of SCI [71]. Crucial studies for our understanding of the potential of Schwann cells are reviewed by Oudega and Xu in 2006 [170]. Tetzlaff and his research group transplanted skin-derived precursors of Schwann cells and Schwann cells isolated from peripheral nerves into injured spinal cord to examine and establish a potential source for autologous Schwann cells for SCI [171]. They observed a more robust endogenous Schwann cell response in the group of transplanted Schwann cells either skin- or nerve-derived. Remarkably, our findings of remyelinated axons did not need the application of Schwann cells or their precursors.

Whether recovery of axonal function was a consequence of remyelination in our model remains an open question. Supporting evidence for this hypothesis comes from the morphological studies of the myelin sheaths. We could observe parallel bundles of myelin

which seemed to resemble a physiological structure around the axon. We could visualize P0-positive structures close to the (PAM-positive) axons. The rostro-caudal orientation of these P0-positive structures around the axons is predominantly perceivable in the bridge of the mMS. The organization within the mMS lumen appears more random. Whether this morphologic disposal can be influenced by different treatment approaches will be an important issue in future studies.

In previous experiments from our group, axonal remyelination could be obtained without transplantation of USSC. These data demonstrate that transplantation of USSC is not indispensable for the remyelination of axons. In contrast, in the current study, the remyelination only in mMS + USSC treated animals has been investigated. It would be interesting to further analyze differences between the treatment groups (with/without USSC) to examine the influence of USSC on remyelination. The fact that remyelination can be observed with and without transplantation of stem cells raises numerous questions: Will paracrine secretion of molecules and neurotrophic factors further enhance and support remyelination? Did remyelination contribute to the improved locomotor function in the combination group?

The fact that regenerating axons were coated with myelin are important findings and might contribute to the observed functional improvement after SCI.

5.6 Functional improvement after combination therapy

5.6.1 Spasticity - Limitation or support for functional improvement?

Spasticity is a common condition arising after disorders of the CNS. Stroke, multiple sclerosis, and SCI typically lead to spasticity [172]. Uncontrolled, rhythmic, and clonic muscle spasms additional affect the quality of life of patients suffering from SCI [173]. Exaggerated reflexes caused by descending overactivity seem to be responsible for muscle hypertonia resulting in a spastic movement disorder [174, 172]. Pathophysiology of spasticity is multifactorial and therefore it is difficult to develop a convincing animal model. Symptoms appear over time excluding loss of inhibitory supraspinal projection as a single cause. Additionally, secondary processes seem to be involved [173].

In accordance with other research groups we observed clinical signs of spasticity in our model rising over time [174, 173]. During functional assessment, we documented observations of clinical signs of spasticity (Fig. 3.11). Spasticity was scored on a scale from 0 to 10 according to Table 3.9. Some animals showed aberrant and exaggerated tail and hindlimb movements. Care was taken not to misinterpret those movement disorders as normal locomotion patterns with large amplitudes.

Significant differences between the four groups could not be observed using our scoring system, impeding further correlation to functional improvement or histological findings. While this newly established scoring system was very well applicable for our experimental setting, it cannot be easily compared with more complex analyses applied by other authors. Reevaluation of the groups using the scoring system established by Bennett et *al.* in 1999 [174] might be a useful strategy in future studies focusing on spasticity. In the current

study, this score was not applicable since it was developed to evaluate spasticity following sacral spinal transection. Movement disorders of hindlimbs are beyond the observation spectrum of the Bennett scale. Only muscle tone and spasm of the tail were taken into account. Different conditions of the assessment can affect the level of movement disorder: passive (clinical), active nonfunctional (laboratory setting), and functional (walking) [172]. These conditions refer to clinical assessment of humans. Variations in the level of spasticity in animals, here rats, might be expected. No further analysis was performed because these observation had no therapeutical consequence and the rats did not appear to be severely impaired.

Particularly with regard to clinical application and conditions in humans, spasticity should not be ignored due to significant influence on the quality of life. In humans, the (modified) Ashworth scale (MAS / AS), the spasm frequency score (SFS), as well as the Reflex score (RS), and the Functional improvement (FIM) are commonly used scoring systems to evaluate spastic and functional outcomes before and during therapy [175]. Treatment should focus on the training of functional movements instead of treating isolated physical signs, such as reflexes [172]. Intrathecal infusion of baclofen can reduce spasticity in chronic SCI (reviewed by McIntyre et *al.* [175]). Further studies will be required for a better understanding of the pathophysiology and development of novel therapies.

5.6.2 Combination of mMS and USSC facilitated functional improvement

The evaluation of functional improvement as well as the question whether the combination is superior to the monotherapies and control groups, were main focuses of this thesis. Loss of locomotor function is regarded as one of the most restrictive conditions for patients suffering from SCI. Therefore, it is likely, that functional improvement or even recovery is the overall aim of SCI research. Even the recovery of only few and small movement patterns can considerably improve the quality of the patient's life.
Schira et *al.* provided evidence in rats that the transplantation of USSC from human umbilical cord blood significantly enhance axonal regeneration and functional improvement [98]. In addition, our research group could demonstrate that implantation of mMS leads to successful reconnection of the separated spinal cord stumps [66] as well as functional improvement (manuscript under consideration).
To verify or falsify the hypothesis that the combination therapy is superior to the individual therapies, observations of locomotor behavior were performed in a 16 week long-term study under blinded conditions. Locomotor function was assessed using the modified Basso, Beattie and Bresnahan (mBBB) rating scale [119]. Results of the functional assessment are shown in Fig. 4.11, Fig. 4.12, and Fig. 4.13. We could show a functional improvement after the individual therapies and demonstrated that the combination therapy was superior to the individual ones. Animals that underwent mMS + USSC treatment showed significantly and consistently improved open field test results than the (Medium-treated) controls. Obviously, more animals of the combination group reached body weight support, clearly visible when analyzing the scatter diagrams (Fig. 4.11 B - E) or the graphs to the different thresholds (Fig. 4.12 A - D). Potential reasons for the functional improvement have already been described and discussed above. A complex interaction of tissue stabilization, prevention of cyst formation, vascularization, axonal regeneration, as well as remyelination

seem to be responsible for the improvement of function. Each aspect is part of the whole and contributes to the overall success.

After the surgery, mBBB values decreased to scores between 0 and 1. This was an important observation to ensure that the transection was complete. Transection of the spinal cord interrupts the electrophysiological signal transduction, resulting in the acute loss of locomotor and sensory function. Local tissue inflammation, cyst formation, and demyelination of undamaged axons occurs days to weeks after the initial trauma. Those events might be responsible for a further exacerbation of the deficits over time [65]. In accordance to other research groups [176, 177], treatment-induced benefits started to become apparent around week 7 post operation.

5.7 Combinatorial therapies - The optimal way to maximize therapeutic effects?

The pathophysiology of SCI is multifactorial and multiphasic and it is likely that effective treatments will require combinations of different strategies. The complexity of the secondary response, involving numerous molecules, factors, and different cells, makes it obvious that SCI is not a "one-molecule or one-cell problem" [65]. Before combining different approaches it was important to discuss and consider the following questions: Which of the approaches established in our laboratory are best suited for combination therapy? What are the effect of the individual treatments? Which effects can be expected by combining? How do treatments affect each other? Do we expect additive and synergistic effects? (If not, why should we combine them?) Which effects might be antagonistic? In our specific case: Will USSC survive within the mMS? Or does the surface of the mMS reduce the survival of the USSC? These and other questions should be considered in advance to reduce unnecessary costs and work as well as the number of animals.

Optimal timing of individual treatments

Further questions refer to the optimal timing of individual treatments. Oudega et *al.* [65] have reviewed and considered the timing of treatmentaccording to the pathophysiological processes. The optimal timing of cellular transplantation has been widely discussed, as the survival of cells is governed by secondary damage including inflammation and apoptosis [65]. For example, neuroprotective strategies appear to have a greater potential when applied immediately after, whereas application of cell-based therapies seems to be more successful at later stages (depending on the applied animal model) [65]. As a consequence, various research groups delay cell transplantation until one week after the initial trauma to avoid poor survival rates [162]. In order to guarantee comparability with previous data, where we achieved good results regarding cell migration and survival, we decided to perform cell transplantation immediately after SCI [98] and mMS implantation.
In general, the majority of SCI patients are in a chronic state. However, most of the studies used acute SCI models, since experiments of chronic SCI often involve higher rates of complication and mortality. Consequently, these experiments require higher numbers of animals [65]. More studies addressing the use of chronic SCI models are needed before

clinical application of different treatments in chronic patients. An additional aim of this study was to pave the way for the implantation of the mMS in a chronic SCI models. Fundamental knowledge to mMS implantation, movement behaviors, and histology of the spinal cord sections could be gained.

Replication and Reproducibility

Replication and reproducibility are fundamental missions in SCI research [131]. Only one of more than 12 studies of experimental SCI has been successfully replicated [131]. Therefore, we aimed to achieve functional improvement and axonal regeneration comparable to our previous results. Independent replication in accordance with the National Institute of Neurological Disorders and Stroke (NINDS) and their program "Facilities of Research Excellence — Spinal Cord Injury" (FORE—SCI) would be desirable [131]. Reasons for deviating results, such as increased cyst formation as potential contributors of comparably lower mBBB values, should be analyzed critically.

The mMS device offers excellent conditions for combinatorial treatment

Our previous results of USSC transplantation and mMS implantation in the acute injured rat spinal cord was successful with regard to axonal regeneration and functional improvement. Explanations why the mMS seems to be a highly suitable device for combinatorial treatments are given in chapter 4.2. and by Brazda et *al.* [66]. The properties of the mMS are listed and explained in detail and the corresponding benefits are highlighted. Importantly, the effects in the examined parameters were larger with the combination than either of the treatments alone, suggesting additive effects of the individual treatments. Combination leads to reduced cyst formation, enhanced axonal regeneration and improved locomotor function that is superior to the individual treatments.

The present thesis demonstrated the successful combination of two individual effective treatments. Further combinations and/or modifications are conceivable. The mMS offers excellent conditions for novel combination therapies in the future. The complexity of the potential interactions between individual components of a combination therapy should be taken into account.

Clinical translation of combinatorial treatments

With regard to clinical translation, it is important to realize that the complexity of clinical trials is far beyond the scope of animal models. Apart from safety aspects when applying new treatment strategies in humans, a great number of participants is needed to reach statistical power when superiority of a new therapy needs to be demonstrated. Thus, the current results are important to generate further hypotheses that might be a next step to clinical application.

5.8 How big is the gap between curability, scientific knowledge, and clinical reality? - Clinical translation of experimental strategies

In this experimental thesis, we first combined a cell-based approach to promote axonal regeneration with a mechanical approach. In summary, we could show that the combination was superior to reach functional improvement compared to each one alone.
With regard to real-life scenarios after SCI, it is a question of debate which therapeutic approaches are feasible and have the potential for translational implication into clinical practice.
Many preclinical studies, including ours, show benefits of different therapeutic strategies relating to functional outcome and axonal regenerating. But so far, there are no efficient and reliable clinical treatments available for SCI patients. Fortunately, due to improved medical care, historical mortality rates of 80 % could markedly reduced. Experimental studies in humans try to improve survival rates and to maintain or regain the patient's independence and quality of life.
Looking at research and development, an ever greater interest on SCI can be detected. Searching PubMed for "spinal cord injury" underlines the growing interest. Between 1900 and 2016 more than 61.000 articles have been published (see fig. 5.1). The graphic representation shows the substantial increase in the last years with an almost exponential growth.

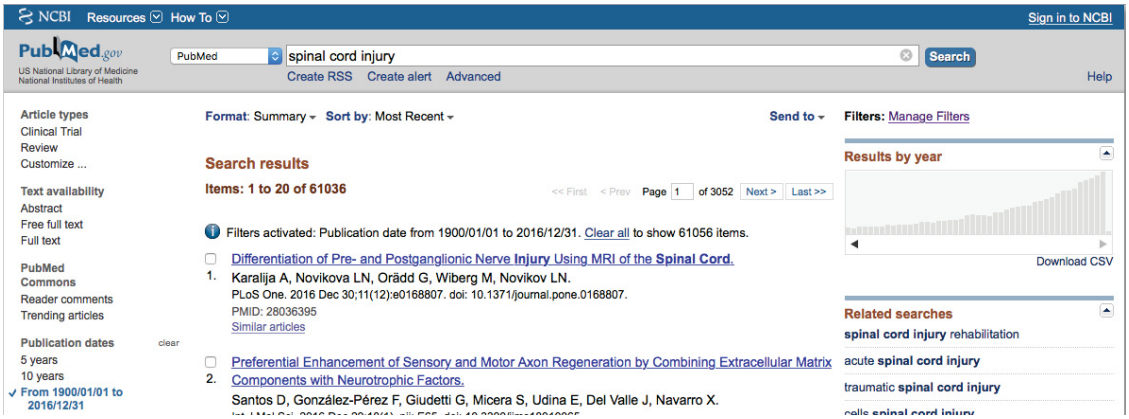

Figure 5.1: **Substantial increase of scientific publications to "spinal cord injury"** The graphic representation shows the rising interest in the field of spinal cord injuries. More than 61000 articles to "spinal cord cord injury" have been published between 1900 and 2016. The graphic shows an almost exponential growth of annual publications. The search was restricted to the search term "spinal cord injury", and articles between 1900/01/01 and 2016/12/31 were included.

With each new study, another piece of the puzzle is found, resulting in a better understanding of the complex mechanisms. To process these large amounts of data, new databases and technologies will be required [178, 179]. Aim of these databases is to reduce the lack of transparency and reproducibility, to enhance the cellular and molecular understanding, and to enable and expedite translation of pre-clinical knowledge into standards of patient care for SCI. The Center for Neuronal Regeneration (CNR) is designed to collect, analyze, and evaluate the globally available knowledge on traumatic injuries of the CNS. The CNR

further aims to enhance and speed up the process of translation of experimental therapies into the clinics and to the patient [180].

Different factors are responsible for the missing translation: First, rats are the most commonly used animals for experimental SCI. In contrast to humans, rats show a quadrupedal organization of locomotion. Therefore, rodents and human differ in the anatomy of their spinal cords [9, 181]. Second, the experimental injury models often differ from clinical reality. Most human patients suffer from contusion injuries with a great heterogeneity and often with an intact *dura*. Although transection models are further away from clinical condition, they may be more appropriate compared to contusion models to evaluate the effectiveness of therapeutic interventions in promoting of axonal regeneration and functional recovery [108]. The accident mechanisms in humans are extremely diverse - and thus the extent of the lesion is difficult to predict.
Experimental scientists try to standardize experimental groups. Frequently, young female rats with nearly the same weight are used to reduce inter-individual differences. Optimally, the lesion models in experimental settings should be consistent and highly reproducible. These standards are often difficult to realize in clinical trials. Also, the demographic changes should be taken into consideration [182].

Despite these methodological difficulties, clinical trials are occasionally realized [183, 74, 184]. For a better overview, Ramer *et al.* categorized studies of spinal cord repair by the "three Rs": rescue, reactivate, and rewire [183]. For each category, examples are given. Rescue operations to prevent the spread of damage beyond the initial site of injury involve surgical decompression, cooling or hypothermia, and pharmacological immune modulation. Rehabilitation, pharmacological or electrical stimulation, as well as remyelination strategies try to reactivate spared tissue. "Rewire" encompasses regrowth strategies of injured axons and re-purposing of spared axons. In his review, some of the most promising experimental treatments for translation to clinical treatment of SCI are highlighted [183]. For each category, Ramer *et al.* highlighted the treatments out for translation to the clinic. It seems to be easier to rescue spared axons compared to axonal regrowth [183]. Local and systemic hypothermia can reduce the rate of biological reactions and secondary damage. A novel and exciting clinical study examined the localized cooling via a custom-made cooling saddles placed extradurally to maintain a dural temperature of 6 °C [185]. Preliminary results indicate promising success of this approach. Thus, local cooling might now be clinically feasible [183]. Another promising therapeutic approach to achieve reactivation and rehabilitation might be epidural stimulation with a good benefit-risk ratio for imminent clinical translation [183]. Rewiring the injured spinal cord is the most difficult goal. Only a few of thousand experimental strategies are ready for clinical trials. Chondroitinase ABC is a good example of an experimental treatment ready for clinical translation [183], and others are likely to follow.
Biomaterials demonstrated beneficial effects in experimental animal models, with regard to a clinical translation, new biotechnological- and/or chemical processes are required [133]. Biodegradability seem to be a key element to obviate invasive surgery to remove non-degradable materials.

In conclusion, it should be emphasized that adherence to the state-of-the art experiments and techniques in preclinical studies is mandatory to restrict clinical failures. A key element

within this effort is continuing to improve replications and reproducibility [186, 184]. To cure SCI still remains a goal that is difficult to achieve, but the knowledge gained by the growing community of SCI scientists gives rise to a promising future.

6 Conclusion and Further Considerations

The results of this thesis confirmed preliminary findings on the therapeutic effects of USSC in SCI. The transplantation of USSC resulted in improved axonal regeneration and functional outcome not only after dorsal-hemisection but also after complete spinal cord transection. In addition to the therapeutic benefit of USSC, the long term study revealed benefits of mMS implantation. Spinal cord tissue remained in place within the mMS after the vacuum was released; regenerating axons and new blood vessels invaded the mMS lumen. Moreover, the results demonstrate superiority of the combinatory treatment. Different factors and aspects that might influence the results have been discussed as possible reasons for the therapeutic effects and the improved functional outcome: E.g. cyst formation, vascularization, and axonal regeneration.

Based on these findings, further modifications are also conceivable. Some of these possibilities have already been mentioned in the individual chapters of the discussion: To prevent further injuries by injecting the stem cells with a glass capillary, USSC could be transplanted directly through the tubing system of the mMS. Further (long-term) drug application could be implemented by connecting the tubing system of the mMS with an osmotic mini-pump. The mMS allows local drug infusion into the lesion site through the internal micro-channels, allowing application of scar-suppressing treatments, growth factor cocktails, or immune modulating drugs.
The implantation of the mMS in a chronic SCI model after resection of the scar should be particularly interesting. With regard to a clinical translation, development of a biodegradable mMS seems to be desirable. Testing of a biodegradable version is on-going and initial successes could be achieved in our laboratory. Regarding clinical translation the ideal mMS device should be individually fitted to any shape or size of lesion and the exact fit will be guaranteed by the fabrication via 3D bioprinting [66].
Additionally, further analyses are required to investigate the exact effects and direct and indirect mechanisms after transplantation of USSC. Which types of immune cells are recruited? How do they modulate the inflammatory response? Which trophic molecules are released? Which cell-cell interactions are essential? How do USSC influence the environment? These and other question have not been completely answered. Moreover, the investigation of any material-cell interactions of USSC and the mMS might be interesting.
On a final note, the effect of physical therapy should not be underestimated. Therefore, additional treadmill training and/or enriched housing environment might positively influence the functional outcome by prevention of muscle atrophy and spasticity.

Abbreviations

5-HT	5-hydroxy-tryptamine
BBB	Basso Beattie Bresnahan locomotor rating scale
BDA	biotinylated dextran amine
BDNF	brain-derived neurotrophic factor
BM-MSC	bone marrow-derived mesenchymal stem cell(s)
BMSC	bone marrow stromal cells
BV	blood vessel(s)
C	consistent
CB	cord blood
ck	chicken
CNR	Center for Neuronal Regeneration
CNS	central nervous system
CST	corticospinal tract
CTB	cholera toxin B subunit
DAPI	4',6-diamidino-2-phenylindole
dk	donkey
DMEM	Dulbecco's modified Eagle medium
DMSO	dimethylsulfoxid
DPX	xylol-containing mounting fluid
e.g.	for example (exempli gratia)
ECM	extracellular matrix
ESC	embryonic stem cell(s)
ESC	embryonic stem cell(s)

etc.	et cetera
EtOH	ethanol
F	frequent
FBS	fetal bovine serum
Fig.	figure
GFAP	glial fibrillary acidic protein
GMP	good manufacturing practice
gt	goat
h	hour
HGF	hepatocyte growth factor
hNuc	human nuclei
IGF-1	insulin-like growth factor-1
IgG	immunoglobulin G
IHC	immunohistochemistry
iPSC	induced pluripotent stem cell(s)
L	left
mBBB	modified Basso Beattie Bresnahan locomotor rating scale
min	minute
mMS	mechanical Microconnector System
ms	mouse
MSC	mesenchymal stem cells
n	number
NF	neurofilament protein
NGS	normal goat serum
NSC	neural stem cell(s)
NSPC	neural stem progenitor cell(s)
NT-3	neutrophin-3
O	occacional

ON	overnight
PAM	panaxonal neurofilament marker
PB	phosphate buffer
PBS	phosphate buffered saline
PFA	paraformaldehyde
PNS	peripheral nervous system
R	right
rb	rabbit
RT	room temperature
s.c.	subcutaneous
SCI	spinal cord injury/injuries
Tab.	table
TH	tyrosine hydroxylase
Th	thoracic level
USSC	unrestricted somatic stem cell
VEGF	vascular endothelial growth factor
vs.	versus
wpo	weeks post operation

Bibliography

[1] F. Biering-Soerensen, J. E. Bickenbach, W. S. El Masry, A. Officer, and P. M. von Groote. Iscos-who collaboration. international perspectives of spinal cord injury (ipsci) report. *Spinal Cord*, 49(6):679–683, Jun 2011.

[2] The National Spinal Cord Injury Statistical Center, 2014.

[3] Michael O'Malley Rob D. Dickerman and Jack E. Zigler. Chapter 15 socioeconomics of spinal injuries. In *Neurotrauma and critical care of the spine*, book; book/illustrated 15, pages 210–219. New York : Thieme, 2009. Includes bibliographical references and index.

[4] Michael Kseeler Jeff S. Silber, Adam S. Levin and Kamal D. Dagly. Chapter 2 pathophysiology of spinal injuries. In Alexander R. Vaccaro Jack Jallo, editor, *Neurotrauma and critical care of the spine*, book; book/illustrated 2, pages 15–27. New York : Thieme, 2009. Includes bibliographical references and index.

[5] Steven C. Kirshblum, William Waring, Fin Biering-Sorensen, Stephen P. Burns, Mark Johansen, Mary Schmidt-Read, William Donovan, Daniel Graves, Amit Jha, Linda Jones, M. J. Mulcahey, and Andrei Krassioukov. Reference for the 2011 revision of the international standards for neurological classification of spinal cord injury. *J Spinal Cord Med*, 34(6):547–554, Nov 2011.

[6] Steven C. Kirshblum, Stephen P. Burns, Fin Biering-Sorensen, William Donovan, Daniel E. Graves, Amitabh Jha, Mark Johansen, Linda Jones, Andrei Krassioukov, M. J. Mulcahey, Mary Schmidt-Read, and William Waring. International standards for neurological classification of spinal cord injury (revised 2011). *J Spinal Cord Med*, 34(6):535–546, Nov 2011.

[7] L. H. Sekhon and M. G. Fehlings. Epidemiology, demographics, and pathophysiology of acute spinal cord injury. *Spine (Phila Pa 1976)*, 26(24 Suppl):S2–12, Dec 2001.

[8] I Klusman and M. E. Schwab. Läsionsmechanismen bei Rückenmarktrauma. In Andreas; Dietz Volker Wallesch, Claus-Werner; Unterberg, editor, *Neurotraumatologie*, chapter 11. Thieme Verlagsgruppe Stuttgart New York Delhi Rio, 2005.

[9] Nuno A. Silva, Nuno Sousa, Rui L. Reis, and Antonio J. Salgado. From basics to clinical: a comprehensive review on spinal cord injury. *Prog Neurobiol*, 114:25–57, Mar 2014.

[10] A.R. Allen. Surgery of experimental lesions of spinal cord equivalent to crush injury of fracture dislocation of spinal column. a preliminary report. *Journal of the American Medical Association*, 57:878–880, 1911.

[11] Samuel David, Juan Guillermo Zarruk, and Nader Ghasemlou. Chapter five - inflammatory pathways in spinal cord injury. In Jeffrey L. Goldberg and Ephraim F.

Trakhtenberg, editors, *Axon Growth and Regeneration: Part 2*, volume 106 of *International Review of Neurobiology*, pages 127 – 152. Academic Press, 2012.

[12] Brian K. Kwon, Wolfram Tetzlaff, Jonathan N. Grauer, John Beiner, and Alexander R. Vaccaro. Pathophysiology and pharmacologic treatment of acute spinal cord injury. *Spine J*, 4(4):451–464, 2004.

[13] Santiago Ramón y Cajal. *Degeneration & regeneration of the nervous system*, volume 1. Oxford University Press, Humphrey Milford, 1928.

[14] S. Y. Fu and T. Gordon. The cellular and molecular basis of peripheral nerve regeneration. *Mol Neurobiol*, 14(1-2):67–116, 1997.

[15] Ramon y Cajal. *Cajal's degeneration and regeneration of the nervous system. Estudios sobre la degeneracion y regeneracion del sistema nervioso. Degeneration and regeneration of the nervous system.* New York [u.a.] : Oxford Univ. Pr., New York [u.a.], 1991.

[16] S. David and A. J. Aguayo. Axonal elongation into peripheral nervous system "bridges" after central nervous system injury in adult rats. *Science*, 214(4523):931–933, Nov 1981.

[17] J. V. Coumans, T. T. Lin, H. N. Dai, L. MacArthur, M. McAtee, C. Nash, and B. S. Bregman. Axonal regeneration and functional recovery after complete spinal cord transection in rats by delayed treatment with transplants and neurotrophins. *J Neurosci*, 21(23):9334–9344, Dec 2001.

[18] Jerry Silver, Martin E. Schwab, and Phillip G. Popovich. Central nervous system regenerative failure: role of oligodendrocytes, astrocytes, and microglia. *Cold Spring Harb Perspect Biol*, 7(3):a020602, Mar 2015.

[19] Michael T. Fitch and Jerry Silver. Cns injury, glial scars, and inflammation: Inhibitory extracellular matrices and regeneration failure. *Exp Neurol*, 209(2):294–301, Feb 2008.

[20] Hitoshi Kawano, Junko Kimura-Kuroda, Yukari Komuta, Nozomu Yoshioka, Hong Peng Li, Koki Kawamura, Ying Li, and Geoffrey Raisman. Role of the lesion scar in the response to damage and repair of the central nervous system. *Cell Tissue Res*, 349(1):169–180, Jul 2012.

[21] E. Preston, J. Webster, and D. Small. Characteristics of sustained blood-brain barrier opening and tissue injury in a model for focal trauma in the rat. *J Neurotrauma*, 18(1):83–92, Jan 2001.

[22] C. C. Stichel and H. W. Müller. Experimental strategies to promote axonal regeneration after traumatic central nervous system injury. *Prog Neurobiol*, 56(2):119–148, Oct 1998.

[23] Jerry Silver and Jared H. Miller. Regeneration beyond the glial scar. *Nat Rev Neurosci*, 5(2):146–156, Feb 2004.

[24] Jill R. Faulkner, Julia E. Herrmann, Michael J. Woo, Keith E. Tansey, Ngan B. Doan, and Michael V. Sofroniew. Reactive astrocytes protect tissue and preserve function after spinal cord injury. *J Neurosci*, 24(9):2143–2155, Mar 2004.

[25] Jared H. Miller and Jerry Silver. Effects of the glial scar and extracellular matrix molecules on axon regeneration. In Michael Selzer, Stephanie Clarke, Leonardo Cohen, Pamela Duncan, and Fred Gage, editors, *Textbook of Neural Repair and Rehabilitation*, volume 1, chapter 22, pages 390–404. Cambridge University Press, 2006. Cambridge Books Online.

[26] D. W. Hampton, K. E. Rhodes, C. Zhao, R J M. Franklin, and J. W. Fawcett. The responses of oligodendrocyte precursor cells, astrocytes and microglia to a cortical stab injury, in the brain. *Neuroscience*, 127(4):813–820, 2004.

[27] J. W. Fawcett and R. A. Asher. The glial scar and central nervous system repair. *Brain Res Bull*, 49(6):377–391, Aug 1999.

[28] Nicole Klapka, Susanne Hermanns, Guido Straten, Carmen Masanneck, Simone Duis, Frank P T. Hamers, Daniela Müller, Werner Zuschratter, and Hans Werner Müller. Suppression of fibrous scarring in spinal cord injury of rat promotes long-distance regeneration of corticospinal tract axons, rescue of primary motoneurons in somatosensory cortex and significant functional recovery. *Eur J Neurosci*, 22(12):3047–3058, Dec 2005.

[29] S. Hermanns, N. Klapka, and H. W. Müller. The collagenous lesion scar–an obstacle for axonal regeneration in brain and spinal cord injury. *Restor Neurol Neurosci*, 19(1-2):139–148, 2001.

[30] S. Hermanns, P. Reiprich, and H. W. Müller. A reliable method to reduce collagen scar formation in the lesioned rat spinal cord. *J Neurosci Methods*, 110(1-2):141–146, Sep 2001.

[31] P. D. Yurchenco and J. C. Schittny. Molecular architecture of basement membranes. *FASEB J*, 4(6):1577–1590, Apr 1990.

[32] M. C. Shearer and J. W. Fawcett. The astrocyte/meningeal cell interface–a barrier to successful nerve regeneration? *Cell Tissue Res*, 305(2):267–273, Aug 2001.

[33] Daniel A. Morgenstern, Richard A. Asher, and James W. Fawcett. Chondroitin sulphate proteoglycans in the cns injury response. *Prog Brain Res*, 137:313–332, 2002.

[34] R. J. Pasterkamp, P. N. Anderson, and J. Verhaagen. Peripheral nerve injury fails to induce growth of lesioned ascending dorsal column axons into spinal cord scar tissue expressing the axon repellent semaphorin3a. *Eur J Neurosci*, 13(3):457–471, Feb 2001.

[35] Liza Q. Bundesen, Tracy Aber Scheel, Barbara S. Bregman, and Lawrence F. Kromer. Ephrin-b2 and ephb2 regulation of astrocyte-meningeal fibroblast interactions in response to spinal cord lesions in adult rats. *J Neurosci*, 23(21):7789–7800, Aug 2003.

[36] M. S. Chen, A. B. Huber, M. E. van der Haar, M. Frank, L. Schnell, A. A. Spillmann, F. Christ, and M. E. Schwab. Nogo-a is a myelin-associated neurite outgrowth inhibitor and an antigen for monoclonal antibody in-1. *Nature*, 403(6768):434–439, Jan 2000.

[37] L. McKerracher, S. David, D. L. Jackson, V. Kottis, R. J. Dunn, and P. E. Braun. Identification of myelin-associated glycoprotein as a major myelin-derived inhibitor of neurite growth. *Neuron*, 13(4):805–811, Oct 1994.

[38] Kevin C. Wang, Vuk Koprivica, Jieun A. Kim, Rajeev Sivasankaran, Yong Guo, Rachel L. Neve, and Zhigang He. Oligodendrocyte-myelin glycoprotein is a nogo receptor ligand that inhibits neurite outgrowth. *Nature*, 417(6892):941–944, Jun 2002.

[39] Marco Domeniconi Tim Spencer and Marie T. Filbin. Inhibitors of axonal regeneration. In Michael Selzer, Stephanie Clarke, Leonardo Cohen, Pamela Duncan, and Fred Gage, editors, *Textbook of Neural Repair and Rehabilitation*, volume 1, chapter 21, pages 365–389. Cambridge University Press, 2006. Cambridge Books Online.

[40] R. J. McKeon, M. J. Jurynec, and C. R. Buck. The chondroitin sulfate proteoglycans neurocan and phosphacan are expressed by reactive astrocytes in the chronic cns glial scar. *J Neurosci*, 19(24):10778–10788, Dec 1999.

[41] J. W. Fawcett. Spinal cord repair: from experimental models to human application. *Spinal Cord*, 36(12):811–817, Dec 1998.

[42] Charles H. Tator. Review of treatment trials in human spinal cord injury: issues, difficulties, and recommendations. *Neurosurgery*, 59(5):957–82; discussion 982–7, Nov 2006.

[43] Martin E. Schwab. Repairing the injured spinal cord. *Science*, 295(5557):1029–1031, Feb 2002.

[44] Toshihiro Takami, Martin Oudega, John R. Bethea, Patrick M. Wood, Naomi Kleitman, and Mary Bartlett Bunge. Methylprednisolone and interleukin-10 reduce gray matter damage in the contused fischer rat thoracic spinal cord but do not improve functional outcome. *J Neurotrauma*, 19(5):653–666, May 2002.

[45] C. Hoffmann. Cox-2 in brain and spinal cord implications for therapeutic use. *Curr Med Chem*, 7(11):1113–1120, Nov 2000.

[46] Naoaki Harada, Yuji Taoka, and Kenji Okajima. Role of prostacyclin in the development of compression trauma-induced spinal cord injury in rats. *J Neurotrauma*, 23(12):1739–1749, Dec 2006.

[47] B. C. Hains, J. A. Yucra, and C. E. Hulsebosch. Reduction of pathological and behavioral deficits following spinal cord contusion injury with the selective cyclooxygenase-2 inhibitor ns-398. *J Neurotrauma*, 18(4):409–423, Apr 2001.

[48] Julio C. Furlan, Vanessa Noonan, David W. Cadotte, and Michael G. Fehlings. Timing of decompressive surgery of spinal cord after traumatic spinal cord injury: an evidence-based examination of pre-clinical and clinical studies. *J Neurotrauma*, 28(8):1371–1399, Aug 2011.

[49] Anita D. Buchli and Martin E. Schwab. Inhibition of nogo: a key strategy to increase regeneration, plasticity and functional recovery of the lesioned central nervous system. *Ann Med*, 37(8):556–567, 2005.

[50] C. C. Stichel, S. Hermanns, H. J. Luhmann, F. Lausberg, H. Niermann, D. D'Urso, G. Servos, H. G. Hartwig, and H. W. Müller. Inhibition of collagen iv deposition promotes regeneration of injured cns axons. *Eur J Neurosci*, 11(2):632–646, Feb 1999.

[51] Nora Schiwy, Nicole Brazda, and Hans Werner Müller. Enhanced regenerative axon growth of multiple fibre populations in traumatic spinal cord injury following scar-suppressing treatment. *Eur J Neurosci*, 30(8):1544–1553, Oct 2009.

[52] Hiroshi Nomura, Charles H Tator, and Molly S Shoichet. Bioengineered strategies for spinal cord repair. *J Neurotrauma*, 23(3-4):496–507, 2006.

[53] I. D. Duncan, A. J. Aguayo, R. P. Bunge, and P. M. Wood. Transplantation of rat schwann cells grown in tissue culture into the mouse spinal cord. *J Neurol Sci*, 49(2):241–252, Feb 1981.

[54] M. Schwartz and E. Yoles. Macrophages and dendritic cells treatment of spinal cord injury: from the bench to the clinic. *Acta Neurochir Suppl*, 93:147–150, 2005.

[55] A. Ramon-Cueto, G. W. Plant, J. Avila, and M. B. Bunge. Long-distance axonal regeneration in the transected adult rat spinal cord is promoted by olfactory ensheathing glia transplants. *J Neurosci*, 18(10):3803–3815, May 1998.

[56] Kanghui Park, Youngjeon Lee, Sookyoung Park, Seunghoon Lee, Yunkyung Hong, Sang Kil Lee, and Yonggeun Hong. Synergistic effect of melatonin on exercise-induced neuronal reconstruction and functional recovery in a spinal cord injury animal model. *J Pineal Res*, 48(3):270–281, Apr 2010.

[57] Camila R. Battistuzzo, Robert J. Callister, Robin Callister, and Mary P. Galea. A systematic review of exercise training to promote locomotor recovery in animal models of spinal cord injury. *J Neurotrauma*, 29(8):1600–1613, May 2012.

[58] Yi Ping Zhang, Christopher Iannotti, Lisa B E. Shields, Yingchun Han, Darlene A. Burke, Xiao-Ming Xu, and Christopher B. Shields. Dural closure, cord approximation, and clot removal: enhancement of tissue sparing in a novel laceration spinal cord injury model. *J Neurosurg*, 100(4 Suppl Spine):343–352, Apr 2004.

[59] Gemma E. Rooney, Toshiki Endo, Syed Ameenuddin, Bingkun Chen, Sandeep Vaishya, Louann Gross, Terry K. Schiefer, Bradford L. Currier, Robert J. Spinner, Michael J. Yaszemski, and Anthony J. Windebank. Importance of the vasculature in cyst formation after spinal cord injury. *J Neurosurg Spine*, 11(4):432–437, Oct 2009.

[60] Alexandre Rasouli, Nitin Bhatia, Paul Dinh, Kim Cahill, Sourabh Suryadevara, and Ranjan Gupta. Resection of glial scar following spinal cord injury. *J Orthop Res*, 27(7):931–936, Jul 2009.

[61] S. Woerly, P. Petrov, E. Sykova, T. Roitbak, Z. Simonova, and A. R. Harvey. Neural tissue formation within porous hydrogels implanted in brain and spinal cord lesions: ultrastructural, immunohistochemical, and diffusion studies. *Tissue Eng*, 5(5):467–488, Oct 1999.

[62] Mindan Wang, Peng Zhai, Xiongbiao Chen, David J. Schreyer, Xiaodan Sun, and Fuzhai Cui. Bioengineered scaffolds for spinal cord repair. *Tissue Eng Part B Rev*, 17(3):177–194, Jun 2011.

[63] Jonathan A Friedman, Anthony J Windebank, Michael J Moore, Robert J Spinner, Bradford L Currier, and Michael J Yaszemski. Biodegradable polymer grafts for surgical repair of the injured spinal cord. *Neurosurgery*, 51(3):742–51; discussion 751–2, Sep 2002.

[64] Karin S. Straley, Cheryl Wong Po Foo, and Sarah C. Heilshorn. Biomaterial design strategies for the treatment of spinal cord injuries. *J Neurotrauma*, 27(1):1–19, Jan 2010.

[65] M. Oudega, E. J. Bradbury, and M. S. Ramer. Combination therapies. *Handb Clin Neurol*, 109:617–636, 2012.

[66] Nicole Brazda, Christian Voss, Veronica Estrada, Homaira Lodin, Nils Weinrich, Klaus Seide, Jörg Müller, and Hans W. Müller. A mechanical microconnector system for restoration of tissue continuity and long-term drug application into the injured spinal cord. *Biomaterials*, 34(38):10056–10064, Dec 2013.

[67] Yi-Cheng Huang and Yi-You Huang. Biomaterials and strategies for nerve regeneration. *Artif Organs*, 30(7):514–522, Jul 2006.

[68] Paul Lu, Yaozhi Wang, Lori Graham, Karla McHale, Mingyong Gao, Di Wu, John Brock, Armin Blesch, Ephron S. Rosenzweig, Leif A. Havton, Binhai Zheng, James M. Conner, Martin Marsala, and Mark H. Tuszynski. Long-distance growth and connectivity of neural stem cells after severe spinal cord injury. *Cell*, 150(6):1264–1273, Sep 2012.

[69] Nicolas N. Madigan, Siobhan McMahon, Timothy O'Brien, Michael J. Yaszemski, and Anthony J. Windebank. Current tissue engineering and novel therapeutic approaches to axonal regeneration following spinal cord injury using polymer scaffolds. *Respir Physiol Neurobiol*, 169(2):183–199, Nov 2009.

[70] Dong-Hyuk Park, Jeong-Hyun Lee, Cesario V. Borlongan, Paul R. Sanberg, Yong-Gu Chung, and Tai-Hyoung Cho. Transplantation of umbilical cord blood stem cells for treating spinal cord injury. *Stem Cell Rev*, 7(1):181–194, Mar 2011.

[71] Wolfram Tetzlaff, Elena B. Okon, Soheila Karimi-Abdolrezaee, Caitlin E. Hill, Joseph S. Sparling, Jason R. Plemel, Ward T. Plunet, Eve C. Tsai, Darryl Baptiste, Laura J. Smithson, Michael D. Kawaja, Michael G. Fehlings, and Brian K. Kwon. A systematic review of cellular transplantation therapies for spinal cord injury. *J Neurotrauma*, 28(8):1611–1682, Aug 2011.

[72] Vibhu Sahni and John A. Kessler. Stem cell therapies for spinal cord injury. *Nat Rev Neurol*, 6(7):363–372, Jul 2010.

[73] Rishi S. Nandoe Tewarie, Andres Hurtado, Ronald H. Bartels, Andre Grotenhuis, and Martin Oudega. Stem cell-based therapies for spinal cord injury. *J Spinal Cord Med*, 32(2):105–114, 2009.

[74] Andrea J. Mothe and Charles H. Tator. Advances in stem cell therapy for spinal cord injury. *J Clin Invest*, 122(11):3824–3834, Nov 2012.

[75] Thomas S. Wilems, Jennifer Pardieck, Nisha Iyer, and Shelly E. Sakiyama-Elbert. Combination therapy of stem cell derived neural progenitors and drug delivery of anti-inhibitory molecules for spinal cord injury. *Acta Biomater*, Sep 2015.

[76] E. Mezey, K. J. Chandross, G. Harta, R. A. Maki, and S. R. McKercher. Turning blood into brain: cells bearing neuronal antigens generated in vivo from bone marrow. *Science*, 290(5497):1779–1782, Dec 2000.

[77] M. A. Eglitis and E. Mezey. Hematopoietic cells differentiate into both microglia and macroglia in the brains of adult mice. *Proc Natl Acad Sci U S A*, 94(8):4080–4085, Apr 1997.

[78] Shuhei Koshizuka, Seiji Okada, Akihiko Okawa, Masao Koda, Mitsuhiro Murasawa, Masayuki Hashimoto, Takahito Kamada, Katsunori Yoshinaga, Masazumi Murakami, Hideshige Moriya, and Masashi Yamazaki. Transplanted hematopoietic stem cells from bone marrow differentiate into neural lineage cells and promote functional recovery after spinal cord injury in mice. *J Neuropathol Exp Neurol*, 63(1):64–72, Jan 2004.

[79] Sandrine Thuret, Lawrence D F. Moon, and Fred H. Gage. Therapeutic interventions after spinal cord injury. *Nat Rev Neurosci*, 7(8):628–643, Aug 2006.

[80] A. J. Friedenstein, K. V. Petrakova, A. I. Kurolesova, and G. P. Frolova. Heterotopic of bone marrow. analysis of precursor cells for osteogenic and hematopoietic tissues. *Transplantation*, 6(2):230–247, Mar 1968.

[81] Karina T. Wright, Wagih El Masri, Aheed Osman, Joy Chowdhury, and William E B. Johnson. Concise review: Bone marrow for the treatment of spinal cord injury: mechanisms and clinical applications. *Stem Cells*, 29(2):169–178, Feb 2011.

[82] Reaz Vawda and Michael G. Fehlings. Mesenchymal cells in the treatment of spinal cord injury: current & future perspectives. *Curr Stem Cell Res Ther*, 8(1):25–38, Jan 2013.

[83] J. Vaquero and M. Zurita. Bone marrow stromal cells for spinal cord repair: a challenge for contemporary neurobiology. *Histol Histopathol*, 24(1):107–116, Jan 2009.

[84] Rakhi Pal, Neelam K. Venkataramana, Abhilash Bansal, Sudheer Balaraju, Majahar Jan, Ravi Chandra, Ashish Dixit, Amit Rauthan, Uday Murgod, and Satish Totey. Ex vivo-expanded autologous bone marrow-derived mesenchymal stromal cells in human spinal cord injury/paraplegia: a pilot clinical study. *Cytotherapy*, 11(7):897–911, 2009.

[85] Fukuki Saito, Toshio Nakatani, Masaaki Iwase, Yuji Maeda, Yoshinori Murao, Yoshihisa Suzuki, Masanori Fukushima, and Chizuka Ide. Administration of cultured autologous bone marrow stromal cells into cerebrospinal fluid in spinal injury patients: a pilot study. *Restor Neurol Neurosci*, 30(2):127–136, 2012.

[86] Ann M. Parr, Iris Kulbatski, and Charles H. Tator. Transplantation of adult rat spinal cord stem/progenitor cells for spinal cord injury. *J Neurotrauma*, 24(5):835–845, May 2007.

[87] Nathalie Picard-Riera, Brahim Nait-Oumesmar, and Anne Baron-Van Evercooren. Endogenous adult neural stem cells: limits and potential to repair the injured central nervous system. *J Neurosci Res*, 76(2):223–231, Apr 2004.

[88] Sherri S. Schultz. Adult stem cell application in spinal cord injury. *Curr Drug Targets*, 6(1):63–73, Feb 2005.

[89] Ninette Amariglio, Abraham Hirshberg, Bernd W. Scheithauer, Yoram Cohen, Ron Loewenthal, Luba Trakhtenbrot, Nurit Paz, Maya Koren-Michowitz, Dalia Waldman, Leonor Leider-Trejo, Amos Toren, Shlomi Constantini, and Gideon Rechavi. Donor-derived brain tumor following neural stem cell transplantation in an ataxia telangiectasia patient. *PLoS Med*, 6(2):e1000029, Feb 2009.

[90] Sharyn L. Rossi and Hans S. Keirstead. Stem cells and spinal cord regeneration. *Curr Opin Biotechnol*, 20(5):552–562, Oct 2009.

[91] Gesine Kögler, Sandra Sensken, Judith A Airey, Thorsten Trapp, Markus Mueschen, Niklas Feldhahn, Stefanie Liedtke, Ruediger V Sorg, Johannes Fischer, Claudia Rosenbaum, Susanne Greschat, Andreas Knipper, Joerg Bender, Ozer Degistirici, Jizong Gao, Arnold I Caplan, Evan J Colletti, Graca Almeida-Porada, Hans W Müller, Esmail Zanjani, and Peter Wernet. A new human somatic stem cell from placental cord blood with intrinsic pluripotent differentiation potential. *J Exp Med*, 200(2):123–135, Jul 2004.

[92] Simone Maria Kluth, Anja Buchheiser, Amelie Pia Houben, Stefanie Geyh, Thomas Krenz, Teja Falk Radke, Constanze Wiek, Helmut Hanenberg, Petra Reinecke, Peter Wernet, and Gesine Kögler. Dlk-1 as a marker to distinguish unrestricted somatic stem cells and mesenchymal stromal cells in cord blood. *Stem Cells Dev*, 19(10):1471–1483, Oct 2010.

[93] Simone Maria Kluth, Teja Falk Radke, and Gesine Kögler. Increased haematopoietic supportive function of ussc from umbilical cord blood compared to cb msc and possible role of dlk-1. *Stem Cells Int*, 2013:985285, 2013.

[94] Meike Winter, Xiao-Nong Wang, Walter Daeubener, Annette Eyking, Michelle Rae, Anne M. Dickinson, Peter Wernet, Gesine Kögler, and Ruediger V. Sorg. Suppression of cellular immunity by cord blood-derived unrestricted somatic stem cells is cytokine-dependent. *J Cell Mol Med*, 13(8B):2465–2475, Aug 2009.

[95] Lieke C J. van den Berk, Helene Roelofs, Tonnie Huijs, Kim G C. Siebers-Vermeulen, Reinier A. Raymakers, Gesine Kögler, Carl G. Figdor, and Ruurd Torensma. Cord blood mesenchymal stem cells propel human dendritic cells to an intermediate maturation state and boost interleukin-12 production by mature dendritic cells. *Immunology*, 128(4):564–572, Dec 2009.

[96] Stefanie Liedtke, Anja Buchheiser, Julia Bosch, Frank Bosse, Fabian Kruse, Xiaoyi Zhao, Simeon Santourlidis, and Gesine Kögler. The hox code as a "biological fingerprint" to distinguish functionally distinct stem cell populations derived from cord blood. *Stem Cell Res*, 5(1):40–50, Jul 2010.

[97] Murat Aktas, Anja Buchheiser, Amelie Houben, Verena Reimann, Teja Radke, Kathrin Jeltsch, Patrick Maier, W Jens Zeller, and Gesine Kogler. Good manufac-

turing practice-grade production of unrestricted somatic stem cell from fresh cord blood. *Cytotherapy*, 12(3):338–348, May 2010.

[98] Jessica Schira, Marcia Gasis, Veronica Estrada, Marion Hendricks, Christine Schmitz, Thorsten Trapp, Fabian Kruse, Gesine Kögler, Peter Wernet, Hans-Peter Hartung, and Hans Werner Müller. Significant clinical, neuropathological and behavioural recovery from acute spinal cord trauma by transplantation of a well-defined somatic stem cell from human umbilical cord blood. *Brain*, 135(Pt 2):431–446, Feb 2012.

[99] Susanne Greschat, Jessica Schira, Patrick Küry, Claudia Rosenbaum, Maria Angelica de Souza Silva, Gesine Kögler, Peter Wernet, and Hans Werner Müller. Unrestricted somatic stem cells from human umbilical cord blood can be differentiated into neurons with a dopaminergic phenotype. *Stem Cells Dev*, 17(2):221–232, Apr 2008.

[100] Katharina M. Iwaniuk, Jessica Schira, Sandra Weinhold, Marc Jung, James Adjaye, Hans Werner Müller, Peter Wernet, and Hans-Ingo Trompeter. Network-like impact of micrornas on neuronal lineage differentiation of unrestricted somatic stem cells from human cord blood. *Stem Cells and Development*, 20(8):1383–1394, 2011.

[101] Jessica Schira. *Transplantation of stem cells from human umbilical cord blood to improve regeneration after spinal cord injury.* PhD thesis, Mathematisch-Naturwissenschaftlichen Fakultaet der Heinrich Heine Universitaet Duesseldorf, Duesseldorf, December 2010.

[102] Gesine Kögler, Teja Falk Radke, Aurelie Lefort, Sandra Sensken, Johannes Fischer, Ruediger V. Sorg, and Peter Wernet. Cytokine production and hematopoiesis supporting activity of cord blood-derived unrestricted somatic stem cells. *Exp Hematol*, 33(5):573–583, May 2005.

[103] Gesine Kögler, Sandra Sensken, and Peter Wernet. Comparative generation and characterization of pluripotent unrestricted somatic stem cells with mesenchymal stem cells from human cord blood. *Exp Hematol*, 34(11):1589–1595, Nov 2006.

[104] Ning Zhang, Marong Fang, Haohao Chen, Fangming Gou, and Mingxing Ding. Evaluation of spinal cord injury animal models. *Neural Regen Res*, 9(22):2008–2012, Nov 2014.

[105] Brian K. Kwon, Tom R. Oxland, and Wolfram Tetzlaff. Animal models used in spinal cord regeneration research. *Spine (Phila Pa 1976)*, 27(14):1504–1510, Jul 2002.

[106] Aysha Z. Akhtar, John J. Pippin, and Chad B. Sandusky. Animal models in spinal cord injury: a review. *Rev Neurosci*, 19(1):47–60, 2008.

[107] Ephron S. Rosenzweig and John W. McDonald. Rodent models for treatment of spinal cord injury: research trends and progress toward useful repair. *Curr Opin Neurol*, 17(2):121–131, Apr 2004.

[108] Stuart I Hodgetts, Giles W Plant, and Alan R Harvey. Chapter 14 - spinal cord injury: experimental animal models and relation to human therapy. In Charles Watson, George Paxinos, Gulgun Kayalioglu, editor, *The Spinal Cord*, pages 209 – 237. Academic Press, San Diego, 2009.

[109] B. T. Stokes and L. B. Jakeman. Experimental modelling of human spinal cord injury: a model that crosses the species barrier and mimics the spectrum of human cytopathology. *Spinal Cord*, 40(3):101–109, Mar 2002.

[110] Mark H. Tuszynski and Oswald Steward. Concepts and methods for the study of axonal regeneration in the cns. *Neuron*, 74(5):777–791, Jun 2012. Einleitung, Diskussion.

[111] Oswald Steward, Binhai Zheng, and Marc Tessier-Lavigne. False resurrections: distinguishing regenerated from spared axons in the injured central nervous system. *J Comp Neurol*, 459(1):1–8, Apr 2003. SKIM.

[112] R. Talac, J. A. Friedman, M. J. Moore, L. Lu, E. Jabbari, A. J. Windebank, B. L. Currier, and M. J. Yaszemski. Animal models of spinal cord injury for evaluation of tissue engineering treatment strategies. *Biomaterials*, 25(9):1505–1510, Apr 2004.

[113] Veronica Estrada and Hans Werner Müller. Spinal cord injury - there is not just one way of treating it. *F1000Prime Rep*, 6:84, 2014.

[114] Nicole Brazda, Veronica Estrada, Christian Voss, Klaus Seide, Hoc Khiem Trieu, and Hans Werner Müller. Experimental strategies to bridge large tissue gaps in the injured spinal cord after acute and chronic lesion. *J Vis Exp*, (110), 2016.

[115] George Paxinos and 1943 Watson, Charles. *The rat brain in stereotaxic coordinates*. Amsterdam : Elsevier Academic Press, 5th ed edition, 2005. At head of title: Paxinos & Watson.

[116] Gudrun Lang. *Histotechnik Praxislehrbuch fuer die Biomedizinische Analytik*. Springer Wien New York, 2 nd edition, 2013.

[117] Alan MRCPath Stevens and John D Bancroft. *Theory and practice of histological techniques*. New York : Churchill Livingstone, 4th ed edition, 1996. Includes bibliographical references and indexes.

[118] D. M. Basso, M. S. Beattie, and J. C. Bresnahan. A sensitive and reliable locomotor rating scale for open field testing in rats. *J Neurotrauma*, 12(1):1–21, Feb 1995.

[119] Veronica Estrada, Nicole Brazda, Christine Schmitz, Silja Heller, Heinrich Blazyca, Rudolf Martini, and Hans Werner Müller. Long-lasting significant functional improvement in chronic severe spinal cord injury following scar resection and polyethylene glycol implantation. *Neurobiol Dis*, 67:165–179, Jul 2014.

[120] Jiri Sedy, Lucia Urdzikova, Pavla Jendelova, and Eva Sykova. Methods for behavioral testing of spinal cord injured rats. *Neurosci Biobehav Rev*, 32(3):550–580, 2008.

[121] R Core Team. *R: A Language and Environment for Statistical Computing*. R Foundation for Statistical Computing, Vienna, Austria, 2013.

[122] Hadley Wickham. *ggplot2: Elegant Graphics for Data Analysis (Use R!)*. Springer, 1st ed. 2009. corr. 3rd printing 2010 edition, 2 2010.

[123] William S. Cleveland. Robust locally weighted regression and smoothing scatterplots. *Journal of the American Statistical Association*, 74(368):829–836, 1979.

[124] Martin Oudega. Molecular and cellular mechanisms underlying the role of blood vessels in spinal cord injury and repair. *Cell Tissue Res*, 349(1):269–288, Jul 2012.

[125] Christopher J. Sontag, Nobuko Uchida, Brian J. Cummings, and Aileen J. Anderson. Injury to the spinal cord niche alters the engraftment dynamics of human neural stem cells. *Stem Cell Reports*, 2(5):620–632, May 2014.

[126] Jun Li, Weichun Guo, Min Xiong, Heng Han, Jie Chen, Dan Mao, Bing Tang, Hualong Yu, and Yun Zeng. Effect of sdf-1/cxcr4 axis on the migration of transplanted bone mesenchymal stem cells mobilized by erythropoietin toward lesion sites following spinal cord injury. *Int J Mol Med*, Sep 2015.

[127] Katja M. Piltti, Sabrina N. Avakian, Gabriella M. Funes, Antoinette Hu, Nobuko Uchida, Aileen J. Anderson, and Brian J. Cummings. Transplantation dose alters the dynamics of human neural stem cell engraftment, proliferation and migration after spinal cord injury. *Stem Cell Res*, 15(2):341–353, Sep 2015.

[128] Katja Rosenkranz, Sandra Kumbruch, Katrin Lebermann, Katrin Marschner, Arne Jensen, Rolf Dermietzel, and Carola Meier. The chemokine sdf-1/cxcl12 contributes to the 'homing' of umbilical cord blood cells to a hypoxic-ischemic lesion in the rat brain. *J Neurosci Res*, 88(6):1223–1233, May 2010.

[129] Chung Heon Ryu, Soon A. Park, Seong Muk Kim, Jung Yeon Lim, Chang Hyun Jeong, Jin Ae Jun, Ji Hyeon Oh, Sun Hwa Park, Won-Il Oh, and Sin-Soo Jeun. Migration of human umbilical cord blood mesenchymal stem cells mediated by stromal cell-derived factor-1/cxcr4 axis via akt, erk, and p38 signal transduction pathways. *Biochem Biophys Res Commun*, 398(1):105–110, Jul 2010.

[130] Thorsten Trapp, Gesine Kögler, Abdelouahid El-Khattouti, Rüdiger V. Sorg, Michael Besselmann, Melanie Foecking, Christian P. Bührle, Ingo Trompeter, Johannes C. Fischer, and Peter Wernet. Hepatocyte growth factor/c-met axis-mediated tropism of cord blood-derived unrestricted somatic stem cells for neuronal injury. *J Biol Chem*, 283(47):32244–32253, Nov 2008.

[131] Oswald Steward, Phillip G. Popovich, W Dalton Dietrich, and Naomi Kleitman. Replication and reproducibility in spinal cord injury research. *Exp Neurol*, 233(2):597–605, Feb 2012.

[132] Rita C. Assuncao-Silva, Eduardo D. Gomes, Nuno Sousa, Nuno A. Silva, and Antonio J. Salgado. Hydrogels and cell based therapies in spinal cord injury regeneration. *Stem Cells Int*, 2015:948040, 2015.

[133] Roger Y. Tam, Tobias Fuehrmann, Nikolaos Mitrousis, and Molly S. Shoichet. Regenerative therapies for central nervous system diseases: a biomaterials approach. *Neuropsychopharmacology*, 39(1):169–188, Jan 2014.

[134] Bikesh Shrestha, Katherine Coykendall, Yongchao Li, Alex Moon, Priyanka Priyadarshani, and Li Yao. Repair of injured spinal cord using biomaterial scaffolds and stem cells. *Stem Cell Res Ther*, 5(4):91, 2014.

[135] Aaron J. Krych, Gemma E. Rooney, Bingkun Chen, Thomas C. Schermerhorn, Syed Ameenuddin, LouAnn Gross, Michael J. Moore, Bradford L. Currier, Robert J. Spinner, Jonathan A. Friedman, Michael J. Yaszemski, and Anthony J. Windebank. Relationship between scaffold channel diameter and number of regenerating axons in the transected rat spinal cord. *Acta Biomater*, 5(7):2551–2559, Sep 2009.

[136] Hiroshi Nomura, Tasneem Zahir, Howard Kim, Yusuke Katayama, Iris Kulbatski, Cindi M. Morshead, Molly S. Shoichet, and Charles H. Tator. Extramedullary chitosan channels promote survival of transplanted neural stem and progenitor cells and create a tissue bridge after complete spinal cord transection. *Tissue Eng Part A*, 14(5):649–665, May 2008.

[137] M. S. Beattie, J. C. Bresnahan, J. Komon, C. A. Tovar, M. Van Meter, D. K. Anderson, A. I. Faden, C. Y. Hsu, L. J. Noble, S. Salzman, and W. Young. Endogenous repair after spinal cord contusion injuries in the rat. *Exp Neurol*, 148(2):453–463, Dec 1997.

[138] M. T. Fitch, C. Doller, C. K. Combs, G. E. Landreth, and J. Silver. Cellular and molecular mechanisms of glial scarring and progressive cavitation: in vivo and in vitro analysis of inflammation-induced secondary injury after cns trauma. *J Neurosci*, 19(19):8182–8198, Oct 1999.

[139] Yukio Someya, Masao Koda, Mari Dezawa, Tomoko Kadota, Masayuki Hashimoto, Takahito Kamada, Yutaka Nishio, Ryo Kadota, Chikato Mannoji, Tomohiro Miyashita, Akihiko Okawa, Katsunori Yoshinaga, and Masashi Yamazaki. Reduction of cystic cavity, promotion of axonal regeneration and sparing, and functional recovery with transplanted bone marrow stromal cell-derived schwann cells after contusion injury to the adult rat spinal cord. *J Neurosurg Spine*, 9(6):600–610, Dec 2008.

[140] Damien Daniel Pearse, Alexander Eduardo Marcillo, Martin Oudega, Michael Paul Lynch, Patrick McGhee Wood, and Mary Bartlett Bunge. Transplantation of schwann cells and olfactory ensheathing glia after spinal cord injury: does pretreatment with methylprednisolone and interleukin-10 enhance recovery? *J Neurotrauma*, 21(9):1223–1239, Sep 2004.

[141] Yang D. Teng, Erin B. Lavik, Xianlu Qu, Kook I. Park, Jitka Ourednik, David Zurakowski, Robert Langer, and Evan Y. Snyder. Functional recovery following traumatic spinal cord injury mediated by a unique polymer scaffold seeded with neural stem cells. *Proc Natl Acad Sci U S A*, 99(5):3024–3029, Mar 2002.

[142] Jeffrey S. Hakim, Melika Esmaeili Rad, Peter J. Grahn, Bingkun K. Chen, Andrew M. Knight, Ann M. Schmeichel, Nasro A. Isaq, Mahrokh Dadsetan, Michael J. Yaszemski, and Anthony J. Windebank. Positively charged oligo[poly(ethylene glycol) fumarate] scaffold implantation results in a permissive lesion environment after spinal cord injury in rat. *Tissue Eng Part A*, Jun 2015.

[143] Xiang Zeng, Yuan-shan Zeng, Yuan-huan Ma, Li-ya Lu, Bao-ling Du, Wei Zhang, Yan Li, and Wood Yee Chan. Bone marrow mesenchymal stem cells in a three-dimensional gelatin sponge scaffold attenuate inflammation, promote angiogenesis, and reduce cavity formation in experimental spinal cord injury. *Cell Transplant*, 20(11-12):1881–1899, 2011.

[144] Kelli G. Sharp, Kelly Matsudaira Yee, and Oswald Steward. A re-assessment of long distance growth and connectivity of neural stem cells after severe spinal cord injury. *Exp Neurol*, 257:186–204, Jul 2014.

[145] C. H. Tator and M. G. Fehlings. Review of the secondary injury theory of acute spinal cord trauma with emphasis on vascular mechanisms. *J Neurosurg*, 75(1):15–26, Jul 1991.

[146] Hyuk Min Kim, Dong Hoon Hwang, Jong Eun Lee, Seung U. Kim, and Byung G. Kim. Ex vivo vegf delivery by neural stem cells enhances proliferation of glial progenitors, angiogenesis, and tissue sparing after spinal cord injury. *PLoS One*, 4(3):e4987, 2009.

[147] Andres Hurtado, Lawrence D F. Moon, Veronique Maquet, Bas Blits, Robert Jerome, and Martin Oudega. Poly (d,l-lactic acid) macroporous guidance scaffolds seeded with schwann cells genetically modified to secrete a bi-functional neurotrophin implanted in the completely transected adult rat thoracic spinal cord. *Biomaterials*, 27(3):430–442, Jan 2006.

[148] Barbara Grimpe and Jerry Silver. The extracellular matrix in axon regeneration. *Prog Brain Res*, 137:333–349, 2002.

[149] E. J. Bradbury, S. Khemani, R. Von, King, J. V. Priestley, and S. B. McMahon. Nt-3 promotes growth of lesioned adult rat sensory axons ascending in the dorsal columns of the spinal cord. *Eur J Neurosci*, 11(11):3873–3883, Nov 1999.

[150] Claire E. Hulsebosch. Recent advances in pathophysiology and treatment of spinal cord injury. *Adv Physiol Educ*, 26(1-4):238–255, Dec 2002.

[151] Paul Lu and Mark H. Tuszynski. Growth factors and combinatorial therapies for cns regeneration. *Exp Neurol*, 209(2):313–320, Feb 2008.

[152] Irja Elliott Donaghue, Charles H. Tator, and Molly S. Shoichet. Sustained delivery of bioactive neurotrophin-3 to the injured spinal cord. *Biomater Sci*, 3(1):65–72, Jan 2015.

[153] Vanessa S. Boyce, Jihye Park, Fred H. Gage, and Lorne M. Mendell. Differential effects of brain-derived neurotrophic factor and neurotrophin-3 on hindlimb function in paraplegic rats. *Eur J Neurosci*, 35(2):221–232, Jan 2012.

[154] Stephanie Lord-Fontaine, Fan Yang, Quy Diep, Pauline Dergham, Scott Munzer, Patrick Tremblay, and Lisa McKerracher. Local inhibition of rho signaling by cell-permeable recombinant protein ba-210 prevents secondary damage and promotes functional recovery following acute spinal cord injury. *J Neurotrauma*, 25(11):1309–1322, Nov 2008.

[155] Paul Lu, Hong Yang, Leonard L. Jones, Marie T. Filbin, and Mark H. Tuszynski. Combinatorial therapy with neurotrophins and camp promotes axonal regeneration beyond sites of spinal cord injury. *J Neurosci*, 24(28):6402–6409, Jul 2004.

[156] Elizabeth J. Bradbury, Lawrence D F. Moon, Reena J. Popat, Von R. King, Gavin S. Bennett, Preena N. Patel, James W. Fawcett, and Stephen B. McMahon. Chondroitinase abc promotes functional recovery after spinal cord injury. *Nature*, 416(6881):636–640, Apr 2002.

[157] Nicholas D. James, Jessie Shea, Elizabeth M. Muir, Joost Verhaagen, Bernard L. Schneider, and Elizabeth J. Bradbury. Chondroitinase gene therapy improves upper

limb function following cervical contusion injury. *Exp Neurol*, 271:131–135, Jun 2015.

[158] H. Cheng, Y. Cao, and L. Olson. Spinal cord repair in adult paraplegic rats: partial restoration of hind limb function. *Science*, 273(5274):510–513, Jul 1996.

[159] Marie-Pascale Cote, Arthi A. Amin, Veronica J. Tom, and John D. Houle. Peripheral nerve grafts support regeneration after spinal cord injury. *Neurotherapeutics*, 8(2):294–303, Apr 2011.

[160] Fernando F. Santos-Benito and Almudena Ramon-Cueto. Olfactory ensheathing glia transplantation: a therapy to promote repair in the mammalian central nervous system. *Anat Rec B New Anat*, 271(1):77–85, Mar 2003.

[161] J. W. McDonald, X. Z. Liu, Y. Qu, S. Liu, S. K. Mickey, D. Turetsky, D. I. Gottlieb, and D. W. Choi. Transplanted embryonic stem cells survive, differentiate and promote recovery in injured rat spinal cord. *Nat Med*, 5(12):1410–1412, Dec 1999.

[162] Hans S. Keirstead, Gabriel Nistor, Giovanna Bernal, Minodora Totoiu, Frank Cloutier, Kelly Sharp, and Oswald Steward. Human embryonic stem cell-derived oligodendrocyte progenitor cell transplants remyelinate and restore locomotion after spinal cord injury. *J Neurosci*, 25(19):4694–4705, May 2005.

[163] Jason Sharp, Jennifer Frame, Monica Siegenthaler, Gabriel Nistor, and Hans S. Keirstead. Human embryonic stem cell-derived oligodendrocyte progenitor cell transplants improve recovery after cervical spinal cord injury. *Stem Cells*, 28(1):152–163, Jan 2010.

[164] Chang-Ching Yang, Yang-Hsin Shih, Miau-Hwa Ko, Shao-Yun Hsu, Henrich Cheng, and Yu-Show Fu. Transplantation of human umbilical mesenchymal stem cells from wharton's jelly after complete transection of the rat spinal cord. *PLoS One*, 3(10):e3336, 2008.

[165] Mingyong Gao, Paul Lu, Bridget Bednark, Dan Lynam, James M. Conner, Jeff Sakamoto, and Mark H. Tuszynski. Templated agarose scaffolds for the support of motor axon regeneration into sites of complete spinal cord transection. *Biomaterials*, 34(5):1529–1536, Feb 2013.

[166] Daniel Becker and John W McDonald, 3rd. Approaches to repairing the damaged spinal cord: overview. *Handb Clin Neurol*, 109:445–461, 2012.

[167] Jason R. Plemel, Michael B. Keough, Greg J. Duncan, Joseph S. Sparling, V Wee Yong, Peter K. Stys, and Wolfram Tetzlaff. Remyelination after spinal cord injury: is it a target for repair? *Prog Neurobiol*, 117:54–72, Jun 2014.

[168] S. Sakiyama-Elbert, P. J. Johnson, S. I. Hodgetts, G. W. Plant, and A. R. Harvey. Scaffolds to promote spinal cord regeneration. *Handb Clin Neurol*, 109:575–594, 2012.

[169] Yukinori Akiyama, Christine Radtke, and Jeffery D Kocsis. Remyelination of the rat spinal cord by transplantation of identified bone marrow stromal cells. *J Neurosci*, 22(15):6623–6630, Aug 2002.

[170] Martin Oudega and Xiao-Ming Xu. Schwann cell transplantation for repair of the adult spinal cord. *J Neurotrauma*, 23(3-4):453–467, 2006.

[171] Joseph S. Sparling, Frederic Bretzner, Jeff Biernaskie, Peggy Assinck, Yuan Jiang, Hiroki Arisato, Ward T. Plunet, Jaimie Borisoff, Jie Liu, Freda D. Miller, and Wolfram Tetzlaff. Schwann cells generated from neonatal skin-derived precursors or neonatal peripheral nerve improve functional recovery after acute transplantation into the partially injured cervical spinal cord of the rat. *J Neurosci*, 35(17):6714–6730, Apr 2015.

[172] Volker Dietz and Thomas Sinkjaer. Spasticity. *Handb Clin Neurol*, 109:197–211, 2012.

[173] Sandra Kapitza, Björn Zörner, Oliver Weinmann, Marc Bolliger, Linard Filli, Volker Dietz, and Martin E. Schwab. Tail spasms in rat spinal cord injury: changes in interneuronal connectivity. *Exp Neurol*, 236(1):179–189, Jul 2012.

[174] D. J. Bennett, M. Gorassini, K. Fouad, L. Sanelli, Y. Han, and J. Cheng. Spasticity in rats with sacral spinal cord injury. *J Neurotrauma*, 16(1):69–84, Jan 1999.

[175] Amanda McIntyre, Rachel Mays, Swati Mehta, Shannon Janzen, Andrea Townson, Jane Hsieh, Dalton Wolfe, and Robert Teasell. Examining the effectiveness of intrathecal baclofen on spasticity in individuals with chronic spinal cord injury: a systematic review. *J Spinal Cord Med*, 37(1):11–18, Jan 2014.

[176] Karim Fouad, Lisa Schnell, Mary B. Bunge, Martin E. Schwab, Thomas Liebscher, and Damien D. Pearse. Combining schwann cell bridges and olfactory-ensheathing glia grafts with chondroitinase promotes locomotor recovery after complete transection of the spinal cord. *J Neurosci*, 25(5):1169–1178, Feb 2005.

[177] Jike Lu, François Féron, Alan Mackay-Sim, and Phil M E. Waite. Olfactory ensheathing cells promote locomotor recovery after delayed transplantation into transected spinal cord. *Brain*, 125(Pt 1):14–21, Jan 2002.

[178] Jessica L. Nielson, Cristian F. Guandique, Aiwen W. Liu, Darlene A. Burke, A Todd Lash, Rod Moseanko, Stephanie Hawbecker, Sarah C. Strand, Sharon Zdunowski, Karen-Amanda Irvine, John H. Brock, Yvette S. Nout-Lomas, John C. Gensel, Kim D. Anderson, Mark R. Segal, Ephron S. Rosenzweig, David S K. Magnuson, Scott R. Whittemore, Dana M. McTigue, Phillip G. Popovich, Alexander G. Rabchevsky, Stephen W. Scheff, Oswald Steward, Grégoire Courtine, V Reggie Edgerton, Mark H. Tuszynski, Michael S. Beattie, Jacqueline C. Bresnahan, and Adam R. Ferguson. Development of a database for translational spinal cord injury research. *J Neurotrauma*, 31(21):1789–1799, Nov 2014.

[179] Vance P. Lemmon, Adam R. Ferguson, Phillip G. Popovich, Xiao-Ming Xu, Diane M. Snow, Michihiro Igarashi, Christine E. Beattie, John L. Bixby, and M. I. A. S. C. I Consortium . Minimum information about a spinal cord injury experiment: a proposed reporting standard for spinal cord injury experiments. *J Neurotrauma*, 31(15):1354–1361, Aug 2014.

[180] N. Brazda and Kruse M. Kirchhoffer T. Klinger R. Cimiano P. Müller H.W. Kruse, F. The cnr preclinical database for knowledge management in spinal cord injury research. *Society of Neurosience*, November 9 - 13 2012.

[181] Charles Watson and Gulgun Kayalioglu. Chapter 1 - the organization of the spinal cord. In Charles WatsonGeorge PaxinosGulgun Kayalioglu, editor, *The Spinal Cord*, pages 1 – 7. Academic Press, San Diego, 2009.

[182] Anne Jaerve, Nora Schiwy, Christine Schmitz, and Hans W Müller. Differential effect of aging on axon sprouting and regenerative growth in spinal cord injury. *Exp Neurol*, Jul 2011.

[183] Leanne M. Ramer, Matt S. Ramer, and Elizabeth J. Bradbury. Restoring function after spinal cord injury: towards clinical translation of experimental strategies. *Lancet Neurol*, 13(12):1241–1256, Dec 2014.

[184] Brian K. Kwon, Jessica Hillyer, and Wolfram Tetzlaff. Translational research in spinal cord injury: a survey of opinion from the sci community. *J Neurotrauma*, 27(1):21–33, Jan 2010.

[185] Robert R. Hansebout and Christopher R. Hansebout. Local cooling for traumatic spinal cord injury: outcomes in 20 patients and review of the literature. *J Neurosurg Spine*, 20(5):550–561, May 2014.

[186] Oswald Steward, Phillip G. Popovich, W. Dalton Dietrich, and Naomi Kleitman. Replication and reproducibility in spinal cord injury research. *Experimental Neurology*, (0), 2011.

Eidesstattliche Versicherung

Ich versichere an Eides statt, dass die Dissertation selbständig und ohne unzulässige fremde Hilfe erstellt und die hier vorgelegte Dissertation nicht von einer anderen Medizinischen Fakultät abgelehnt worden ist.

Düsseldorf, January 5, 2017 Theresa Sophie Kehl

Danksagung

Wie bereits in der Eidesstattlichen Versicherung bestätigt habe ich diese Arbeit alleine geschrieben - doch bei deren Entstehung und Gelingen habe ich von vielen Menschen Unterstützung erfahren, denen ich an dieser Stelle gerne danken möchte.

An erster Stelle möchte ich meinem Doktorvater Prof. Dr. rer. nat. Hans Werner Müller für die einzigartige Betreuung in den vergangenen Jahren herzlichst danken. Insbesondere für seine engagierte, ehrliche, zielführende und warmherzige Art mit der er mich geduldig begleitet hat. Ansteckend war für mich nicht nur sein Enthusiasmus für die wissenschaftliche Grundlagenforschung sondern auch die Freude an der Jazz Musik in New Orleans.

Ein ganz besonderer Dank geht auch an meine Betreuerin Frau Dr. rer. nat. Veronica Estrada, die mir bei der Planung, Durchführung und Auswertung dieser Arbeit jederzeit sachkundig und erfahren zur Seite stand. Auch in Zeiten von Motivationstiefs und längeren Durststrecken verstand sie es, durch ihre Gelassenheit, meine manchmal ungeduldige und unbändige Art zu beruhigen, meine Kräfte zu bündeln und tiefere Täler mit Eiscreme zu füllen. Für deine uneingeschränkte, liebevolle Unterstützung bin ich dir sehr dankbar Vero. Unsere gemeinsame Sumpftour durchs Mississippi-Delta mit riesigen Alligatoren hat großes Vertrauen geschaffen und wird mir immer in Erinnerung bleiben.

Auch den vielen anderen Mitarbeitern des Labors für molekulare Neurobiolgie möchte ich danken. Insbesondere Frau Dr. rer. nat. Jessica Schira für ihre jederzeit freundliche Hilfsbereitschaft und Expertise im Bereich der USSC, ohne deren Hilfe die Studie in diesem Ausmaß nicht möglich gewesen wäre. Christine möchte ich danken für die hervorragende Einarbeitung in die verschiedenen Techniken in unserem Labor. Von ihr das Operieren lernen zu können war für mich großes Glück und die Voraussetzung, die Tiere in dieser Arbeit selbstständig operieren zu können. Marion danke ich für das präzise Kultivieren der USSC als wichtige Grundvoraussetzung für diese Arbeit, Steffi für die Unterstützung bei den Färbungen, Lei für die Hilfe bei der Auswertungen zur Vaskularisierung und Zystenausbildung und Valentina für die kulinarischen Bereicherungen.

Dem Graduiertenkolleg ’1033’ der HHU und insbesondere dessen Vorsitzender Prof. Dr. med. Guido Reifenberger, der sich zusätzlich bereit erklärt hat meine Arbeit mit zu betreuen, möchte ich für die finanzielle Unterstützung danken.

Mein ganz besonderer Dank gilt meinen Eltern, die mich während meiner gesamten Ausbildung begleitet haben und mich in meinen Plänen und Vorstellungen bestärkt und unterstützt haben. Sie standen und stehen mir jederzeit mit Rat und Tat zur Seite, auch wenn ich die ein oder andere Erfahrung selber machen durfte, vor der sie mich bewahren wollten. Für euren uneingeschränkten Rückhalt und eure Liebe bin ich euch unendlich dankbar.